

The impact of extreme events on mudflats

The Guyana case

Master of Science Thesis



May 2021

The impact of extreme events on mudflats

The Guyana case

By

Vasileios Ntriankos

Student Number 4403347

In partial fulfilment of the requirements for the degree of

Master of Science
in Hydraulic Engineering

at the Delft University of Technology

Supervisor:	Ir. Ü.S.N. (Üwe) Best	IHE, TU Delft
Assessment committee:	Dr. Ir. B.C. (Bram) van Prooijen	TU Delft
	Dr. Ir. M. (Mick) van der Wegen	IHE, Deltares
	Dr. B. K. (Bregje) van Wesenbeeck	TU Delft, Deltares

Thessaloniki, May 2021

An electronic version of this report is available at <http://repository.tudelft.nl/>

Cover: Guyana coast at the study area. Picture by Üwe Best, 2020

«Η φύσις μηδέν ατελές ποιεῖ, μήτε μάτην» - “Nature does nothing without purpose or in vain”, Aristotle
(Greek philosopher, 384 – 322 BC)



Aristotle by sculptor Lysippos – 4th century B.C.

To my godfather, Leonidas Tsoukalas

Preface

This MSc Thesis is performed as the final part of my studies for the Master of Science in Hydraulic Engineering at Delft University of Technology. It lasted from September 2020 when I first contacted Dr. Bram van Prooijen till my presentation on May 2021. All the study and the meetings with the members of the assessment committee were held online due to the corona restrictions and because this was possible by the nature of this study that had no lab experiments and no field work.

The learning objectives of a Master Thesis, according to the study guide, is for the student to demonstrate scientific and technological skills, to show ability to work independently, to demonstrate capacity to manage –both technically and time-wise– a research or design project and to familiarize with fundamental research, possibly to prepare for a PhD study.

The aim of this study is to understand the processes taking place in a vegetated (mangroves) mudflat and to test the resilience of the system under extreme cases. As a case study, a part of the coast of Guyana, where in 2011 a mangrove restoration project was held is used and the model for the computations is the Mflat model.

Acknowledgements

The Master Thesis work is not a team work but an individual study and the independent work by the student is a prerequisite by the study guide. However, it is very important for somebody who works intensely for months on a study to have the right psychological support by family and friends and the right scientific support and guidance by the supervisors. I am really glad that I had both of these very important supports!

I would like to especially thank my godfather Leonidas who gave me the moral and financial motive to return back to Delft and finish my Master that I interrupted in 2015. Also, my brother and my father for their support and especially my mother who, once again, gave me the chance to leave from our job in Greece for months to complete this very important part of my education. I would also like to thank my friend and old fellow student Robert for his important support according to everything that had to do with my stay and life in The Netherlands.

Finally, I would like to thank my four supervisors: Üwe, you were a real daily support for this study who helped me a lot not only according to the pure scientific part, but also for understanding the study area and for the preparation of this report. Bregje, your field experience and knowledge on vegetation helped me to understand better all the vegetation dynamic, represent them more realistically in the model and interpret the results. Mick, your weekly support was very important for me to understand the model and the hydrodynamic processes and be able to give realistic results and explanations. Bram, your answer to my first email on September 2020, when I asked to have a Thesis with you was very encouraging for me to start this hard work. Thank you for your trust on me and for the real guidance through this whole study.

*Vasileios Ntriankos
Thessaloniki, May 2021*



Contents

List of Figures	iv
List of Tables	ix
Abstract	x
Graphical Abstract	xi
1 Introduction	1
1.1 Mudflats and vegetation	1
1.2 Knowledge motivation and research objectives	1
1.3 The study area	2
1.3 Modelling development	4
1.5 Thesis outline	5
2 Theoretical Framework for Guyana coast	6
2.1 Bathymetry and profiles	6
2.2 The normal hydrodynamic conditions	8
Tide in Guyana coast	8
Waves in Guyana coast	10
Wind	11
2.3 The extreme hydrodynamic conditions	11
Extreme swell event	12
Extreme storm event	13
Summary of extreme events	15
2.4 Sediment dynamics	15
2.5 The Mflat model	16
Morphological factor	16
Model limitations and advantages	17
3 The role of vegetation	18
3.1 General information on vegetation	18
3.2 The height of mangroves	20
3.3 Pneumatophores	21
3.4 Zone of Influence theory	22
3.5 Biomass	23
3.6 Influence on the flow	24
Increase of the critical erosion shear stress	24
Increase of drag coefficient	24
Increase of bed level by organic deposition	25
Dissipation of wave energy due to vegetation	25
3.7 Vegetation dynamics	26
Inundation stress	26
Competition stress	26
Growth of vegetation	27
Establishment of initial vegetation	27
Establishment of new plants	28

Mortality of vegetation	29
3.8 Impact of extreme events on vegetation.....	29
3.9 Summary of vegetation	30
4 Model calibration.....	31
4.1 Importance of calibration.....	31
4.2 Hydrodynamic and sediment dynamic calibration.....	31
The cross-shore flow case	35
Comparison between the cross-shore and the alongshore case	37
4.3 Vegetation calibration.....	38
Equilibrium profile	44
4.4 Summary of calibration	45
5 Sensitivity analysis.....	46
Critical shear stress.....	46
Sediment boundary concentration.....	47
Settling velocity.....	48
Erosion Coefficient.....	49
Wave height.....	50
Wave period.....	50
Morphological factor.....	52
Summary of sensitivity analysis	54
6 Results.....	55
6.1 Extreme swell event.....	55
6.2 Extreme storm event.....	60
6.3 Sensitivity analysis for the storm case.....	64
The slope effect	68
Forcing erosion	70
6.4 Impact of extreme events on vegetation.....	73
7 Discussion	74
The presence and migration of mudbanks	74
The hydrodynamic processes	75
Vegetation dynamics.....	75
The storm case	76
Expected bed level changes	77
The swell case	78
The impact of extreme events on vegetation.....	78
8 Conclusion	79
The response of vegetated mudflat on extreme events	79
The impact of extreme events on the mangrove-mudflat system.....	79
References	80
Appendix A – Wind and wave roses.....	83
Appendix B – Mudbank migration in Guyana coast.....	85

List of Figures

Figure 1 - The plume from Amazon River runs along the coast of Guiana basin in a zone of 20-40km wide up to the mouth of Orinoco River. A proportion of the fine sediment is transported as mud banks (Figure taken by Froidefond et al., 1988) -----	2
Figure 2 – The location of the study area together with aerial pictures before and after the mangrove restoration project – Satellite images by Google Earth -----	3
Figure 3 - The full interaction between hydrodynamics, morphodynamics and vegetation dynamics are considered by the Mflat_vege, forming a unique bio-geomorphological model-----	4
Figure 4 - Flow diagram of the work of this study. The necessary input data and the processes followed through this study. -----	5
Figure 5 - The three cross sections used to study the bathymetry of study area -----	6
Figure 6 - Mudbank migration along Guyana coast according to NEDECO, 1972. In the vertical axis it is the year and in the horizontal the location along the coast. Dots represent observations and lines the trends. The full sheet of the report is presented in Appendix B. -----	7
Figure 7 - 3D view of 1970 bathymetry. In the vertical axis is the water depth and in the horizontal axes the location according to a general grid of that area. -----	8
Figure 8 - Tidal wave during a day (above) and a month (below) according to the 5 measured tidal constituents by Demerara Beacon-----	9
Figure 9 – The position of the offshore buoy compared to the study area and the average annual roses for winds and waves (more information on roses at Appendix A)-----	10
Figure 10 - Wave height computed by van Ledden et al. (2009) using SWAN model for Guyana coast, for the swell event of October 2005 with the indication of the study area-----	12
Figure 11 - Schematized description of the processes and the interactions in Mflat model -----	17
Figure 12 - Avicennia Germinans with its well developed pneumatophores (Toorman et al. 2018) -----	18
Figure 13 - Aerial photo of the study area taken on 2012, one year after mangrove planting campaign. Photo by Toorman et al. (2018)-----	19
Figure 14 - Relationship between literature (red line – modified equation 3.2) and field data (blue dots) together with the new equation to adjust to field data (green line – modified equation 3.3) -----	21
Figure 15 – Sketch of a mangrove with its pneumatophores roots -----	21
Figure 16 - control volume, Mazda et al. 1997-----	24
Figure 17 - Aerial picture of the study area of 2020 (taken by Üwe Best). The growth of initial vegetation is visible as well as the establishment of new vegetation, compared with Figure 13 that refers to the same location at 2012. -----	28
Figure 18 - Impact of fmd on wave energy through the domain for fmd=0.0001-----	33
Figure 19 - The evolution of the initial 1970 profile (blue line) through the decades for 40 years of simulation for the cross-shore flow case. Different lines, representing different decades are almost on top of each other, showing a profile in equilibrium. -----	36
Figure 20 – The range of water depth, sediment concentration, wave height, cross-shore flow velocity and shear stresses during a 12-hour tidal period with 2-hours intervals at the end of the 40 years simulation time for the cross-shore flow case. -----	37
Figure 21 – Comparison of bed level profiles between the cross-shore flow case (blue line), the cross-shore plus alongshore flow case (red line) and the initial profile (black line) after 40 years of simulation using the parameters of Table 5 -----	37
Figure 22 - Evolution of the profile through decades for the alongshore flow case. With blue line it is presented the initial bed level and with different colors it is presented different decades. -----	38

Figure 23 - Vegetation after 10 years of simulation. Green line indicated the position and the height of mangroves, while black line the bed level profile. Blue line indicated the water level (in the figure is at around Mean Sea Level).-----	39
Figure 24 - Vegetation diameter in cm, vegetation height in m and number of plants per grid cell (10x10m) for the 10 years of simulation starting only with initial vegetation in the first 100m. The three pictures show only the last kilometer of the profile where vegetation is actually present. The color scale is the same for the first and the second picture. -----	40
Figure 25 - Bed level evolution and tidal cycles of spring and neap tide. The model uses a morphological factor of 50, thus 10 years are represented by 2.4 months that correspond to 5 spring and 5 neap tides (as there are 2 spring and 2 neap tides during every month). Bed level oscillates at the seaward boundary, following the spring and neap tides. This is a boundary effect limited up to the first 500m of the profile. In the last 500m of the profile, accretion due to the presence of dense vegetation and erosion just in front of it is gradually occurring. -----	40
Figure 26 - 10 years of simulation with vegetation (red line) and without vegetation (blue line) compared with the initial profile (black line)-----	41
Figure 27 - The range of water depth, sediment concentration, wave height, cross-shore flow velocity and shear stresses during a 12-hour tidal period with 2-hours intervals at the end of the 10 years of simulation time with vegetation. The vertical green line shows the position where vegetation becomes denser, at 3200m. -----	42
Figure 28 - Diameter in cm (blue line) and mangrove height in m (red line) after 10 years of simulation. Horizontal lines represent the average height (red line) and the average diameter (blue line) from field measurements. Black line shows the initial 1970 profile.-----	43
Figure 29 - Number of plants per grid cell (100m ²) (blue line) and the height of plants in 10*m (red line). Black line represents the initial 1970 profile. Horizontal lines represent the average height (red line) and the average number of plants per grid cell (blue line) from field measurements. -----	43
Figure 30 - Evolution of the profile through the years for 10 years of simulation with vegetation for the landward, densely vegetated part -----	44
Figure 31 – The evolution of the profile through the decades for a 40 years simulation with a zooming into the vegetated area. Blue line represents the initial 1970 profile, while different colors refer to different decade of evolution. -----	44
Figure 32 - Sensitivity on critical shear stress: The initial 1970 profile (purple line) together with the equilibrium profile after 40 years of simulation (blue line). Comparison with a profile with higher critical shear stress (red line – $\tau_{cr}=1.5*\tau_{crinitial}$) and with lower critical shear stress (green line – $\tau_{cr}=0.5*\tau_{crinitial}$). Horizontal axis: the length of the profile (m). Vertical axis: water depth (m).-----	47
Figure 33 - Sensitivity on sediment boundary concentration: The initial 1970 profile (purple line) together with the equilibrium profile after 40 years of simulation (blue line). Comparison with a profile with higher boundary concentration (red line – $bc=2*bc_{initial}$) and with lower boundary concentration (green line – $bc=0.5*bc_{initial}$). Horizontal axis: the length of the profile (m). Vertical axis: water depth (m).-----	47
Figure 34 - Evolution of bed level profile for the case of increased (two times higher) sediment boundary concentration. In the upper figure the time step of plotting the profile is 1 year and in the second it is 10 years. With blue line it is the initial 1970 profile and with different color it is presented a different year (upper figure) or a different decade (lower figure).-----	48
Figure 35 - Sensitivity analysis for settling velocity: The initial 1970 profile (purple line) together with the equilibrium profile after 40 years of simulation (blue line). Comparison with a profile with higher settling velocity (red line – $ww=2*ww_{initial}$) and with lower settling velocity (green line – $ww=0.5*ww_{initial}$). Horizontal axis: the length of the profile (m). Vertical axis: water depth (m).-----	49
Figure 36 – Sensitivity for erosion factor: The initial 1970 profile (purple line) together with the equilibrium profile after 40 years of simulation (blue line). Comparison with a profile with higher erosion factor (red line – $MM=2*MM_{initial}$) and with lower erosion factor (green line – $MM=0.5*MM_{initial}$). Horizontal axis: the length of the profile (m). Vertical axis: water depth (m).-----	49

Figure 37 - Sensitivity for wave height: The initial 1970 profile (purple line) together with the equilibrium profile after 40 years of simulation (blue line). Comparison with a profile with higher wave height (red line – $H_{rms}=2*H_{rms_{initial}}$) and with lower wave height (green line – $H_{rms}=0.5*H_{rms_{initial}}$). Horizontal axis: the length of the profile (m). Vertical axis: water depth (m).-----	50
Figure 38 - The evolution of the bed level profile through decades for a 40 years of simulation with a wave height of $H_{rms} = 0.1m$, the half of the one used for the normal hydrodynamic conditions. -----	50
Figure 39 – Sensitivity for wave period: The initial 1970 profile (purple line) together with the equilibrium profile after 40 years of simulation (blue line). Comparison with a profile with higher wave period (red line – $T_p=2*T_{p_{initial}}$) and with lower wave period (green line – $T_p=0.5*T_{p_{initial}}$). Horizontal axis: the length of the profile (m). Vertical axis: water depth (m).-----	51
Figure 40 - Dissipation of wave energy ($J/m^2/sec$) due to wave breaking during flood tide at the beginning of the 40 years simulation. The initial 1970 profile (purple line) together with the distribution of wave energy dissipation during normal hydrodynamic conditions (blue line). Comparison with the dissipation using higher wave period (red line – $T_p=2*T_{p_{initial}}$) and lower wave period (green line – $T_p=0.5*T_{p_{initial}}$). Horizontal axis: the length of the profile (m). Vertical axis: dissipation of wave energy ($J/m^2/sec$).-----	51
Figure 41 - Evolution of the profile through decades for the 40 years of simulation with a MF = 50 -----	52
Figure 42 – Evolution of the profile through decades for the 40 years of simulation with a MF = 100 – the case that is used for this study -----	52
Figure 43 – Evolution of the profile through decades for the 40 years of simulation with a MF = 200 -----	53
Figure 44 – Evolution of the profile through decades for the 40 years of simulation with a MF = 400 -----	53
Figure 45 - Comparison between the equilibrium profile came out of calibration with diffusion coefficient $Dif = 1.5$ (red line), the case with much higher diffusion coefficient $Dif = 5$ (blue line) and the initial 1970 profile (black line).-----	53
Figure 46 - Bed level profiles after 5 days of extreme swell event. The green line representing the case of normal hydrodynamic conditions is under the black one, representing the initial bed level profile. The red line represents the bed level after 5 days of extreme swell conditions and is almost the same with the other two, having only erosion in the order of 10cm at the very offshore boundary (boundary effect). -----	55
Figure 47 – Root mean square wave height (m) during flood tide – high water for normal hydrodynamic conditions (green line) and for extreme swell conditions (red line). The water level is shown by the blue line and the bed level by the black line. -----	56
Figure 48 – Comparison of wave height (m) between the case of extreme swell event with vegetated mudflat (green line) and the hypothetical case of the same event occurring on the same mudflat without vegetation (red line) during flood tide – high water. The water level is shown by the blue line and the bed level by the black line. Only the landward half of the profile is presented as vegetation is only present landward. -----	56
Figure 49 - Total shear stress profiles (Pa) for flood tide – high water during normal hydrodynamic conditions (green line) and during extreme swell conditions. The water level (m) is shown by the blue line and the bed level (m) by the black line. -----	57
Figure 50 – Comparison of total shear stress (Pa) between the simulation for extreme swell event with vegetation (green line) and the hypothetical case of the same event occurring on the same mudflat without vegetation (red line) during flood tide – high water. The water level (m) is shown by the blue line and the bed level (m) by the black line. Only the landward half of the profile is presented as vegetation is present landward.-----	58
Figure 51 – Suspended sediment concentration (kgr/m^3) during flood tide – high water for normal conditions (green line) and for extreme swell conditions (red line). The water level (m) is shown by the blue line and the bed level (m) by the black line.-----	58
Figure 52 - Comparison of suspended sediment concentration (kgr/m^3) between the case of extreme swell event with vegetated mudflat (green line) and the hypothetical case of the same event occurring on the same mudflat without vegetation (red line) during flood tide – high water. The water level (m) is shown by the blue line and the	

bed level (m) by the black line. Only the landward half of the profile is presented as vegetation is present landward. -----	59
Figure 53 - Cross-shore flow velocity (m/sec) in case of extreme swell event and in case of normal hydrodynamic conditions during flood tide (both velocity profiles are on top of each other, represented by red line). The water level (m) is shown by the blue line and the bed level (m) by the black line. -----	59
Figure 54 – Bed level profiles (m) after 5 days of extreme storm event. The green line representing the case of normal hydrodynamic conditions is under the black one, representing the initial bed level profile. The red line represents the bed level after 5 days of extreme storm conditions and is almost the same with the other two, having only erosion in the order of 10cm at the very offshore boundary (boundary effect). -----	60
Figure 55 - Root mean square wave height (m) during flood tide – high water for normal hydrodynamic conditions (green line) and during extreme storm conditions (red line). The water level (m) during storm is shown by the blue line and the bed level (m) by the black line. -----	60
Figure 56 - Comparison of wave height (m) between the case of extreme storm event with vegetated mudflat (green line) and the hypothetical case of the same event occurring on the same mudflat without vegetation (red line) during flood tide – high water. The water level (m) is shown by the blue line and the bed level (m) by the black line. Only the landward half of the profile is presented as vegetation is present landward. -----	61
Figure 57 - Total shear stress profiles (Pa) during flood tide – high water for normal hydrodynamic conditions (green line) and during extreme storm conditions (red line). The water level (m) during storm is shown by the blue line and the bed level (m) by the black line. -----	61
Figure 58 - Comparison of total shear stress (Pa) between the case of extreme storm event with vegetated mudflat (green line) and the hypothetical case of the same event occurring on the same mudflat without vegetation (red line) during flood tide – high water. The water level (m) is shown by the blue line and the bed level (m) by the black line. Only the landward half of the profile is presented as vegetation is present landward.-----	62
Figure 59 – Suspended sediment concentration (kg/m^3) during flood tide – high water for normal conditions (green line) and for extreme storm conditions (red line). The water level (m) during storm is shown by the blue line and the bed level (m) by the black line.-----	62
Figure 60 - Comparison of sediment concentration (kg/m^3) between the case of extreme storm event with vegetated mudflat (green line) and the hypothetical case of the same event occurring on the same mudflat without vegetation (red line) during flood tide – high water. The water level (m) is shown by the blue line and the bed level (m) by the black line. Only the landward half of the profile is presented as vegetation is present landward.-----	63
Figure 61 - Cross-shore flow velocity (m/sec) in case of extreme storm event (red line) and in case of normal hydrodynamic conditions (green line) during flood tide. The water level (m) during storm is shown by the blue line and the bed level (m) by the black line.-----	63
Figure 62 - Bed level profiles (m) for the last tide of the five days of extreme storm simulation. Profile plot for every 2 hours. Only in the seaward boundary the initial bed level is distinguished from the final one, while during the whole tidal period bed level remains stable.-----	64
Figure 63 - Water level (m) and bed level (m) variation during the 5 days of storm conditions-----	64
Figure 64 - Cumulative deposition (m) for normal conditions (red line), cumulative erosion for normal conditions (blue line, hidden behind the red one), cumulative deposition (m) for storm conditions (purple line) and cumulative erosion for storm conditions (orange line) through the model domain for 5 days of simulation. Bed level is shown by the black line. -----	65
Figure 65 - Bed level profiles (m) after 5 days of storm conditions for the extreme storm (blue line), for the extreme storm using a four times higher settling velocity – $w_w = 0.0048 \text{ m/sec}$ instead of $w_w = 0.0012 \text{ m/sec}$ – (red line) and for the extreme storm using the half settling velocity – $w_w = 0.0006 \text{ m/sec}$ instead of $w_w = 0.0012 \text{ m/sec}$ – (magenta line) -----	66
Figure 66 - Bed level profiles (m) after 5 days of storm conditions for the extreme storm (blue line), for the extreme storm using higher diffusion coefficient – $dif = 5$ instead of $dif = 1.5$ – (red line) and for the extreme storm using	

lower diffusion coefficient – dif = 0.5 instead of dif = 1.5 – (magenta line). All the profiles are on top of each other. -----	66
Figure 67 – Bed level profiles (m) after 5 days of storm conditions for the extreme storm (blue line) and for the extreme storm using lower critical shear stress – $\tau_{cr} = 0.05$ Pa instead of $\tau_{cr} = 0.18$ Pa – (red line). The initial bed level is shown by the black line. -----	67
Figure 68 - Bed level profiles (m) after 5 days of storm conditions for the extreme storm (blue line) and for the extreme storm using higher boundary sediment concentration – bcs = 0.2 kgr/m ³ instead of bcs = 0.1 kgr/m ³ – (red line)-----	67
Figure 69 - Wave height profiles (m) for flood tide – high water during the 5 days of extreme storm simulation. Comparison between the normal storm conditions (blue line) and the conditions with a storm using double wave height (red line). Bed level is shown by the black line. -----	68
Figure 70 - Bed level profiles (m) for the case of Guyana coast slope (black line) and for the hypothetical case of 10 times steeper coast (magenta line). The differences after 5 days of storm conditions are not visible in the scale of water depth. -----	68
Figure 71 - Differences on bed level between the starting bed level and the final one after 5 days of storm conditions for Guyana coast (blue line) and for the hypothetical case of 10 times steeper coast (red line). With black line is represented the horizontal axis. -----	69
Figure 72 - Differences on bed level (m) between the starting bed level and the final one after 5 days of storm conditions for Guyana coast (blue line) and for the hypothetical case of 10 times steeper coast (red line). With black line is represented the horizontal axis. The figure shows a magnification into the landward part of the profile. The point (at 3310m) where the profile jumps from erosion to deposition is where the initial slope changes and becomes milder. -----	69
Figure 73 - Suspended sediment concentration (kgr/m ³) for the normal storm case (blue line) and for the “forced erosion” storm case (red line) during flood tide – high water. With black line is shown the bed level (m) in the beginning of the storm. -----	70
Figure 74 – Suspended sediment concentration (kgr/m ³) for the normal storm case (blue line) and for the “forced erosion” case (red line) during ebb tide – high water + 4 hours. With black line is shown the bed level (m) in the beginning of the storm. -----	70
Figure 75 - Erosion and deposition (kgr/m ² /sec) during flood tide – high water. Erosion for normal storm case (green line), deposition for normal storm case (red line), erosion for “forced erosion” storm case (blue line) and deposition for “forced erosion” storm case (black line). -----	71
Figure 76 – Erosion and deposition (kgr/m ² /sec) during ebb tide – high water + 4 hours. Erosion for normal storm case (green line), deposition for normal storm case (red line), erosion for “forced erosion” storm case (blue line) and deposition for “forced erosion” storm case (black line). -----	71
Figure 77 - Final bed level profiles (m): The initial profile (black line) and the profiles after 5 days of simulation under normal storm conditions (blue line) and under “forced erosion” storm conditions (red line). -----	72
Figure 78 - Number of plants and wave energy dissipation for the last 1,000m of the profile, where vegetation is present during the 5 days of storm conditions -----	73
Figure 79 – The various profiles (m) used for this study: the measured 2020 profile (black line), the measured 1970 profile (red line), the simulated 2020 profile (blue line) -----	74

List of Tables

Table 1 - The characteristics of the tidal constituents from Demerara Beacon close to the study area-----	9
Table 2 - Table taken from van Ledden et al. (2009), presenting wind and wave data from a buoy at the offshore of Georgetown, Guyana-----	11
Table 3 - The hydrodynamic parameters for normal, extreme swell and extreme storm cases-----	15
Table 4 - Sediment characteristics from 8 samples at the study area-----	15
Table 5 - Comparison between vegetation parameters from literature and from field data analysis -----	23
Table 6 - Parameters that are subject of calibration with the symbols used in Mflat code-----	32
Table 7 – The set of parameters that can result in an equilibrium profile for the cross-shore flow case -----	35
Table 8 - Vegetation parameters used for the 10 years simulation (third column) compared with literature data (second column)-----	38
Table 9 - The variation of sediment and hydrodynamic parameters to apply sensitivity analysis -----	46
Table 10 – Description of the behavior of bed level profile for the tested cases of sensitivity analysis -----	54
Table 11 - The parameters of storm sensitivity analysis together with their physical explanation -----	65
Table 12 - Reduction of various parameters at the landward end of the model domain for a random flood tide – high water during the 5 days of extreme event simulation, compared with the same simulation using normal hydrodynamic conditions -----	79

Abstract

Mudflats are coastal features present in numerous locations around the planet. Depending on the latitude and local conditions, mudflats can be vegetated by salt marshes or by mangroves and play an important role in coastal evolution. Vegetated mudflats can create a remarkable sea defence and their high ecosystem value has been proven by various studies worldwide. In this study, the response of a vegetated mudflat under extreme hydrodynamic forcing is analysed using, as case study, a specific part of the Guyana coast at South America.

The sediment dynamics of the Guyana coast are dominated by Amazon River plume that shifts northwards and travels along the coast of South America till the Orinoco River delta in Venezuela. Mudflats are quite wide reaching tens of kilometres in width because of the high supply of sediment by Amazon and the formation of mudbanks along the coast travelling northwards and then westwards. The hydrodynamic environment is relatively mild as Guyana is located far from the track of tropical hurricanes; however swell events can occur caused by the North Atlantic cyclones. Despite of its mild hydrodynamic environment, there are often cases of overtopping of the seawall along Guyana coast every year with a severe and characteristic one been held on October 2005. This was the motive for the mangrove restoration project of the study area in 2011 and for the initiation of this study.

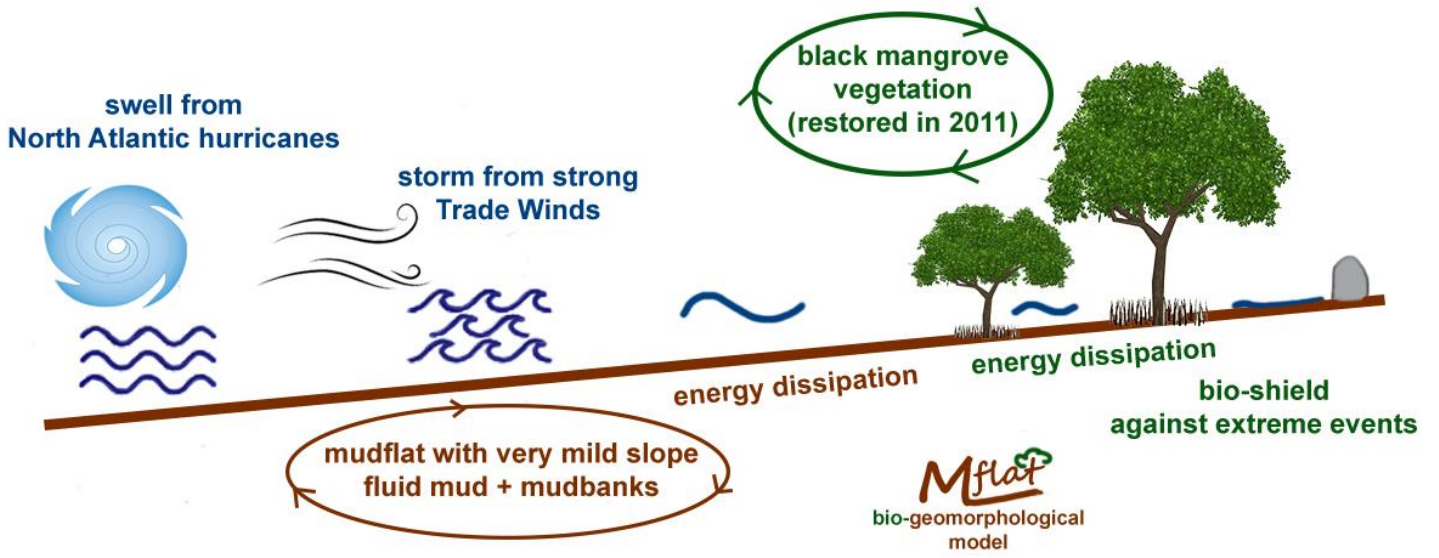
The purpose of this study is to analyze the response of a vegetated mudflat under extreme swell and storm events and investigate the impact of vegetation on this response. Furthermore, the impact of the extreme hydrodynamic event on probable damage of vegetation is tested presenting the complete interaction between hydrodynamics and vegetation.

The study area is the area of Chateau Margot, southern of Georgetown, where a mangrove restoration project took place in 2011 by planting *Avicennia Germinans* mangroves and field measurements were applied in the end of 2019 by the researcher Üwe Best. Using the 1-D process based model Mflat, based on an open source Matlab code, a 3.5km portion of the mudflat extending offshore is modelled. Vegetation dynamics and its influence on the flow is part of the model, so a full interaction between hydrodynamics, sediment dynamics, vegetation and morphological evolution can be simulated, establishing a complete bio-geomorphological model.

Using field measurements and literature data, the model is calibrated for hydrodynamic conditions and for the vegetation parameters giving a profile in equilibrium. A sensitivity analysis is applied to understand the behaviour of the model and the interaction between various hydrodynamic and sediment parameters and morphodynamics. After calibration, two extreme cases are tested in the model: an extreme storm that could be expected in Guyana coast and an extreme swell event based on the real case occurred in October 2005.

The Mflat model, after calibration, is able to reproduce a stable profile with mangrove vegetation similar to the observations. Vegetation appears to be quite effective in reducing the wave energy and thereby protecting the coast behind it during the extreme events, while in long term results in accretion of the landward part of the mudflat. The impact of the extreme hydrodynamic conditions on vegetation is difficult to be quantified, but for the extreme cases corresponding to the hydrodynamics of Guyana coast, vegetation is expected to be resilient enough having minor damages that could be restored in a short time period. The very mild slope of the coast is a factor that prevents the bed level of being highly dynamic contributing to the stability of the profile.

Graphical Abstract



1 Introduction

1.1 Mudflats and vegetation

Mudflats are coastal environments with muddy sediments as a major component that governs the behaviour of the morphodynamics (Healy, 2005). They consist of fine sediment with particles of silt and clay, smaller than $63\mu\text{m}$ and they usually occur in places where low-sloping coastlines coincide with large tidal ranges and high sediment inflows (Murray et al., 2019). The shape of mudflat's profile depends on the characteristics of the wave and tidal environment that dominate the hydrodynamic processes, with a more concave shape when wave action is dominant and a more convex shape when tide is prevailing in the overall balance (Petti et al., 2019). When averaged over annual or longer timescales, the morphology of a mudflat can approximate a dynamic equilibrium with external forces (Friedrichs, 2011). Fluid mud can be formed in extensive mudflats exposed on the cyclical stresses of incoming waves, forming internal waves that can dissipate a large percentage of the wave energy (Winterwerp et al., 2007) contributing on the self-protection of the coast from wave action.

Mangroves occupy the upper inter-tidal zone of many mudflats worldwide in tropical and subtropical areas up to the latitude of 25 to 30° (de Vos, 2004). They are plants adapted with aerial roots developed mostly in coastal and estuarine environments (Ilka et al., 1996). Mangroves form very active ecosystems that provide multiple services, as they can: absorb and store large carbon quantities, provide nutrients and safety for fish to grow, contribute to water purification and enrich water ecosystems with nutrients, provide timber and can be beneficial even for the development of tourism (Spalding et al. 2014). One more very important ecosystem service of mangroves is their ability to attenuate wave energy and to reduce the impact of extreme events on coastal areas (Hashim et al., 2013), thereby protecting these areas from extreme wave events, with the benefit of their contribution to the adaptation of coasts to the sea level rise (van Wesenbeeck et al., 2016).

1.2 Knowledge motivation and research objectives

The scope of this study is to enlighten the field of the response of vegetated mudflats under short and extreme events, focusing more to vegetation parameters and dynamics that remain a field with poor literature information. To succeed this, it is important to understand the processes that take place in the dynamic environment of a vegetated mudflat: hydrodynamics, morphodynamics and their interaction with vegetation. Then two different cases of extreme wave events are tested: One storm event with high wind generated waves (relatively high wave height and the corresponding wave period together with a storm surge) and one swell event with long waves (normal wave height with high wave period). The research questions that this study is intended to answer, taking as a case study a specific area along the coast of Guyana, South America, are the following:

- How do mudflats with mangrove vegetation respond to extreme wave events?
In order to answer to this question, the 1-D process based model Mflat is used, after calibrated for the specific case of Guyana, taking into account field measurements. Extensive sensitivity analysis is applied for both hydrodynamic, morphodynamic and vegetation parameters.
- What is the impact of extreme wave events on the mangrove-mudflat system and how does this system recovers after an extreme event?
The resilience of vegetation on extreme events is studied after the calibration of vegetation parameters for growth and death. To be able to understand better the processes that take place during extreme hydrodynamic conditions, a sensitivity analysis for the storm case is applied together with the investigation of the effect of very mild slope that could increase the stability of the mangrove-mudflat system.

1.3 The study area

Guyana is located in South America and its coasts have latitude between N 5.8° at the south borders with Suriname and N 8.5° at the north borders with Venezuela. The coastal environment is rich in muddy sediment originating mainly from the Amazon River, through a plume that travels northwards and remain close to the coast due the Trade Winds that dominate the wind conditions of this part of the continent and because of the cross-shore gravitational circulation caused by salinity gradient. Huge mud banks travel along the coast north-westerly of the Amazon River and regulate the erosion and accretion rates with a periodicity of about 30 years. These mud banks, together with mangrove fringes that are scattered along the coast, form a highly dynamic coastal environment (Winterwerp et al., 2007). A schematic illustration of the origin and the journey of mudbanks is presented in the Figure 1.

In this thesis, the study is focused on the Chateau Margot area, about 9km to the east of the estuary of Demerara River. The coast in this area is muddy with a very gentle slope in the order of 1:1,500 that initially was ending in a concrete wall used for sea defense. The mangroves of this area were restored by the Guyana Mangrove Restoration Project in 2011, with the planting of 13,000 seedlings in a fringe of 100m wide and 800m long. This fringe is located between two outfalls which provide the mangroves with fresh water. The dominant species is *Avicennia Germinans* with a secondary establishment of *Lunguncularia Racemosa*. Since 2011, the mangroves grew up and extended in the mudflat providing a bio-shield in front of the existing sea wall defense. The location of the study area is shown in Figure 2. Field data on hydrodynamics and vegetation are available from the field survey of PhD researcher Üwe Best, the period between November 2019 and January 2020.

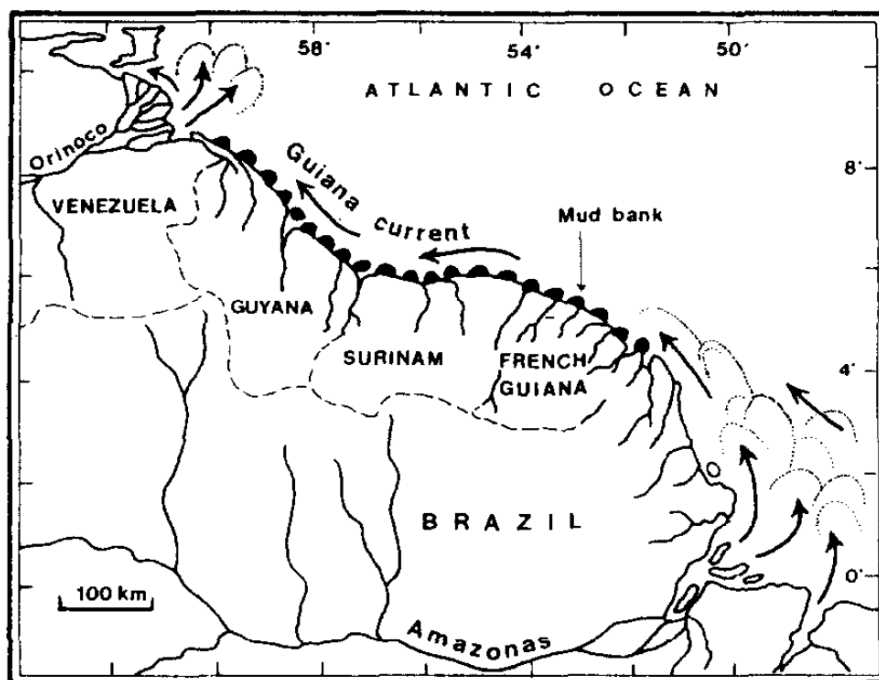


Figure 1 - The plume from Amazon River runs along the coast of Guiana basin in a zone of 20-40km wide up to the mouth of Orinoco River. A proportion of the fine sediment is transported as mud banks (Figure taken by Froidefond et al., 1988)



Figure 2 – The location of the study area together with aerial pictures before and after the mangrove restoration project – Satellite images by Google Earth

1.3 Modelling development

The response of a mudflat to the hydrodynamic forcing is a continuous interaction between the hydrodynamic conditions (wind, waves and tide), the sediment dynamics (critical shear stress, settling velocity, presence of fluid mud, etc), the local topography and vegetation, if present. To be able to understand, study and simulate the behavior of a mudflat under all the applied conditions, various numerical models have been developed based on field measurements and observations the last 3 decades (Pitchard et al., 2003). Models are usually based on specific areas or they focus on the impact of specific processes on mudflats according to the case they are made to study. The complexity of the processes and the range of knowledge are such that different models may need to be used by coupling results from wave propagation, morphodynamics and vegetation dynamics models. Especially in the field of vegetation dynamics, there is not much information found on modeling and the most of it concerns the impact of vegetation on flow and on dissipation of wave energy (Tang et al., 2015) and not the opposite process: the impact of hydrodynamic processes on vegetation.

In this study, Mflat, a new one dimensional process-based model developed on an open source Matlab code is used to study the morphodynamics of the study area. This model was initially developed to simulate a mudflat in South San Francisco Bay with quite good skill (van der Wegen et al., 2019). Then, vegetation dynamics and their interaction with the morphodynamics of the profile were added (Legay, 2020), following the work and guidelines of previous studies (van Maanen et al., 2015) and forming the model Mflat_vege. This model is still under experimental verification. This study is contributing to its development but also it uses the advantage of this “all in one”, unique bio-geomorphological model, as shown in Figure 3, and of its flexibility to extract valuable conclusions for the response of a vegetated mudflat under swell and storm conditions.

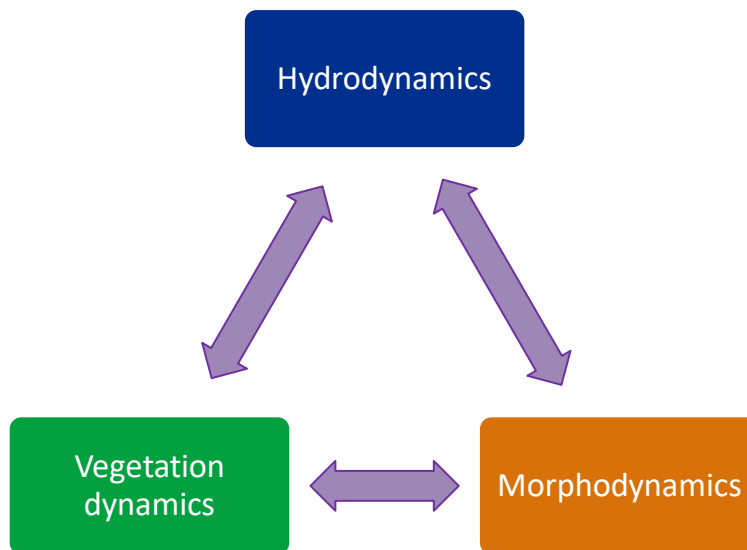


Figure 3 - The full interaction between hydrodynamics, morphodynamics and vegetation dynamics are considered by the Mflat_vege, forming a unique bio-geomorphological model

1.5 Thesis outline

The outline of this study starts with the basic theory and the theoretical framework concerning basic of the bathymetry, normal and extreme hydrodynamic conditions, sediment dynamics, as well as an analysis of the model used for this study in chapter 2. In chapter 3 the vegetation parameters and all the necessary assumptions are explained, analysing the field data and presenting a complete description of vegetation dynamics, including growth and death of vegetation, as well as the expected behaviour under extreme conditions. Then, in chapter 4 it is explained the procedure to calibrate the model both for hydrodynamic and for vegetation parameters based on literature and on the field measurements and it is derived the final set of parameters that is used further by the model. The purpose of calibration is to achieve a profile in equilibrium. In chapter 5 a sensitivity analysis is applied to the equilibrium profile derived from calibration procedure for the hydrodynamic conditions, to understand better the behaviour of the model.

After having a stable, realistic profile as well as the desirable extreme conditions from literature, the results of the simulations of the two extreme cases are presented in chapter 6, together with their sensitivity to hydrodynamic and vegetation changes. To understand better the results for the storm case, a sensitivity analysis is also applied for extreme storm condition. In chapter 7 the whole process is evaluated and discussed and in chapter 8 the final conclusions are presented. The source of wind and wave data as well as the mudbank migration for Guyana coast is presented in the appendices. The flow diagram of this study is shown in Figure 4.

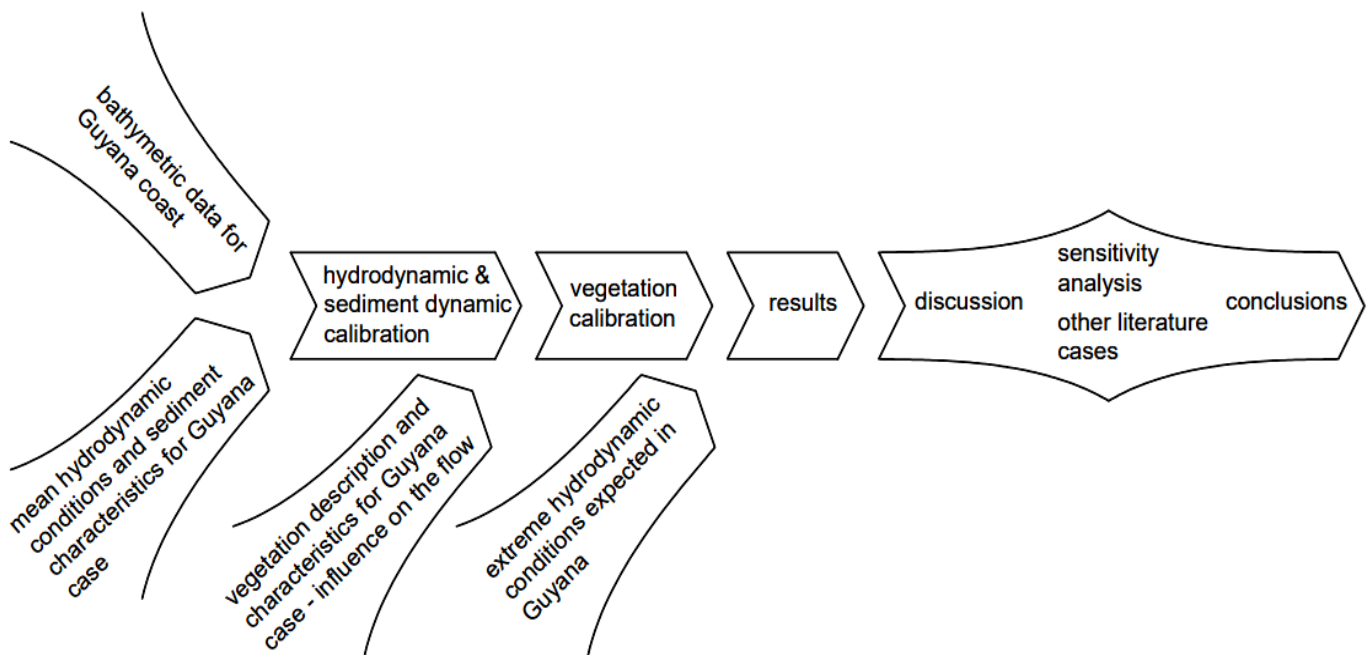


Figure 4 - Flow diagram of the work of this study. The necessary input data and the processes followed through this study.

2 Theoretical Framework for Guyana coast

Before deepening into the study of specific cases, it is important to understand the system around the study area, consisted of the bathymetry, the sediment and the hydrodynamic characteristics that determine the behavior of the profile and the dominant processes. It is also important to get familiar with the model and its ability to simulate physical procedures, together with the interaction between different dynamic conditions and processes. By understanding the system and the simulation capability of the model, it can be defined the framework of the study and the results of the model can be interpreted reliably.

2.1 Bathymetry and profiles

The bed level profile is the very first characteristic of a study area that can affect its response under hydrodynamic conditions and determine its morphological evolution. For the study area, there are no continues (annual) bathymetry data available. According to the year of interest, data can be derived by GEBCO database (General Bathymetric Charts of the Oceans – www.gebco.net) or by field surveys of the area taken place the period of interest, if available. For 1970 the profile is generated by the data of 1968 and 1972 reports of Netherlands Engineering Consultants (NEDECO) in which a slope of 1:1,500 extending from +0.30m at the landward end is mentioned. The 2008 profile is derived using the GEBCO database processed by the PhD researcher Üwe Best. The 2020 profile is generated by field measurements of the PhD researcher Üwe Best between November 2019 and January 2020. In parts of the study area where the access was not possible (in very shallow muddy areas just in front of the mangrove belt), the profile data are corrected using the GEBCO 2020 profile for this area.

All the above data are provided in a 2-dimensional grid with square discretization of $dx=10m$. The width of the grid is 900m and the length of the grid to the offshore is 3,500m. Mflat is a 1-D model, so the input in the model needs to be only one cross section of this 2-D profile. These cross sections are chosen to be visually representative of the 2-D profile. The cross sections of 1970, 2008 and 2020 are presented in Figure 5.

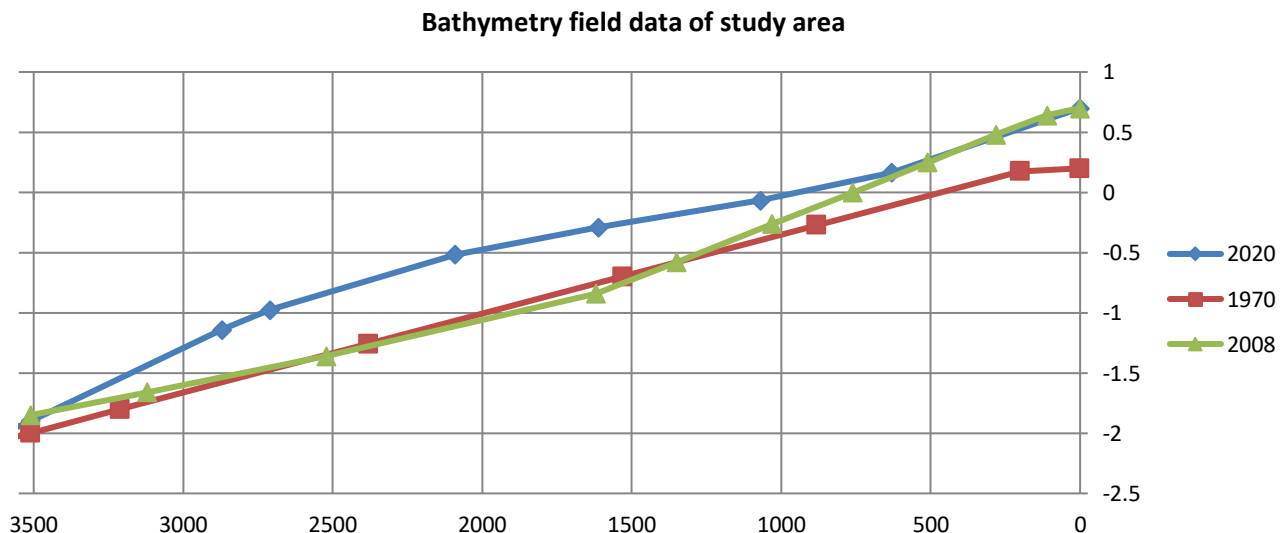


Figure 5 - The three cross sections used to study the bathymetry of study area

It is observed that the 2008 profile is similar with the 1970 one between 3,500m and 1,300m and with the 2020 one between 500m and 0m. Between 1,300m and 500m, the profile is in between 1970 and 2020 profile.

Along the coast from Amazon to Orinoco River, there is formation of huge mudbanks that extend up to 30km offshore and migrate under the influence of tides and currents generated by winds and waves. Mudbanks are spaced at intervals of 15-25km and migrate with a rate of 0.5-4.5km per year creating a periodicity of 10 to 20 years in their appearance at a specific coastal location. In their appearance they offer extra protection to the coast and a large sediment supply, favoring the accretion of the coast and the development of mangroves (Anthony et al., 2013).

The migration of mudbanks along the Guyana coast is presented in NEDECO 1972 report and the relevant picture is shown in Figure 6. This migration could give an explanation of the profile changes along the years presented in Figure 5. A possible scenario is that the appearance of a mudbank caused accretion of the coast starting some years before 2008 and developing further at least until 2020, when the profile appears to be generally more elevated. This scenario is not in fully accordance with the migration prediction of NEDECO 1972, but it should be mentioned that this prediction is performed about 50 years ago and it is already old. The fact is that according to the field measurements of researcher Uwe Best between November 2019 and January 2020, a mudbank is now present in front of the study area.

The mudbank migration and their impact on the coast is a procedure that is not included in the model simulations. According to the profiles shown in Figure 5, it is assumed that without the impact of the mudbank, the 1970 profile is in equilibrium and this is used as a reference for the calibration process analyzed further in chapter 4.2. The mild uniform slope of 1970 profile used by the model is presented in Figure 7.

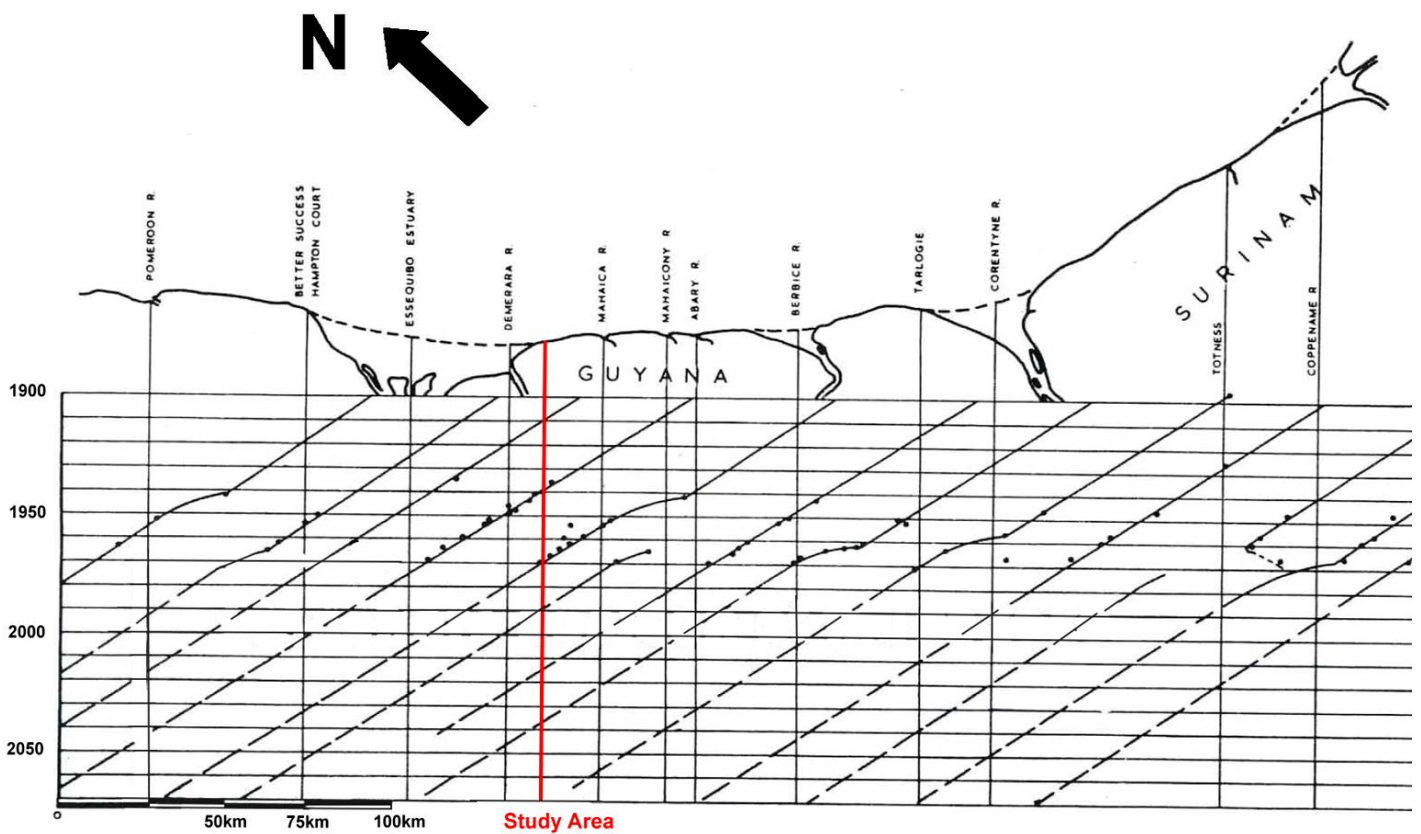


Figure 6 - Mudbank migration along Guyana coast according to NEDECO, 1972. In the vertical axis it is the year and in the horizontal the location along the coast. Dots represent observations and lines the trends. The full sheet of the report is presented in Appendix B.

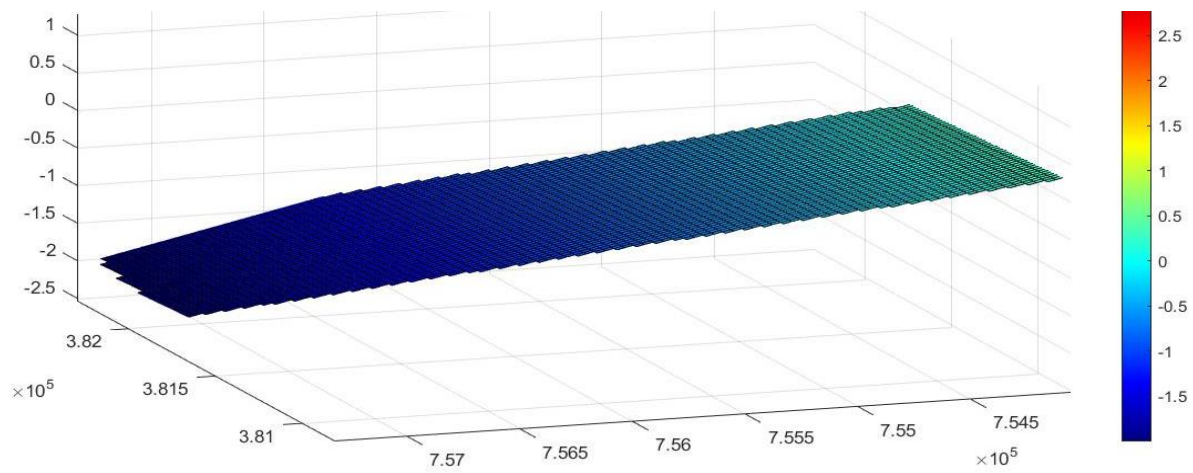


Figure 7 - 3D view of 1970 bathymetry. In the vertical axis is the water depth and in the horizontal axes the location according to a general grid of that area.

2.2 The normal hydrodynamic conditions

The intertidal flat hydrodynamics are governed by several processes and characteristics, like tidal propagation, cross-shore and alongshore currents, tidal asymmetry, wind-induced circulations, wave propagation and drainage processes. Bed friction is important for the attenuation of wave energy and together with the slope it defines the maximum wave height that a tidal flat can experience (Le Hir et al., 2000). For this study, the main hydrodynamic processes that are taken into account are the tide as the full signal with its asymmetries, the waves as a single stationary wave through its energy balance and the wind as an energy supply for the waves. Other hydrodynamic processes are neglected by the model and their effect is taken into account through the calibration procedure by modifying the input parameters as the final profile is known.

Tide in Guyana coast

Tide, when present in a coastal system, according to its range and its characteristics, can be a very important hydrodynamic process for the coastal evolution. The continuous repetitive oscillation of the water level due to tide can create cross-shore and alongshore currents which mobilize sediment and act on the morphology of the coast. Flood tide can bring sediment to the shore, while ebb tide returns it back to the offshore maintaining a balance or leading to slow but continuous changes of the profile. The type of the changes and the final shape of the coastal profile depend on the tidal range and on the shape of the tidal wave that forms the tidal asymmetry (Le Hir et al., 2000). The combination of different tidal constituents and the characteristics of each one of them form the final tidal wave and determine its behavior.

The characteristics of a tidal constituent are the amplitude, the phase lag relatively to the theoretical equilibrium tide and the angular frequency of the wave. The main tidal constituents are 37 and some of the most important of them are the principal lunar semidiurnal (M2), the principal solar semidiurnal (S2), the larger lunar elliptic semidiurnal (N2) and the lunar diurnal constituents (K1 and O1) (NOAA, 2021).

The tidal environment in the coast between Amazon and Orinoco River is semidiurnal with a large range in the order of 8m in the area of Amazon River decreasing northwards to a range in the order of 2m in the area of Orinoco River (Anthony et al., 2013). For this study, the tidal data from Demerara Beacon, located 18km NE of Georgetown at a depth of 5m are used. According to this station, the characteristics of the tidal constituents are shown in Table 1.

Table 1 - The characteristics of the tidal constituents from Demerara Beacon close to the study area

Parameter		Tidal constituent				
Symbol	Description	O1	K1	N2	M2	S2
A (m)	amplitude	0.09	0.14	0.14	0.9	0.33
ω (rad/sec)	angular frequency	0.0000676	0.0000729	0.0001379	0.0001405	0.0001454
ϕ (rad)	phase lag	3.05432361	3.420842444	1.483528611	1.919860556	2.3561925

According to the table above, Guyana experiences a mesotidal environment with a tidal range between 1m and 3m, and a tidal cycle with two spring and two neap tides per month. The tide is quite symmetric, with about 6 hours of flood and 6 hours of ebb tide, while the high water and low water peaks are symmetric around the Mean Sea Level. The shape of the tidal wave is shown in Figure 8 below:

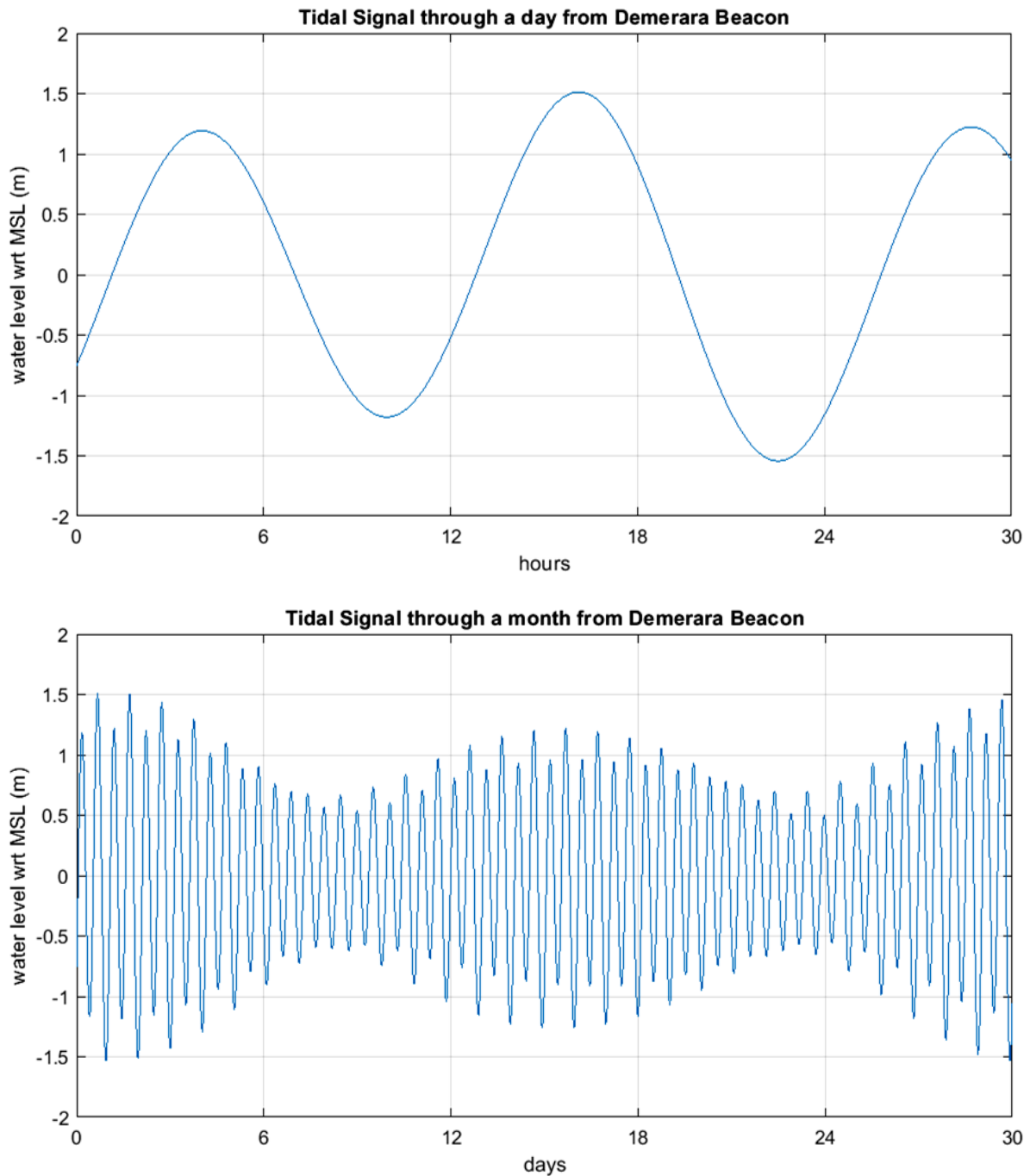


Figure 8 - Tidal wave during a day (above) and a month (below) according to the 5 measured tidal constituents by Demerara Beacon

Waves in Guyana coast

The coast between Amazon River and Orinoco River is affected by Trade Winds that have a predominant direction from North East and are mainly active from January to May. Trade Winds are the main wave generator in this part of Atlantic, with significant wave periods in the order of 6sec to 8sec and significant wave height at the offshore in the order of 1m to 2m. Longer swell waves can reach the coast originating from North Atlantic and are more severe during autumn and winter, due to the North Atlantic depression and Central Atlantic cyclones. Swell waves have a direction from the North West (Anthony et al., 2013).

There are available wind and wave data from a study of Delft Hydraulics the period 1997-2003 by a station at location 8°N, 57.5°W, at about 150km offshore of Georgetown (Appendix A). The location of the station and corresponding roses are presented in Figure 9.

The main direction of the waves according to the roses of the offshore buoy is 45° to the east compared with the orientation of the coast at the study area. The waves when they start feeling the sea bed they start to refract becoming more perpendicular to the coast. The 20m isobath curve is located approximately 30km to the offshore of Guyana coast (s.R.L., Navionics, 2021) and the mean slope of the shallow water is 1:1,500. For this study, because of the large trajectory of the waves on the mudflat before reaching the model domain, it is assumed that due to refraction wind waves approach vertically the coast of the study area.

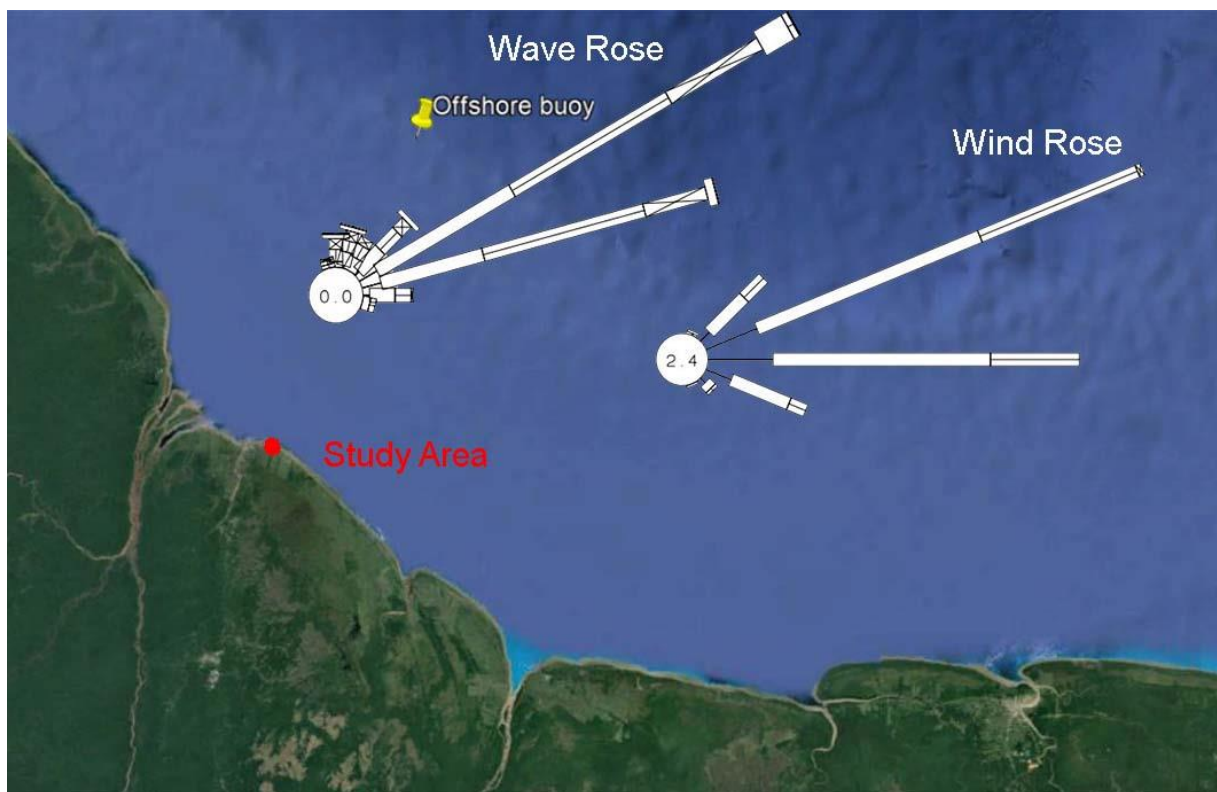


Figure 9 – The position of the offshore buoy compared to the study area and the average annual roses for winds and waves (more information on roses at Appendix A)

The model domain extends 3,500m to the offshore in a depth of 2m according to the field data. The wave height in normal conditions is 1.3m to the offshore and becomes about 0.3m close to the coast, while the wave period from 6sec to the offshore becomes around 3sec close to the coast (Winterwerp et al., 2007). For the calibration of the morphodynamic model it is necessary to assume one wave height that represents the mean hydrodynamic conditions over a long period, including the periods with very small and negligible waves, so the height of 0.3m is further reduced.

For the normal hydrodynamic simulations, it is assumed one wave reaching perpendicular the coast with a mean square root height of $H_{rms}=0.20m$ and a peak period of $T_p=3sec$.

Wind

In this study, having as an input the wave data, the role of the wind is only to amplify the waves while they propagate through the model domain. As soon as the model domain is relatively small, compared to the ability of the wind to determine the wave conditions (the length of the domain is 3.5km), the effect of the wind on hydrodynamics is not crucial. However, a representative wind velocity (u_{10}) is chosen, based on the resulting offshore wave height of 1.3m for fully developed conditions, due to the very long fetch available for Trade Winds to form waves through the Atlantic.

According to Recio et al., 1999, a good approximation for the significant wave height in fully developed seas can be given by Equation 2.1:

Equation 2.1 - Significant wave height in fully developed sea

$$H_s \cong 0.056 \cdot \frac{u_{10}^{2.488}}{g}$$

To achieve a wave height of 1.3m that is the case for normal conditions at the offshore, a wind velocity of 8.9m/sec (32km/hour) is necessary, so this is the velocity assumed for the amplification of wave height while waves propagate through the model domain.

2.3 The extreme hydrodynamic conditions

Guyana is located far from the track of tropical hurricanes and its wave environment is driven by Trade Winds directed from the east and swell waves coming from the North Atlantic. The presence of mud in the form of fluid mud and of long mudbanks along the coast of Guyana protect the coast from high waves succeeding a high percentage of wave energy dissipation and resulting in a mild wave environment along the Guyana coastline (van Ledden et al. 2009).

An analysis of NOAA data from a buoy located at 7°N, 57.75°W at a depth of 25m offshore of Georgetown made by van Ledden et al. (2009) can be a good indicator of the wave environment and the extreme conditions expected in Guyana coast and is presented in Table 2.

Table 2 - Table taken from van Ledden et al. (2009), presenting wind and wave data from a buoy at the offshore of Georgetown, Guyana

Parameter	NOAA location 7°N 57.75°W					
	Mean	>30%	>10%	1/year	1/10 years	1/50 years
Wind speed (m/sec)	5.8	7.4	8.1	9.9	10.4	10.7
Wind direction (deg w.r.t. north)	76	72	70	-	-	-
Wave height (m)	1.4	1.8	2	2.6	2.9	3
Wave period (sec)	7.6	8.4	8.9	16.7	18	18.7
Wave direction (deg w.r.t. north)	52	48	45	-	-	-

Extreme swell event

During October 2005 an extreme swell event hit the coast of Guyana causing floods and damages to the seawall defence due to overtopping. This event, according to the study of van Ledden et al. (2009) was originated from the North Atlantic. This swell event coincided with the spring tide resulting in easier wave propagation landward due to higher water levels. However, using the water level data from Georgetown's tidal gauge, no further water level set-up was observed and the water level was in the levels of the expected astronomical tide.

Van Ledden et al. (2009) studied an extensive area around Georgetown using the SWAN model to compute the propagation of waves landward accounting also for the effect of fluid mud and for the presence of mudbanks. After their data analysis, they chose to use an offshore wave with a significant wave height of $H_s=1.3\text{m}$, a peak period of $T_p=18.4\text{sec}$ and a direction of $\theta_{\text{wave}}=20^\circ$ from the North. The model shows a wave height of 0.3-0.8m near shore, depending on the location and a wave period that is capable of "penetrating" towards the coast without any reduction. In the study area of this Thesis, the wave height is in the order of 0.4m as shown in Figure 10.

The study of van Ledden concludes that the severe overtopping in some areas of Guyana coastline and the damages on the sea defense is a product of the high run-up resulting from the relatively high surging waves approaching the coast with an extremely high peak period coinciding with the spring tidal cycle. This event is considered rare and severe for Guyana coast and its characteristics are adopted by this Thesis to study the interaction of such an event with the vegetated mudflat.

Finally, the chosen hydrodynamic characteristics for the extreme swell analysis are the followings:

- $H_s = 0.50\text{m}$, assuming a severe condition compared with the one computed by van Ledden et al. (2009)
- $T_p = 18\text{sec}$, keeping the same period with offshore conditions as this is proven by van Ledden et al. (2009)
- $u_{10} = 8.9\text{m/sec}$, assuming the same wind conditions as for the normal hydrodynamic parameters

The wave direction is perpendicular to the coast as by assuming waves coming with an angle of 20° NE, they reach the coast of the study area (without considering the change of direction due to refraction) at an angle of 85° from the coastline.

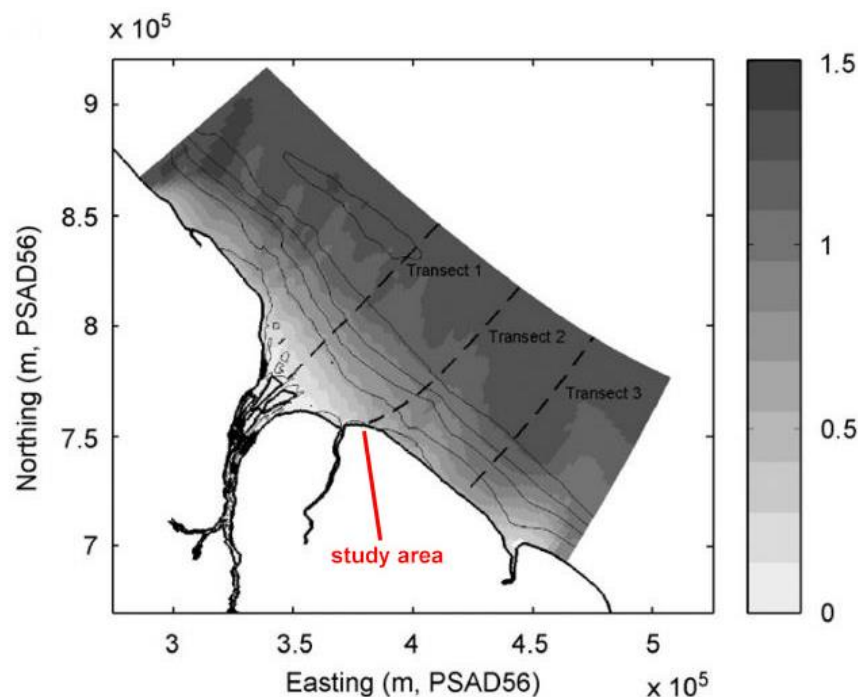


Figure 10 - Wave height computed by van Ledden et al. (2009) using SWAN model for Guyana coast, for the swell event of October 2005 with the indication of the study area

Extreme storm event

Guyana wave environment is dominated by Trade Winds and is not affected by extreme conditions that could be the case for tropical or subtropical cyclones in other areas of the planet. According to wave data from Table 2, an offshore wave height with a return period of 50years (extracted from the available data using a Weibull distribution) is in the order of 3m. In another study about Guyana coast (Winterwerp et al., 2007) it is mentioned that under extreme conditions waves can reach 4m height at the offshore that is reduced to 1.2m more inshore. The wave period is affected by the dissipation of wave energy and is reduced while waves propagate through the mudflat. However, no quantify data was found on the reduction of wave period in case of a storm along Guyana coast.

An important issue in case of a storm (strong winds and high waves) is the increase of the water level near the coast. This increase is a result of the storm surge and the water level set-up due to wave breaking. These two phenomena together can intensify the extremity of an event and result into more severe damages along a coast.

Wave induced water level set-up

The water level set-up is computed by using the gradient of cross-shore radiation stresses caused by wave propagation on shallow water especially when waves break. The wave induced radiation stresses are not calculated by Mflat model, as the model does not include the full momentum equation. Thus, the exact calculation of the water level set-up could be a difficult case and would demand generous changes of the way that Mflat model is constructed.

More simplistic ways to compute the maximum water level set-up does exist in literature with a characteristic one being on the study of R.A. Holman (1985), shown by Equation 2.2.

Equation 2.2 - Maximum wave induced water level set-up

$$\frac{\bar{\eta}_M}{H_b} = 0.38 \cdot \gamma$$

Using this formula, for wave height at breaking point $H_b=1,0\text{m}$ and for $\gamma=0.6$ (spilling waves) as used for this study, the maximum water level set-up is 0.23m. This could be used as an approximation, but this doesn't count for the impact of vegetation. Moreover, no data on wave induced set-up for Guyana coast are available.

Storm surge

Storm surge is the increase of the water level near the shore caused by high winds and low atmospheric pressure that are present during storm conditions. This phenomenon is very intense in case of strong tropical storms and can have duration of several hours up to a few days and extend along several kilometers along the coast (McIvor et al., 2012).

Storm surge height can be measured as the difference between the observed water level during storm conditions and the expected one caused by astronomical tide. However, the exact propagation of the storm surge wave is influenced by tidal wave propagation (both by currents and by water level changes) making these two phenomena slightly correlated. For this study, storm surge is considered as a uniform water level increase along the model domain as any further effort of including it into the model with more accurate way would create more uncertainty than the accuracy it would offer.

The height of the storm surge is strongly depended on the intensity of the storm that creates it, while regional topography can also affect it. Historical data from records around the world mention storm surges of up to 10m for tropical cyclones and of up to a few meters for extra-tropical storms. The peak water level storm surge height measured in the Netherlands during the 1953 storm was 3.0m for winds of up to 21m/sec (Mclvor et al., 2012)

For Guyana coast, there are no historical records found concerning storms surges. The expected wind speed corresponded to the extreme wave height (for Guyana case) of 4m is in the order of 14m/sec (have a look also at the wind roses in Appendix A). So, a reasonable assumption for the storm surge could be in the order of 1.5m.

Impact of vegetation on water level set-up and on storm surges

Vegetation can reduce the storm surge height mainly because of the obstacles it creates to the flow of water through it. This reduction was measured for several cases and it is described analytically in the study of Mclvor et al. (2012). Depending on the structure of vegetation, the type or mangrove roots, the density of vegetation and local topographic parameters, the reduction of storm surge height is in the order of 10cm per kilometer of mangrove width.

For Guyana case, the width of vegetation in the study area is in the order of a few hundred meters, so the expected reduction of the storm surge height is very low, in the order of a few centimeters. For this reason, and because there are not enough arguments found on how to quantify exactly this reduction, it is assumed a uniform storm surge along the whole model domain, without any reduction due to vegetation.

However, the effect of mangroves on reducing the wave induced setup is larger as even a narrow band of mangroves can reduce significantly the wave height, which is directly connected with the water level setup, as discussed in previous chapters of this study and this reduction is quantified. Thus, the wave induced set-up that is depended on the wave energy is strongly reduced. Because of the relatively low wave height (for a storm) expected in the breaking zone of Guyana coast and the corresponding low set-up (in the order of 20cm without the impact of vegetation), and because of the complexity of describing it in an analytical way using the Mflat model, it is decided to neglect the wave induced set-up for testing of the storm case.

Finally, the chosen hydrodynamic characteristics for the extreme storm analysis are listed below:

- $H_s = 1.0\text{m}$, assuming an offshore wave height of 4.0m that is strongly reduced due to depth restrictions and due to fluid mud and friction energy dissipation
- $T_p = 6\text{sec}$, assuming an offshore period in the order of 9sec partly reduced but without available field data reference
- $u_{10} = 14\text{m/sec}$ (50.4km/hour), assuming wind conditions that correspond to fully developed offshore wave height of 4m
- wave induced set-up: reasonably totally neglected
- storm surge height: 1.5m as a uniform increase of the water level through the whole model domain

Summary of extreme events

Summarizing the two extreme event cases that are analyzed in this study, the parameters for each case are presented in Table 3. The duration of the extreme events is chosen to be 5 days. This could be an upper limit for the duration of extreme hydrodynamic conditions and it is assumed so as the most severe scenario.

Table 3 - The hydrodynamic parameters for normal, extreme swell and extreme storm cases

Parameter	Comments	Normal mean conditions	Extreme 1 - Swell event According to the 2005 event	Extreme 2 - Storm event According to the offshore records, with a return period >> 50 years
duration		40 years	5 days	5 days
MorFac		100	1	1
H _s (m)	Assumed in water depth of -2m offshore value -> onshore value	1.3m -> 0.2m	1.3 -> 0.5	4 -> 1
T _p (sec)	Assumed in water depth of -2m offshore value -> onshore value	6 -> 3	18 -> 18	9 -> 6
wave direction	Due to refraction through the long shallow mudflat, it is assumed that waves reach the coast perpendicularly for all the cases			
tidal amplitude (m)	The full tidal cycle, starting with spring tide, so the extreme events coincide with high tide that is the most severe case			
wind-u ₁₀ (m/sec)	The same as the offshore wind	8.9	8.9	14
storm surge (m)	Uniform water level increase	0	0	1.5

2.4 Sediment dynamics

From the available data analysis of the field campaign of researcher Üwe Best, the average percentage of soil that passes from the No 200 sieve for 8 different sample locations is 99.2%, which means that the sand content of mud is only 0.8%.

The information of data processing of soil samples of 8 different locations (Samples 1 to 5 from mangroves and seaward and samples 6 to 8 from seawall and seaward) from the study area are summarized in Table 4 below:

Table 4 - Sediment characteristics from 8 samples at the study area

Sample	Moisture (%)	Specific Gravity (-)	Organic content (%)	Bulk Density (kgr/m ³)	Dry Density (kgr/m ³)	Liquid Limit	Plastic Limit	Plasticity Index
Sample 1	103.50	2.66	6.28	1612.00	967.61	53	22	31
Sample 2	79.01	2.63	3.88	1662.00	1048.65	45	24	21
Sample 3	47.22	2.67	1.51	1852.00	1356.61	35	20	15
Sample 4	87.81	2.65	3.48	1532.00	837.95	52	20	32
Sample 5	60.54	2.64	2.95	1792.00	1259.36	38	16	22
Sample 6	116.98	2.66	5.94	1388.00	604.56	99	33	66
Sample 7	116.71	2.62	4.01	1656.00	1038.93	87	33	54
Sample 8	95.34	2.67	6.47	1460.00	721.25	79	32	47
Average	88.39	2.65	4.32	1619.25	979.37	61	25	36

Using the average values of sediment characteristics together with relevant literature research, a realistic range for the characteristic parameters of the muddy bed can be derived. These parameters are the critical shear stress, the settling velocity and the Chézy friction factor as well as other calibration parameters analyzed in chapter 4.2.

2.5 The Mflat model

Mflat is a one dimensional process based model developed on an open source Matlab code. It applies a simplification of the shallow water equation to describe the cross-shore and alongshore tidal hydrodynamics as well as a stationary wave model (van der Wegen et al., 2019). It was first presented by van der Wegen et al. (2019) and the impact of vegetation was included in Mflat model by Legay (2020). Vegetation is further modified for the scope of this study as explained analytically in chapter 3.

To calculate the cross-shore velocities, inertia and friction effects of the momentum equation are neglected due to the relatively low velocities assumed. So the mass-balance equation is used instead of the momentum equation. The alongshore velocities are derived from the alongshore momentum equation assuming Neumann boundary along the profile. The wave-driven alongshore flow and the wave action impact on the alongshore shear stress are neglected. This is justified by the small wave height applied for this case study, as the domain is small and the wave energy has already been attenuated through the propagation on the mudflat before reaching the study domain. The wave energy is dissipated by the wave breaking and friction (also by vegetation when included) and amplified by wind energy supply. An advection – diffusion equation solves sediment transport while bed level changes occur by the divergence of the sediment transport field.

The bed level is updated by the net effect of local sediment transport gradient while erosion and deposition are enhanced by a morphological factor. The choice of the right morphological factor is important for the reliability of the results and for the wise use of time, thus it is further analyzed below.

Morphological factor

Morphological changes take place on a much longer time scale than hydrodynamic flows. To be able to scale up the morphological processes to a rate that has a significant impact on hydrodynamic flows, the term of the morphological time scale factor is introduced. Morphological factor is a coefficient that acts on morphological processes aiming to accelerate these processes with respect to the hydrodynamic processes (Lesser et al., 2004). The maximum morphological factor that can be used in a morphodynamic model depends on the particular processes being modeled and on how much dynamic is the hydrodynamic environment, so it is a matter of judgment. Tests have shown that even a morphological factor of 1000 can work for moderate morphologically active conditions (Deltares, 2020), albeit that, values of 50 are more appropriate if wave forcing is applied.

In Mflat, the morphological factor (MF) acts on every process related with bed erosion and deposition (both due to hydrodynamics and vegetation) and on the formula for the growth of mangroves' diameter. A starting point for long term simulation is set to 100, a typical value for coastal problems (Roelvink et al., 2005). For the Guyana case, it is tested to reduce the MF to 50 and no remarkable changes in morphological response are observed, so a value of 100 for the long term processes (the 40 years simulations without vegetation) it is considered as a good choice. The morphological factor is tested as part of sensitivity analysis in chapter 5. For shorter simulations (i.e. for the 10 years simulation with vegetation) a MF of 50 is used. For the very short duration of extreme events (5 days duration), there is no need to accelerate the morphological changes and a MF of 1 is used.

Model limitations and advantages

Mflat model is a relatively simple model compared to the much more sophisticated Delft3D model that is able to solve the unsteady shallow-water equations in two or in three dimensions. Delft3D consists of the horizontal momentum equations, the continuity equations, the transport equations (advection – diffusion equation) and a turbulence closure model. Several choices for the grid (rectangular, curvilinear, spherical and flexible) can be made by the user to properly simulate every specific case. A full spectrum for waves can be considered through the DELFT3D-WAVE module that co-operates with SWAN or other wave models and the full impact of waves is taken into account (radiation stress gradients, etc). For the sediment transportation, it considers the full advection diffusion equation together with bedload sediment transport and turbidity models (Lesser et al., 2004).

Mflat model is a 1D model, with constant grid that simplifies the shallow water equations, neglecting the inertia and friction effects and solving the mass-balance equation instead of the full momentum equation in the cross-shore direction. The cross-shore sediment transport is calculated with a simple advection diffusion equation and the alongshore sediment transport is neglected.

The Mflat model it may be simpler than other available models, it may include less processes in a more simplified way, but its simplicity makes it faster in calculation and its open code makes it “malleable”, easy to be modified for specific conditions and to adapt in specific cases. For this study this advantage is quite important especially for the vegetation part as it is easy to adjust the model to the specific field data for Guyana case. Another advantage is that it includes the full dynamics of vegetation, as analyzed further in chapter 3 and a complete interaction between vegetation, hydrodynamics and morphodynamics. A schematized description of the processes taken into account in the model as well as the interactions between them is presented in Figure 11. For an analytical description of Mflat model, the processes and the way that these processes are taken into account for the morphodynamic response of the profile, as well as for an analysis of the mathematical relations used by the model, please have a look at van der Wegen et al. (2019).

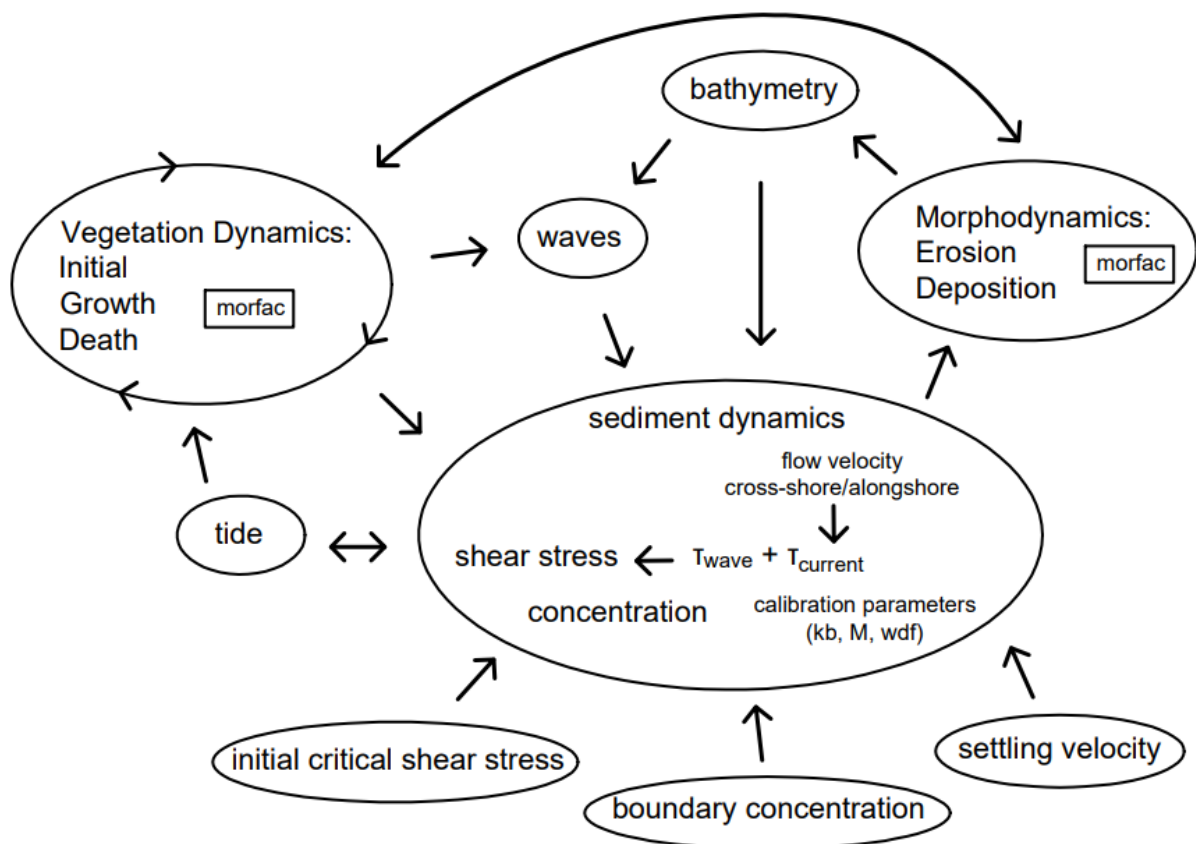


Figure 11 - Schematized description of the processes and the interactions in Mflat model

3 The role of vegetation

Vegetation is considered as a fundamental parameter, as its interaction with the mudflat under extreme hydrodynamic conditions is the core of this study. In this chapter, an extend analysis of vegetation characteristics by deepening into the relevant literature is applied together with the comparison between literature findings and the available field observations, while an analysis of the set-up of the model and how these characteristics are included in Mflat model is shown. Finally, a literature research on the impact of extreme events on vegetation provides a first impression of limitations of the model and of the expected response of vegetation.

3.1 General information on vegetation

Vegetation is an important parameter of coastal behaviour, when present, as it has a direct impact on hydrodynamics by dissipating wave energy (Mclvor et al., 2012a) and a direct impact on morphodynamics as it can stabilise the bed level in its area. Its importance is an extra motive to study it in detail and investigate further its impact on the response of the bed level profile.

Mangroves are highly productive ecosystems and have been highlighted as areas of global importance because of the variety and the importance of the ecosystem services they provide (van Maanen et al., 2015). Mangrove vegetation can dissipate wave energy playing an important role in coastal protection (Mclvor et al., 2012). The degree of protection depends on various parameters, like the mangrove species and its root system (rhizophora or pneumatophora), the density of the mangrove forest, the width of vegetation on the mudflat, the structure of the forest (stem configuration, diameters of roots and branches, etc), the age and the height of vegetation (if canopy is also –partly– submerged, how stiff are the stems, etc) (Hashim et al., 2013).

Avicennia Germinans is the main mangrove species in the area of Guyana. Fromard et al. (1998) measured for French Guiana that this species can reach 30m height, have a diameter at breast height (at 1.37m above ground) of 90cm, reach an age of 60-70 years old and have a density of around 300 trees per ha for mature stands. A characteristic *Avicennia Germinans* individual with its developed pneumatophores is shown in Figure 12.



Figure 12 - *Avicennia Germinans* with its well developed pneumatophores (Toorman et al. 2018)

Vegetation dynamics and their impact on the flow are described by van Maanen et al. (2015) and included in Mflat model by Legay (2020). In both of the above studies, it is used as a reference the *Avicennia Marina* mangrove species. In Guyana coast the dominant species is *Avicennia Germinans*. They both belong to the same, *Avicennia* genus of *Acanthaceae* family and they both develop pneumatophores aerial roots. Their characteristics can be considered to be similar as the literature feedback for this field is quite poor compared with the probable effect that any difference could result in the final behaviour of the vegetated profile. For this study, the main structure of the model described by Legay (2020) is followed, but various formulas and coefficients are modified according to the mangrove species of Guyana and based on field data collected on December 2019 – January 2020 by the researcher Uwe Best.

There are two important considerations to be taken into account before deepening into the details of vegetation dynamics:

- Vegetation in the study area is relatively young, as the mangrove restoration project took place in Guyana coast on 2011, thus it is a young mangrove forest with the oldest trees being now 10 years old. This may explain some differences from literature studies that refer to fully developed mangroves fringes. An aerial photo after mangrove restoration is presented in Figure 13.
- Vegetation is defined in the model separately for every grid cell, but in the same grid cell vegetation is considered to have the same characteristics (diameter, height, number of pneumatophores roots). The dimensions of a grid cell for this study are 10x10m.



Figure 13 - Aerial photo of the study area taken on 2012, one year after mangrove planting campaign. Photo by Toorman et al. (2018)

3.2 The height of mangroves

In a lot of literature studies, the height of mangroves 'H' is represented as a function of their stem diameter at breast height 'D'. The breast height is formalized at 137cm above ground level (van Maanen et al., 2015). Various studies agree on the following formula:

Equation 3.1 - General formula connecting mangroves' height and diameter

$$H = 137 + b_2 \cdot D - b_3 \cdot D^2$$

In which 'b₂' and 'b₃' are dimensionless coefficients that for *Avicennia Germinans* have the value of b₂=48.04, b₃=0.172 according to Berger et al., 2000.

So, the starting formula for this study is:

Equation 3.2 - Berger's formula for mangroves' height and diameter

$$H = 137 + 48.04 \cdot D - 0.172 \cdot D^2$$

'H' is the height and 'D' the diameter at breast height in cm.

From field measurements the mean tree height is 9.6m and the mean tree diameter at breast height is 7.5cm. With the above formula and coefficients, for a diameter of D=7.5cm the height of the tree is only H=4.91m. It is observed that the mangroves measured at the field have generally thinner stem and relatively higher height than the predicted ones by literature, which might be explained by the fact that the modelled vegetation is planted and not natural.

To be able to simulate the field data by keeping the same way of thinking with literature, the coefficients b₂ and b₃ are modified such as by keeping the constant parameter the same (137cm as the height for D=0), the result are close to the measurements. This leads to the following adjusted formula:

Equation 3.3 - Final formula for mangroves' height and diameter

$$H = 137 + 136 \cdot D - 3.5 \cdot D^2 \text{ and thus } b_2=136 \text{ and } b_3=-3.5$$

The Equation 3.3, as well as the Equation 3.2, may be able to connect the mangroves' height with their diameter, but they cannot be representative for very young trees as for the theoretical case of D=0 they give a mangrove height of 1.37m. To overcome this paradox and to be able to describe young mangroves, the following process is chosen to be followed:

1. It is chosen that the update for the new vegetation in the model is every 3 months.
2. An initial starting point is defined for the seedlings: It is assumed that a seedling has a diameter of 0.4cm and a height of 34.25cm. The value for the height of 34.25 is chosen as 137/4, since every 4 times per year vegetation is generated by the model.
3. A turning point is chosen for the description of the vegetation height: At D=1.37cm the height is the one derived by the equations 3.2 and 3.3 accordingly.
4. Between diameters of 0.4cm and 1.37cm, the mangrove height is given by linear interpolation

With this way of thinking, it is provided a realistic height for very young trees, as well as a continuous equation that can relate any diameter with the mangrove height. The above process for the field data and for the literature proposal is shown graphically in Figure 14 below:

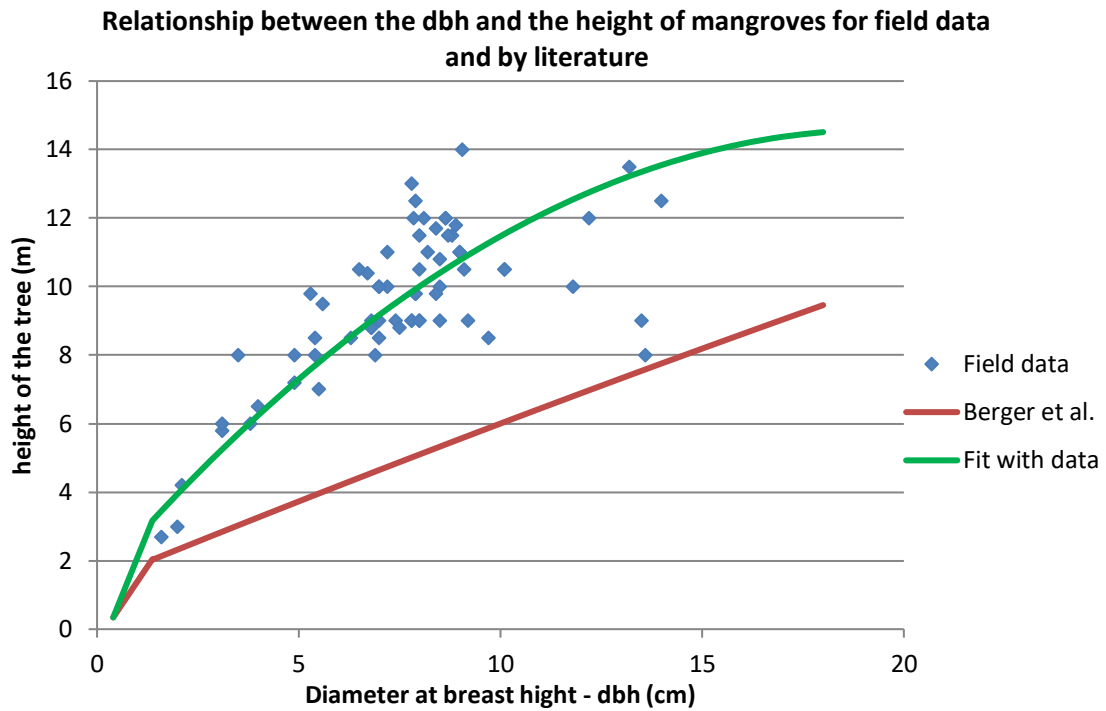


Figure 14 - Relationship between literature (red line – modified equation 3.2) and field data (blue dots) together with the new equation to adjust to field data (green line – modified equation 3.3)

The maximum diameter for this specific study is chosen to be 20cm corresponding to a height of 14.6m using the adjusted formula presented above (Equation 3.3). This diameter is relatively small compared to literature but it is chosen so because of the young age of the mangroves at the study area. By the above procedure, it is created a formula that may be unrealistic for long term runs, but it is very representative of the current conditions of vegetation in Guyana area and of the assumed evolution between 2011 and today.

3.3 Pneumatophores

Pneumatophores form an aerial root system around the stem, as shown in Figure 15, that allows the mangrove to breath during flooding and in anoxic soils. In *Avicennia* species the height of pneumatophores can reach 30cm, while an average spacing is 2.5cm (de Vos, 2004). Topographic variability results in variability in pneumatophores’ density, as the plant try to adjust its root system to be able to breathe sufficiently. Thus, in local topographic depressions pneumatophores are denser and higher as the flooding period is longer. Their density can reach high numbers, such as 2,500 roots per m², but a typical value is 200 roots per m² (Guebas et al., 2007).



Figure 15 – Sketch of a mangrove with its pneumatophores roots

For this study, the number of pneumatophores is considered as a number per tree, using the diameter of the tree to estimate their number:

Equation 3.4 - Number of pneumatophores per mangrove tree

$$N_{pneu} = 10025 \cdot \frac{1}{1 + e^{f \cdot (D_{0.5} - D)}}$$

'D' is the diameter at breast height in cm, $f = 0.3 \text{ cm}^{-1}$ and $D_{0.5} = 20 \text{ cm}$. These parameters are chosen such that a mature tree gets 10,000 pneumatophores (supplementary material of van Maanen et al., 2015).

All the pneumatophores are considered to have the same diameter, the average one from the field measurements, 0.26cm and a constant height of 10cm.

Feedback from field data:

Concerning the amount of pneumatophores per tree, according to Equation 3.4, the result is 230 pneumatophores for a $D=7.5\text{cm}$, while by the field measurements the number is 316 per tree. To reach 316 pneumatophores per tree, a diameter of 8.6cm at breast height is necessary, according to the above formula. A nice fit can be achieved if the parameter 'f' is changed from $f=0.30\text{cm}^{-1}$ to $f=0.274\text{cm}^{-1}$ and this modification is considered at the model.

3.4 Zone of Influence theory

The "Zone Of Influence" (ZOI) theory is based on the assumption that each individual tree exploits resources within a circular zone around its stemming point. Wherever the zones of influence of different individuals overlap, competition stresses are developed and the growth slows down or even mortality of vegetation can occur. However, the ZOI theory does not consider the variation in the strength of the influence of a tree with the variation of the distance from its stem (Berger et al., 2000).

The radius of the zone of influence of each tree is defined as:

Equation 3.5 - Radius of influence of a mangrove

$$R_{inf} = \alpha \cdot \sqrt{0.5 \cdot D}, \text{ according to Berger et al. (2000)}$$

The parameter α is taken as $10\text{m}^{0.5}$ by literature and it is the same for *Avicennia Marina* and *Avicennia Germinans* species. This parameter is subject of calibration as it is described in chapter 4.3.

The area of influence is defined as the area corresponding to the above radius:

Equation 3.6 - Area of influence of a mangrove

$$A_{inf} = \pi \cdot R_{inf}^2$$

The best way to pack circles in a plane is a well known and solved mathematical problem and can be achieved with the hexagonal packing with maximum packing density of 0.9069. Thus, the maximum number of plants that can be arranged in a specific square area with dimension dx before competition stresses start developing between them is:

Equation 3.7 - Maximum number of plants per grid cell without competition stresses

$$N_{inf} = 0.9069 \cdot \frac{dx^2}{A_{inf}}$$

This leads to an initial mangrove density of 3,000 individuals per hectare for a diameter of 1.92cm that is in accordance with van Maanen et al. (2015).

Feedback from field data:

From field data analysis, a mean number of trees per hectare is 4,664 individuals, with a mean diameter at breast height of 7.5cm and a mean height of 9.6m. These values are much higher than the ones predicted by van Maanen et al. (2015). For $D=7.5\text{cm}$, Equation 3.7 gives only 770 trees per ha.

To count for this difference, the area of influence of each tree can be reduced to allow more trees per hectare: According to Berger et al. (2000), $R_{inf} = a \cdot \sqrt{R} = a \cdot \sqrt{0.5 \cdot D}$, with 'a' a scaling factor, assumed 10. So, by changing 'a', it is possible to reach similar results with the field observations:

Using a value of $a=4.1$, for a $D=7.5\text{cm}$, the number of trees per hectare is 4580, close to the mean of 4664. With this value of a , the maximum number of trees per hectare for the initial diameter of seedlings, $D_{min}=0.4\text{cm}$ is 85900 trees. Following the thinking of van Maanen for using a value of diameter 1.92cm to

determine the maximum allowed trees per hectare, using $\alpha=4.1$, the maximum trees per hectare are 17900. However, this number is also too large compared with the maximum number from literature used by van Maanen that is 3,000. The maximum observed number of trees per hectare in the study area during field measurements in 2020 is 7,000 trees and this number is adopted for use in the model.

The above parameter settings are concluded in Table 5, comparing the field data with literature findings:

Table 5 - Comparison between vegetation parameters from literature and from field data analysis

Parameter	Theory (van Maanen, 2015)	Field data analysis
Height vs Diameter	$H = 137 + 48.04 \cdot D - 0.172 \cdot D^2$	$H = 137 + 136 \cdot D - 3.5 \cdot D^2$
Characteristics	Mangroves can reach 30m height for mature trees that can reach the age of 70 years old	maximum 10 years old trees, with $H_{\max}=14\text{m}$
Number of pneumatophores per tree $N_{pneu} = 10025 \cdot \frac{1}{1 + e^{f \cdot (D_{0.5} - D)}}$	$D_{0.5}=20\text{cm}$ and $f=0.300\text{cm}^{-1}$	$D_{0.5}=20\text{cm}$ and $f=0.274\text{cm}^{-1}$
Diameter and height of pneumatophores	$d=1\text{cm}$, $h=15\text{cm}$	$d=0.26\text{cm}$ measured $h=10\text{cm}$ assumed (no field data)
Zone of influence $R_{inf} = a \cdot \sqrt{R} = a \cdot \sqrt{0.5 \cdot D}$	$\alpha = 10$	$\alpha = 4.1$
Maximum number of trees per hectare	3,000	7,000

3.5 Biomass

The biomass of the mangroves is important because it determines both the increase of the critical shear stress and the organic deposition, as it is analyzed bellow.

The above ground (ag) and below ground (bg) biomass in kilograms as a function of the diameter of the stem in centimetres can be given as:

Equation 3.8 - Above ground biomass

$$W_{\text{tree,ag}} = 0.308 \cdot D^{2.11}$$

Equation 3.9 - Below ground biomass

$$W_{\text{tree,bg}} = 1.28 \cdot D^{1.17}$$

The above formulas are adopted by van Maanen et al. (2015) for *Avicennia Marina* and are described in its supplementary material. These formulas are chosen by Legay (2020) for use in Mflat model.

3.6 Influence on the flow

The presence of vegetation is very important for the stability of a coast, as it can increase the critical shear stress for erosion, increase the drag coefficient for shear stress, increase the bed level because of organic deposition and dissipate the wave energy (van Maanen et al., 2015).

Increase of the critical erosion shear stress

The critical shear stress is increased due to the presence of vegetation and for this study the guidelines of Mariotti et al., 2010 are followed: The increase of critical shear stress is proportional to the bellow ground biomass of vegetation following the equation bellow:

Equation 3.10 - Increase of critical shear stress due to biomass

$$\tau_{cr} = \tau_0 \cdot \left(1 + K_{cr} \cdot \frac{W_{bg}}{W_{bg,max}} \right)$$

In which ' τ_0 ' is the critical shear stress without vegetation, ' K_{cr} ' a dimensionless coefficient, ' W_{bg} ' the bellow ground biomass and ' $W_{bg,max}$ ' the maximum bellow ground biomass that can occur.

$K_{cr} = 0.1$, assumed by Mariotti et al. 2010.

The maximum bellow ground biomass, considering that the maximum amount of trees that can occur is $N_{max} = 1.5 \cdot N_{inf}$ and for the maximum stem diameter can be calculated as:

Equation 3.11 - Maximum below ground biomass in a grid cell

$$W_{bg,max} = 1.5 \cdot N_{inf} \cdot W_{bg,tree} = 1.5 \cdot \frac{0.9069 \cdot dx^2}{\pi \cdot (\alpha \cdot \sqrt{0.5 \cdot D_{max}})^2} \cdot 1.28 \cdot (D_{max} \cdot 100)^{1.17}$$

Increase of drag coefficient

Following the work of Mazda et al. (1997), a vegetation length scale can be defined, for the control volume of Figure 16, as:

Equation 3.12 - Definition of vegetation length

$$L = \frac{V_c - V_v}{A_v}$$

In which ' V_c ' is the control volume ($dx \cdot dx \cdot$ water depth), ' V_v ' is the vegetation volume (stem plus pneumatophores) and ' A_v ' is the projected area of vegetation on the flow (stem plus pneumatophores).

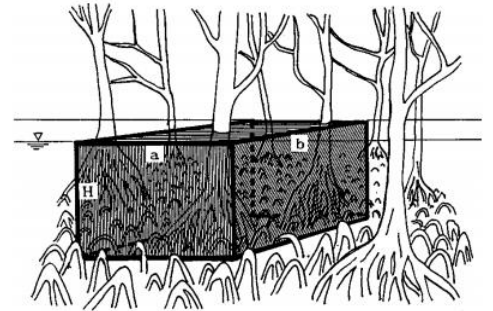


Figure 16 - control volume, Mazda et al. 1997

The vegetation length depends on the mangrove species that can define the relationship between the vegetation volume, the projected area and the water depth.

Then, the drag coefficient is related with vegetation length using the Equation 3.13:

Equation 3.13 - Increase of drag coefficient due to vegetation

$$C_{D,veg} = C_{D0} + \frac{e}{L}$$

The parameter 'e' is set to e=5m. This assumption is made by van Maanen et al. (2015) – supplementary material for *Avicennia Marina* mangrove species and is adopted for this study as no further information is available to modify and calibrate it.

For the above consideration, it is assumed that the water level does not reach the canopy of mangroves. This could be a realistic assumption (except of the very young trees) as mangroves are mostly developed above the MSL in the study area and the maximum water level due to tide variation is +1.5m.

Increase of bed level by organic deposition

According to Mariotti et al. (2010), the organic deposition can be calculated as:

Equation 3.14 - Organic deposition formula (literature)

$$Z_{org} = k_b \cdot \frac{W}{W_{max}}$$

In which $k_b=9\text{mm/year}$ and 'W' refers to the above ground biomass.

In this study, following the supplementary material of van Mannen et al. (2015), a similar formula is used by Legay (2020) but for the bellow ground biomass and for $K_{org}=1\text{mm/year}$:

Equation 3.15 - Organic deposition formula (used)

$$Z_{org} = K_{org} \cdot \frac{W_{bg}}{W_{bg,max}}$$

This formula is used for this study as no further information is available to judge about the biomass choice or to calibrate the organic deposition coefficient ' K_{org} '.

Dissipation of wave energy due to vegetation

An extra term in the equation of dissipation of wave energy is added, due to the presence of vegetation, according to van Rooijen et al. (2015), as described by Equation 3.16.

Equation 3.16 - Wave energy dissipation due to vegetation

$$D_v = \frac{1}{2 \cdot \sqrt{\pi}} \cdot \rho \cdot \hat{C}_D \cdot D \cdot \frac{N}{dx^2} \cdot \left(\frac{k \cdot g}{2 \cdot \omega}\right)^3 \cdot \frac{\sinh^3(k \cdot H_{uw}) + 3 \cdot \sinh(k \cdot H_{uw})}{3 \cdot k \cdot \cosh^3(k \cdot h)} \cdot H_{rms}^3$$

In Equation 3.16, 'D' is the vegetation diameter at breast height, 'k' is the wave number, 'g' the gravitational acceleration, 'ω' the wave frequency, 'h' the water depth, ' H_{uw} ' the underwater vegetation height and $\hat{C}_D = 0.4$ the bulk drag coefficient after calibration of van Rooijen's model. The bulk drag coefficient is a completely different parameter from the drag coefficient used for the calculation of shear stresses mentioned above and it's only a subject of calibration, depended on the kind of mangrove species of vegetation.

The above formula counts for both the stem and the pneumatophores contribution to wave energy attenuation, as ' H_{uw} ' is calculated for both of them. However, this formula does not count for canopy contribution to wave energy dissipation. This contribution can become important when the water depth is increasing (due to the combination of tide and storm surge) and reaches the canopy (Mclvor et al., 2012), but there is still not enough information on literature about how to quantify canopy, depending also on the age of the tree, so this effect is neglected for this study.

3.7 Vegetation dynamics

Vegetation dynamics are very important for the long term evolution of a coast as they can determine how representative can be the characteristics of vegetation. To define vegetation dynamics, four different processes are considered:

- The initial establishment of vegetation
- The establishment of new vegetation every year
- The growth of vegetation
- The mortality of vegetation

An important factor that drives the vegetation dynamics is the inundation and competition stresses that vegetation experiences. These stresses can define how favourable are the conditions for vegetation to be established and grow. In case of high stresses, vegetation stops growing and after a period dies.

Inundation stress

Inundation stress determines the stress that a mangrove tree experiences due to the period when the area around its stem is flooded and breathing is restricted. According to van Maanen et al. (2015), the inundation stress can be defined by Equation 3.17.

Equation 3.17 - Inundation stress

$$I = \begin{cases} a \cdot P + b \cdot P^2 + c & \text{for } P < 0.6 \\ 0 & \text{for } P \geq 0.6 \end{cases}$$

'P' represents the hydroperiod, the percentage of time that the area around the mangrove tree is submerged under water level and is given by Equation 3.18.

Equation 3.18 – Definition of hydroperiod

$$P = \frac{T_{\text{inundated}}}{T_{\text{tide}}}$$

a=4, b=-8, c=0.5, according to the supplemented material of van Maanen et al. (2015).

Competition stress

Competition stress is the stress that a mangrove tree experiences due to the presence of other individual in its vicinity and it is defined by van Maanen et al. (2015) using the Equation 3.19:

Equation 3.19 - Competition stress (literature)

$$C = \frac{1}{1 + e^{d \cdot (B_{0.5} - B)}},$$

In which 'B' is the total biomass and 'B_{0.5}' is the value of 'B' that gives C=0.5. 'd' is a constant set to -0.00005.

For C = 1 mangroves grow without any competition stress, while for C = 0.5 they grow with high competition and at this point is defined the limit for mortality.

To be able to model the above stresses, Legay (2020) uses a sigmoid function assuming that the competition stress is a function of the number of plants 'N' and that for $N = N_{inf}$, $C = 0.9$ and for $N = 1.5 \cdot N_{inf}$ the competition stress reach the level of mortality and $C = 0.5$.

Thus, competition stress is modelled using the Equation 3.20:

Equation 3.20 - Competition stress (used)

$$C = \frac{1}{1+e^{d \cdot (N-1.5 \cdot N_{inf})}}, \text{ with } d = \frac{\ln(9)}{N_{inf}} \cong \frac{4.39}{N_{inf}}$$

The above formulas about competition stresses are kept unchanged for this study as no further information that could define them more precisely is available for the study area. The control of the stresses for every grid cell is done by the model on a monthly basis.

Growth of vegetation

Based on the theory of Berger et al. (2000), which is also used by van Maanen et al. (2015), the growth of vegetation can be represented by the growth of the diameter at breast height with the following formula:

Equation 3.21 - Vegetation growth formula

$$\frac{dD}{dt} = \frac{G \cdot D \cdot \left(1 - \frac{D \cdot H}{D_{max} \cdot H_{max}}\right)}{274 + 3 \cdot b_2 \cdot D - 4 \cdot b_3 \cdot D^2} \cdot I \cdot C$$

'G' is a growth constant given by Berger et al. (2000) for *Avicennia Germinans* as 162, 'D' is the diameter at breast height in meters, 'H' the height of vegetation in meters, 'b₂' and 'b₃' coefficients as defined in chapter 3.1, 'I' the inundation stress and 'C' the competition stress.

The growth is calculated for every time step and in every grid cell that there is already vegetation and vegetation. Diameter of vegetation increases following the Equation 3.21.

After the calibration procedure it was found that for $G = 162$, after 10 years of growing, vegetation is unable to reach the observed heights. To approximate the field measurements, the growth constant is set to the value of $G = 750$ as explained in chapter 4.3. This is another probable consequence of the fact that vegetation was planted having thinner and higher stems compared to the naturally developed vegetation, as explained in chapter 3.2.

Establishment of initial vegetation

The initial vegetation is added after an entire tidal cycle, as this is necessary to be able to calculate the hydroperiod P. Vegetation is developed only if $P < 0.5$. The initial diameter normally is selected randomly from the range of the possible diameters that can be found in the field and the height is calculated accordingly.

The threshold of $P=0.5$ for the development of vegetation is a common used threshold, also adopted by van Maanen et al. (2015).

In Guyana case, vegetation was established during the mangrove restoration project of 2011, so for this study the initial vegetation has the same diameter in all the grid cells. This diameter is chosen to be $D_{ini}=1.0\text{cm}$

Furthermore, vegetation was established in a certain width for Guyana case. This width, was about 100m and only for this width it is allowed by the model the initial establishment of vegetation, in case of $P < 0.5$. After the 10-years simulation analyzed in chapter 4.3, it appears that the restriction of the 100m is stricter than the one of $P < 0.5$.

The probability that vegetation is initially established in a grid cell is assumed to be 80% (no field data or literature findings on this, but as vegetation is planted, it is assumed a high probability).

Establishment of new plants

It is assumed that every no-vegetated grid cell has a probability to be vegetated, if the hydroperiod is lower than 0.5. The initial number of plants is set to $N = 1.5 \cdot N_{inf}$ (50% more than the ideal number for no competition stresses) and their diameter to the seedling diameter: $D_{seedling} = 0.4\text{cm}$.

The probability that vegetation is developed in an empty grid cell is taken as 10%. New vegetation is chosen to be established after the hydroperiod check every three months. There are no field data or literature findings on how to define this probability or on how often is the optimum for the model to establish new vegetation, but this choice is tested and gives representative results as analyzed in chapter 4.3

An aerial view of the study area after 9 years of vegetation development is shown in Figure 17. The difference with the initially established vegetation is obvious if compared with Figure 13.



Figure 17 - Aerial picture of the study area of 2020 (taken by Üwe Best). The growth of initial vegetation is visible as well as the establishment of new vegetation, compared with Figure 13 that refers to the same location at 2012.

Mortality of vegetation

Vegetation is assumed that can die because of one of the following reasons:

1. Combination of high inundation and competition stresses: If the product of the two stresses calculated as above is lower than 0.5, there is no more vegetation growth (van Maanen et al., 2015), and a number of plants can die:

Equation 3.22 - Number of trees that die due to stresses (literature)

$$N_{\text{death}} = N \cdot (0.6 - I \cdot C)$$

This check is applied once per month.

After the calibration procedure it is found that too much vegetation dies because of the stresses and almost no initial vegetation is left after 10 years of modeling. This is not the case for Guyana coast, as the largest part of the initial vegetation is still alive. Thus, the amount of trees that die due to stresses is reduced and the Equation 3.22 is modified as:

Equation 3.23 - Number of trees that die due to stresses (used)

$$N_{\text{death}} = N \cdot (0.5 - I \cdot C)$$

2. High deposition rates: According to Ellison, 1998, a sudden high deposition of mud on the mangroves can lead to their death. The threshold limit is hard to be identified, but a reasonable limit for *Avicennia Germinans* species could be 15cm, a value that is in the order considered by Ellison, 1998. So, if this happens in one time step for a grid cell, then vegetation in this grid cell dies.
3. High erosion rate: If the erosion in a grid cell since the birth of vegetation becomes higher than the 50% of its current height, vegetation dies. This percentage is an assumption, as no relevant literature was able to be found, but the phenomenon is known (Toorman et al., 2018).

Even for storm conditions, as presented in chapter 6, bed level changes are very small, so only the first criterion about death due to stresses is finally active for Guyana case.

3.8 Impact of extreme events on vegetation

An extreme hydrodynamic event can result in damage of vegetation with various ways: Uprooting due to wind, breaking of branches or stems, defoliation of the canopy, death due to high erosion when roots are uncovered or death due to high deposition, when aerial roots are buried by sediment and the tree is unable to breathe (Smith et al., 2009).

In Mflat model only the death by erosion, deposition and stresses is included, as described in chapter 3.7, but for this death to occur it is necessary for the extreme event to result in remarkable bed level changes where vegetation is present. The mortality due to high stresses is not relevant for the extreme event case, as the duration of the event is too short for a probable high inundation stress to damage vegetation (the update of stresses is on a monthly base). According to other death mechanisms (branch breaking, uprooting, defoliation), literature sources are not enough yet to be able to be quantified and described in the model code expecting a reliable result. However, the extreme hydrodynamic conditions expected in Guyana, as analyzed in chapter 2.3 can be compared with other extreme cases worldwide that have already been studied according to their impact on vegetation.

Servino et al. (2018) studied the impact of an extreme hailstorm on June 2016 at southeast Brazil, with wind gusts of 100km/hour (double the extreme wind expected in Guyana). The damage of mangroves at the impacted areas was from 59% to 89%. Areas with severe damages (more than 75%), one year after the storm, were further degraded while areas with moderate damages (50% to 75%) started recovering. However, this damage is also related with the presence of hail and with the previous long drought period before the hailstorm occurred.

Various studies have been done about the impact of hurricanes on mangrove vegetation. However, all these studies refer to events much more severe than the extreme storm expected in Guyana coast. The mildest hurricane, Category 1 of Saffir-Simpson system, starts with winds above 119 km/hour (Krauss et al. 2020), which is a wind velocity more than the double of the most extreme one expected in Guyana (50.4km/hour). For category 1 hurricanes, not much damage is expected on vegetation.

Wind is not the only factor that can determine the amount of damage on a mangrove forest because of a hurricane. There are mangrove species that are more resilient to extreme events (*Avicennia Germinans*, *Laguncularia Racemosa*) than others (*Rhizophora Mangle*) and the trajectory of the hurricane compared with orographic positioning could also be important. Another parameter that can determine the amount of damage is the structure of the mangrove forest: Smaller mangroves trees in a less dense arrangement could be more resilient than very dense and high mangrove forests (Krauss et al. 2020).

3.9 Summary of vegetation

Research that has already been done on vegetation can give valuable information on how to quantify vegetation dynamics and their impact on the flow and on the bed level morphology. The complexity of the processes is realized by the variety of formulas and calibration coefficients that are used to describe the behaviour and the development of vegetation. However, using the current knowledge and reasonable assumptions based on literature findings as analyzed in this chapter, it is possible to simulate most of the processes around vegetation and create a bio-geomorphological model that describes the full interaction between vegetation, hydrodynamics and morphodynamics. This model is further analyzed and calibrated in the following chapter, before being used for the test cases.

4 Model calibration

Calibration is an important intermediate step after defining the theoretical framework of a study and before using the model for the test cases. The model is calibrated for two different cases: First the calibration of sediment parameters takes place for a simulation of 40 years with normal hydrodynamic conditions and without vegetation to succeed a profile in equilibrium. Then, using the set-up of parameters of this calibration, vegetation parameters are further calibrated for a simulation of 10 years to succeed similar results with field observations. Then, the model is considered to be ready for use.

4.1 Importance of calibration

Scientists in their effort to understand natural processes and predict their outcomes make experiments and create models using the calculation power the technology offers to them. Due to the complexity of natural systems, in most of the cases it is impossible to create formulas and mathematical relations that can represent exactly natural processes. To overcome this problem, scientist use coefficients in which it is hidden a part of uncertainty and of inability to be precise. The procedure to determine the appropriate coefficients and to adjust the mathematical formulas for a specific case in order to be able for a model to approach natural processes is usually referred to as “calibration”.

The importance of calibration for the subsequent progress of a study is great, since it can determine the accuracy of further results or how representative these results are for the desirable case. The scope of calibration is to make the model able to reproduce an already known condition that is similar, but not the same with the unknown condition that researchers want to test. There are various methods to calibrate a model, with inverse modeling being a famous, but a complex one, because of problems of insensitivity, non-uniqueness and instability and because sometimes the inverse process is also complex and unknown as the strait-forward one (Hill, 1998). For this study, another maybe more famous method is used: The trial and error. Thus, different trials are tested in the model, judging from the error the parameters are modified and tested again, until the desirable result is reached.

4.2 Hydrodynamic and sediment dynamic calibration

To calibrate the hydrodynamic parameters of the model, only the 1970 bathymetry profile is used as analyzed in chapter 2.1. The calibration simulations are applied for 40 years, from 1970 to 2010, as in 2011 took place the Mangrove Restoration Project with the plantation of new vegetation in the study area. The aim of calibration is to keep the 1970 profile stable through the decades, as it is expected to be without the impact of mudbanks, resulting in a set of parameters that can keep the profile in equilibrium.

The parameters that influence the response of the profile and are subject of calibration are presented in Table 6 and analyzed below.

The parameter ‘wdf’:

The wave dissipation factor ‘ f_w ’ acts for two different cases in the model:

To calculate the shear stress due to the wave action, as shown by Equation 4.1:

Equation 4.1 - Wave induced shear stress

$$\tau_w = 0.5 \cdot \rho \cdot f_w \cdot u_{orb}^2$$

And to calculate the wave energy dissipation due to friction, as shown by Equation 4.2:

Equation 4.2 - Wave energy dissipation due to friction (initial)

$$D_f = \rho \cdot f_w \cdot |u_{rms}|^3$$

Through the calibration process, too much landward deposition is observed. For that reason, the two functions of 'f_w' are separated to be able to change them differently: 'f_w' remain for the calculation of wave induced shear stress connected with 'k_b' as initially is set in the model, but a new parameter, the 'wdf' (wave dissipation factor) is used for the calculation of wave energy dissipation due to friction 'D_f', as shown by Equation 4.3:

Equation 4.3 - Wave energy dissipation due to friction (final)

$$D_f = \rho \cdot wdf \cdot |u_{rms}|^3$$

By this way and by setting $wdf < f_w$ it is possible to achieve less dissipation of wave energy by keeping the same effect of waves on shear stress. Thus, wave action is higher landward than before and more erosion can occur there.

However, finally, it appeared that it is better not to use the 'wdf' parameter with a different value than the 'k_b' parameter as this serves better the formation of an equilibrium profile after a lot of simulation trials.

Table 6 - Parameters that are subject of calibration with the symbols used in Mflat code

Parameter	Explanation	Units	Use in the model
u₁₀	wind velocity	m/sec	Energy input to the wave energy balance
bcs	sediment concentration at the sea boundary	kgr/m ³	To calculate initial sediment concentrations and the feed of sediment during floods tide
ww	settling velocity of the sediment	m/sec	$depo = ww \cdot concentration$ to calculate deposition
taucr	critical shear stress for erosion	Pa	$ero = MM \cdot (\tau - \tau_{cr})$ to calculate erosion
MM	erosion factor	Kgr/m ² /sec	$ero = MM \cdot (\tau - \tau_{cr})$ to calculate erosion
Ch	Chezy friction factor	m ^{1/2} /sec	$C_d = \frac{g}{Ch^2}$ for drag coefficient to calculate the shear stress
HH	root mean square wave height	m	$E = \frac{1}{8} \cdot \rho \cdot g \cdot H_{rms}^2$ for the wave energy equation
Tpp	peak wave period	sec	In various equations for the wave energy calculations
gamma	breaking index	-	For the calculation of energy dissipation due to wave breaking
kb	wave friction related parameter	-	For calculation of f _w , the wave friction factor
wdf	wave dissipation factor due to bed friction	-	New parameter explained in this chapter
fmd	dissipation of energy due to fluid mud	-	New parameter explained in this chapter

The parameter 'fmd':

Fluid mud is an important factor that can dissipate significantly the wave energy. In the field of Suriname and Guyana, a dissipation of wave energy of up to 96% with a dissipation of more than 70% of wave height has been observed. The study of Winterwerp et al. (2007) using the SWAN model shows a "fairly constant" dissipation of energy towards the coast, a strong decrease of the wave period and an additional decrease of wave height due to fluid mud in the order of 50% from the depth of 25m to the depth of 5m.

Because of the importance of fluid mud on energy dissipation, it is initially considered as a necessary step to find a way to include it in Mflat code. The complexity of this interaction between the waves and the fluid mud layer, with the formation of internal waves in the interface of water with the fluid mud layer is such that an analytical mathematical description would be difficult to be established in Mflat and would be beyond the scope of this study. To overpass this complexity, a very simple parameter, the 'fmd' (fluid mud dissipation) is used in the wave energy dissipation equation that acts in every spacial step of the model:

Equation 4.4 - Energy dissipation due to fluid mud

$$E(x + 1) = (1 - fmd) \cdot E(x)$$

By this way, the 'fmd' can reduce the wave energy with a very small percentage, but in every spacial step, so in a large domain the total dissipation can be significant, as shown in Figure 18.

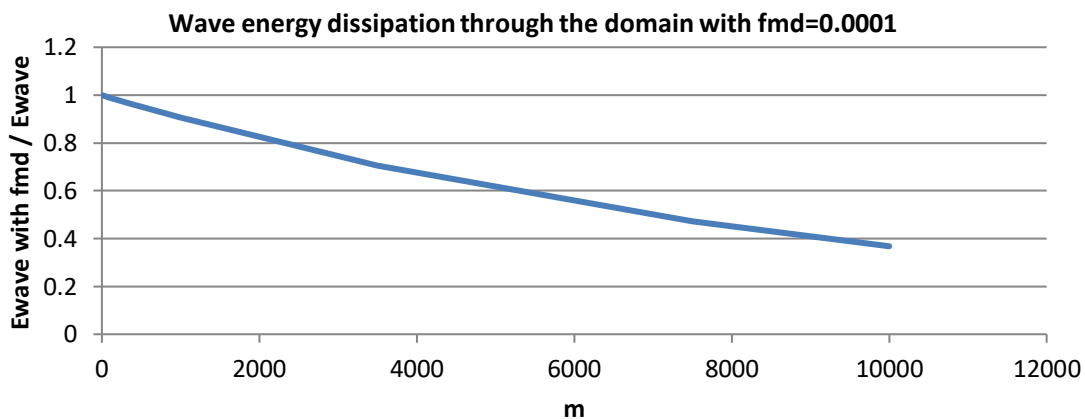


Figure 18 - Impact of fmd on wave energy through the domain for fmd=0.0001

The modification of the code to apply 'fmd' with the above explained way is done and the parameter is used during calibration procedure but finally it is set to zero, because:

- The wave height that is finally adopted is already quite low, so a further dissipation would make it unrealistically low.
- There is a need to dissipate less the wave energy through the domain, to be able to have relatively higher wave action landward. This is the reason of the new parameter 'wdf', as explained above. So, another parameter like 'fmd' that would enhance dissipation, especially landward, would rather make it more difficult the desirable equilibrium profile than contributing to it.

Gradual fixing of parameters:

The above mentioned parameters presented at Table 6 are 12 in total. To modify all of these parameters simultaneously and to test different combinations of them is something very difficult that can result to misleading. Thus, a gradual fixing of the above parameters is adopted according to the uncertainty on their values and on the influence they have on the profile, during the testing of different combinations.

The first parameters fixed are those of the hydrodynamic input: The wave height, the wave period and the wind velocity. These parameters are considered as representative parameters for the long term normal hydrodynamic conditions of Guyana coast at a location 3.5 km offshore with a water depth of 2m below mean seal level. The values chosen, as explained in chapter chapter 2.2 are:

$$u_{10} = 8.9\text{m/sec}$$

$$H_{rms} = 0.2\text{m}$$

$$T_p = 3\text{sec}$$

Breaking index 'γ' depends on bottom slope and wave steepness and various formulas have been created to be able to calculate it. Very gentle slopes, like the slopes found on mudflats, are connected with spilling breaking waves and a good approximation for breaking index for this type of waves is $\gamma=0.6$ (Kuznetsov et al., 2017). So this parameter is fixed to 0.6 because of the above clear literature reference.

The Chézy coefficient 'Ch' is a subject of calibration: A typical value for Chézy coefficient for muddy beds is 80 to 100 $\text{m}^{0.5}/\text{sec}$ (van Rijn, 2018). The 'Ch' determines the value of drag coefficient with which the shear stresses are calculated. The starting point for 'Ch' is 80 $\text{m}^{0.5}/\text{sec}$, but a lower value showed that a smoother slope closer to the observed one is possible to be achieved. Thus, a value of $\text{Ch}=60 \text{ m}^{0.5}/\text{sec}$ is chosen for the model.

Critical shear stress is an important parameter for determining the erosion, as it is directly connected with it. According to van Rijn 2020, for weakly consolidated mud beds with a dry bulk density of $\rho_{\text{bulk}} < 400 \text{kg}/\text{m}^3$, the critical shear stress is in the order of $0.2 \pm 0.15 \text{Pa}$, while for firmly consolidated mud beds with a dry bulk density of $\rho_{\text{bulk}} > 800 \text{kg}/\text{m}^3$, the critical shear stress is in the order of $1 \pm 0.5 \text{Pa}$. In Guyana case, $\rho_{\text{bulk}} > 800 \text{kg}/\text{m}^3$ but it couldn't be claimed that the mud is firmly consolidated, especially the upper layer that is subjected to erosion, because of the high dynamic tidal and wave environment that keeps sediment in motion. So, a value in the order of $\tau_{\text{cr}} = 0.2 \text{ Pa}$ is tested for calibrating the model.

The erosion factor 'M', usually referred also as "erosion rate parameter" is a calibration parameter that connects the shear stress that is above the critical one with the erosion. It may vary with time and depth but in most of the cases it is kept constant. The typical values for 'M' are $0.1 \cdot 10^{-4} < M < 5 \cdot 10^{-4} \text{ kg}/\text{m}^2/\text{sec}$ (Winterwerp et al., 2012). The initial value of M is set to $M = 1 \cdot 10^{-4} \text{ kg}/\text{m}^2/\text{sec}$.

Sediment concentration is calculated by the model, according to the hydrodynamic conditions in each spacial and time step. The input in the model is the boundary sediment concentration seaward. According to the study of Wells et al. (1981) in Suriname coast the typical sediment concentration is in the order of some thousands of mgr/lt . This is in accordance with the study of Winterwerp et al. (2007) about Guyana coast. As in calibration trials the influence of the mudbank is neglected on sediment supply, an initial value of $0.1 \text{kg}/\text{m}^3$ is used.

Settling velocity is a parameter depended on the type and the percentage of mud (the particle size and the structure formation), the sediment concentration (that leads to hindered or not hindered settling) and the degree of flocculation, if present. The degree of flocculation depends on the sediment concentration and on salinity. Higher concentration and higher salinity favor flocculation. For Guyana case, sediment concentrations are in the order of some hundreds of mgr/lt , so there is no hindered settling. Flocculation it may exist as the water is saline but is not intense as the concentration is not too high. The average percentage of mud is 99.2% and the average percentage of organic content is 4.32% by field measurements. According to a literature and experiments review by van Rijn (2020), settling velocity for the characteristics of Guyana coast is in the order of 0.1 to 0.4 mm/sec if there is no flocculation and in the order of 1 mm/sec in case of weak flocculation. An initial value of 0.3 mm/sec is used. However, settling velocity is further increased as it turned out to be an important parameter to keep the profile in equilibrium.

Diffusion coefficient 'Dif' is a parameter in the advection diffusion equation used in Mflat model to calculate the cross-shore sediment transport in combination with bed interaction (Equation 4.5). To be able to have a stable profile, the criterion for diffusion coefficient, according to Rogers et al. (2002), is $\text{Dif} \cdot \text{dt}/\text{dx}^2 < 0.5$. After some trials, the diffusion parameter is set to $\text{Dif} = 1.5$, a value that satisfies the above conditions, for $\text{dt}=5\text{sec}$ and $\text{dx}=10\text{m}$ that is the setup for this study.

Equation 4.5 - Advection - diffusion equation

$$\frac{\partial hc}{\partial t} + \frac{\partial uhc}{\partial x} - \text{Dif} \cdot \frac{\partial h \cdot \frac{\partial c}{\partial x}}{\partial x} = \text{ero} - \text{depo}$$

The cross-shore flow case

The calibration process is focused on the cross-shore flow case, because for this case it is possible to create a very stable profile. The stability of the profile after calibration is considered to be very important as only with an initially stable profile it is possible to have a clear result on the impact of vegetation or extreme events on the profile without misunderstanding by changes that run in parallel due to the normal hydrodynamic processes. Thus, the cross-shore flow case simulation it may not be able to represent all the processes that take place in a coastal mudflat, but the equilibrium profile that it produces is very useful for continuing this study effectively.

After a lot of “trial and error” simulations, by first fixing the hydrodynamic conditions and then gradually the sediment parameters and the calibration coefficients, the final set of parameters chosen is presented in Table 7 below.

Table 7 – The set of parameters that can result in an equilibrium profile for the cross-shore flow case

Parameter	Explanation	Units	Value chosen after calibration
MF	morphological factor	-	100
u₁₀	wind velocity	m/sec	8.9
HH	root mean square wave height	m	0.2
Tpp	peak wave period	sec	0.3
bcs	sediment concentration at the sea boundary	kgr/m ³	0.1
ww	settling velocity of the sediment	m/sec	0.0012
taucr	critical shear stress for erosion	Pa	0.18
Ch	Chézy friction factor	m ^{1/2} /sec	60
gamma	breaking index	-	0.6
fmd	dissipation of energy due to fluid mud	-	0
kb	wave friction related parameter	-	0.001
wdf	wave dissipation factor due to bed friction	-	0.001
MM	erosion factor	Kgr/m ² /sec	1*10 ⁻⁴

Using the above parameter set-up, the result is shown in Figure 19. The initial, blue line profile is the one of 1970. Then, the evolution of the profile for every decade is presented. It is shown that this set of parameters, is able to create an almost stable profile through the decades of simulation. This is the reason why the above combination is adopted for the next steps of this study although some parameters are a bit out of literature range, like the low Chézy factor and the high settling velocity. Especially for settling velocity, the value of 1.2mm/sec it could be an upper limit for the case of mild flocculation that could be present in the saline water with concentrations up to 0.3kgr.m³ that appear through the domain during a tidal period.

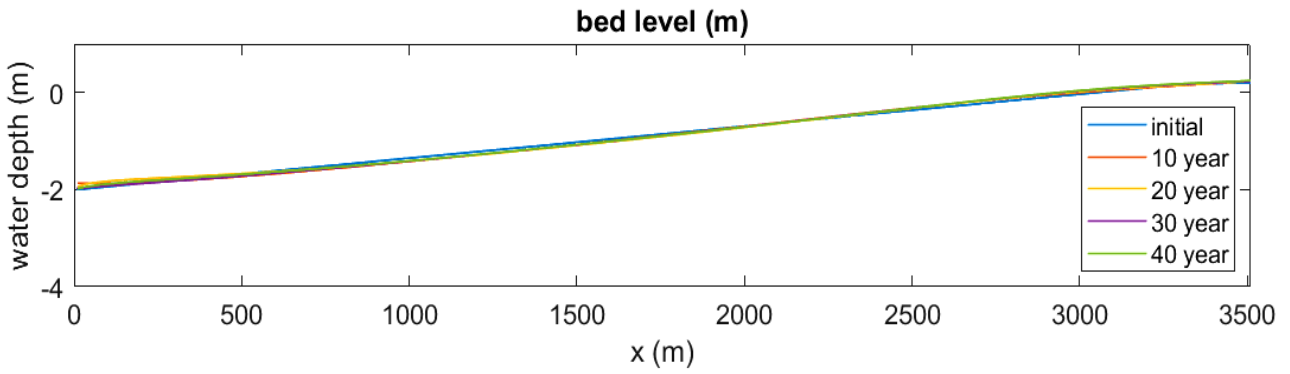
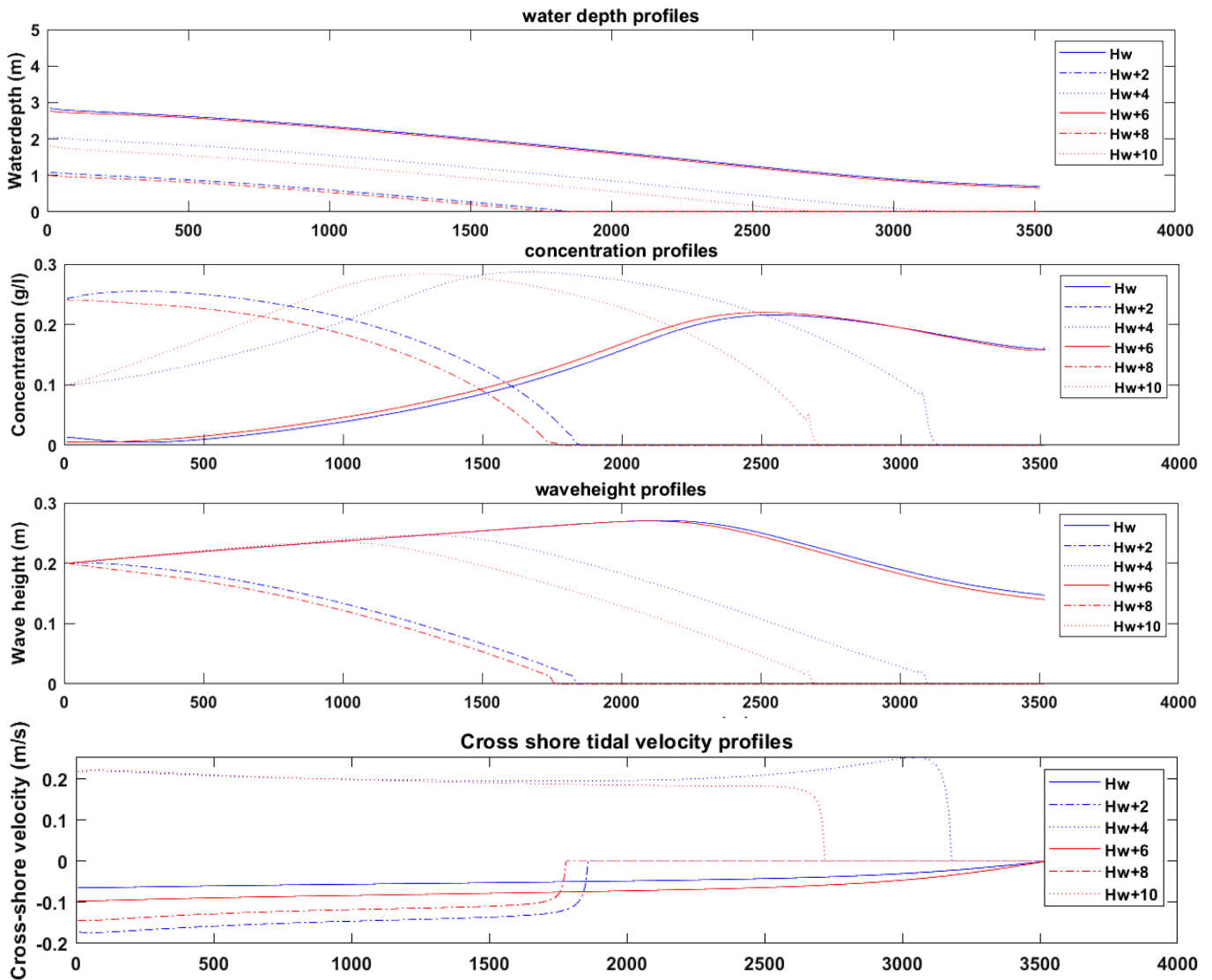


Figure 19 - The evolution of the initial 1970 profile (blue line) through the decades for 40 years of simulation for the cross-shore flow case. Different lines, representing different decades are almost on top of each other, showing a profile in equilibrium.

Other important parameters of the simulation, like the variation of the water depth profile, the suspended sediment concentration, the wave height, the cross-shore flow velocity and the total shear stress are presented in Figure 20 to give a sense of their range during a 12-hour tidal period at the end of the 40 years simulation period.



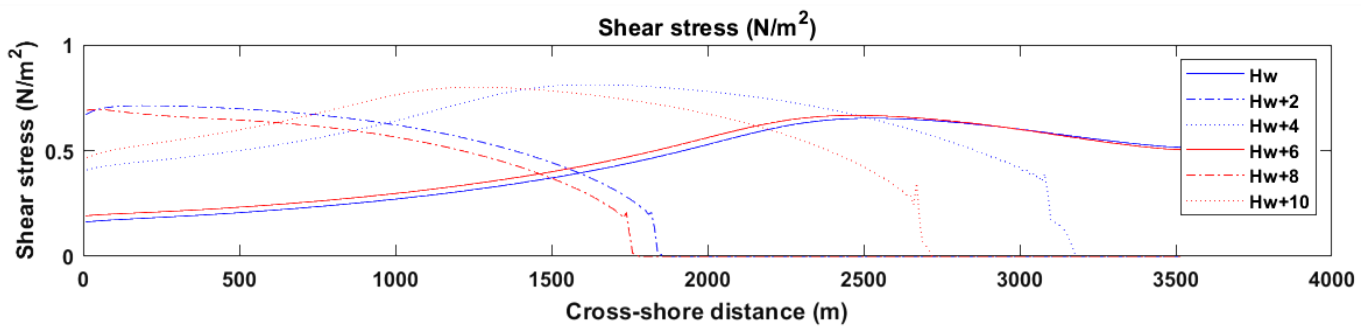


Figure 20 – The range of water depth, sediment concentration, wave height, cross-shore flow velocity and shear stresses during a 12-hour tidal period with 2-hours intervals at the end of the 40 years simulation time for the cross-shore flow case.

Comparison between the cross-shore and the alongshore case

The same set of parameters presented in Table 7 is used for a simulation including also the alongshore flow due to tide described by van der Wegen et al. (2019), to indicate the differences between the two cases. The alongshore velocity mobilizes more sediment than only the cross-shore velocity. The suspended sediment is either transported to the onshore by flood tide and remains there due to milder hydrodynamic conditions resulting in more accretion landward or leaves the profile during ebb tide resulting in more erosion seaward, where hydrodynamic conditions are stronger, as shown in Figure 21:

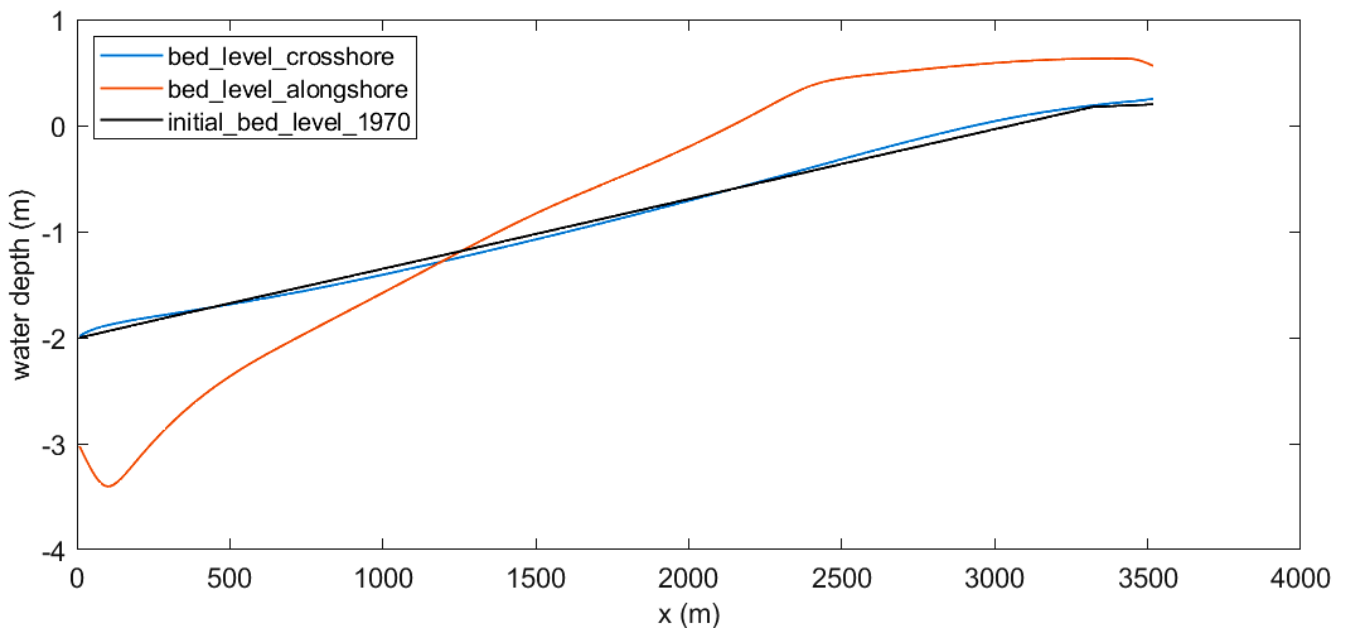


Figure 21 – Comparison of bed level profiles between the cross-shore flow case (blue line), the cross-shore plus alongshore flow case (red line) and the initial profile (black line) after 40 years of simulation using the parameters of Table 7

The evolution of the profile through the decades for the alongshore case is presented in Figure 22. Probably, a different set of parameters could result in a profile closer to the initial one of the 1970 and in a higher stability but this would double the work of calibration, sensitivity analysis and maybe of the extreme scenarios testing so it is not included in this study. The cross-shore flow case is chosen because, by using a reasonable set of parameters in the range proposed by literature for the characteristics of Guyana coast, it is possible to create a profile in equilibrium.

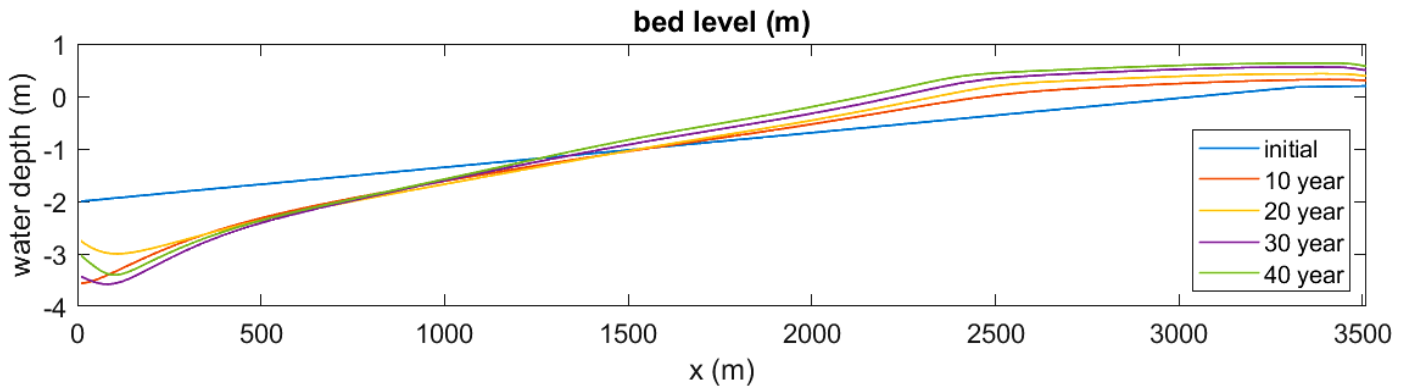


Figure 22 - Evolution of the profile through decades for the alongshore flow case. With blue line it is presented the initial bed level and with different colors it is presented different decades.

4.3 Vegetation calibration

Hydrodynamic and sediment dynamic calibration results to a set of parameters that allows the model to reproduce a profile in equilibrium. The next step before testing the extreme events is to calibrate vegetation parameters to be able to have simulation results from the model that are close to field observations. The input profile for the vegetation cycle of calibration is the 1970 profile as this profile is made to be in equilibrium. The vegetation parameters used for this process are based on the analysis of chapter 3 and are presented in the third column of Table 8 below, compared with the literature proposition in the second column:

Table 8 - Vegetation parameters used for the 10 years simulation (third column) compared with literature data (second column)

Parameter	Theory (van Maanen et al., 2015)	Field data analysis and calibration feedback
Height vs Diameter	$H = 137 + 48.04 \cdot D - 0.172 \cdot D^2$	$H = 137 + 136 \cdot D - 3.5 \cdot D^2$
Characteristics	Dmax = 40cm Hmax = 17.8m	maximum 10 years old trees, with Hmax=14m
Number of pneumatophores per tree $N_{pneu} = 10025 \cdot \frac{1}{1 + e^{f \cdot (D_{0.5} - D)}}$	$D_{0.5}=20\text{cm}$ and $f=0.300\text{cm}^{-1}$	$D_{0.5}=0.20\text{cm}$ and $f=0.274\text{cm}^{-1}$
Diameter and height of pneumatophores	d=1cm, h=15cm	d=0.26cm measured h=10cm assumed (no data)
Zone of influence $R_{inf} = a \cdot \sqrt{R} = a \cdot \sqrt{0.5 \cdot D}$	$\alpha = 10$	Initial value for calibration: $\alpha = 4.1$ final used after calibration: $\alpha = 6.0$
Maximum number of trees per hectare	3000	7000
Seedling parameters	No dealing with so low vegetation. Only for $H > 1.37\text{m}$	$H=0.3425\text{m}$ $D=0.004\text{m}$ renewal every 3 months
Growth factor G	162	Initial value for calibration: 300 Final used after calibration: 750
Death due to stresses	$N_{death} = N \cdot (0.6 - I \cdot C)$	$N_{death} = N \cdot (0.5 - I \cdot C)$
Probability of initial vegetation to occur	No data	80%
Probability of new vegetation to occur every 3 months	No data	10%

The calibration procedure for vegetation aims to reproduce the observed vegetation 10 years after the mangrove restoration project. As a criterion for the quality of the produced results is used the density of vegetation (i.e. the number of plants per grid cell), the diameter and the height of vegetation, as well as the extend of vegetation after 10 years of simulation.

Some of the parameters determined in chapter 3 are modified further to succeed a simulation that is close to the natural process during the last 10 years in Guyana coast. As shown in Table 8, the modified parameters is the growth coefficient 'G' that is increased significantly to allow vegetation to grow till the observed height and the parameter 'α' that indicates the zone of influence of each mangrove tree which is increased to increase the influence of mangroves and thus decrease the number of plants per grid cell.

Vegetation is created initially in the first 100m of the profile (3,400m – 3,500m) as it was planted in 2011 and then it is free to develop under the normal hydrodynamic forcing and with the parameters presented above for 10 years. The result, after 10 years of simulation is shown in Figure 23. Through the years, vegetation is quite dynamic in the zone between 3,100m and 3,500m (at the last 400m of the profile) with its average height and diameter continuously growing and the number of plants gradually decreasing. Sometimes death of vegetation takes place at some grid cells due to competition stresses. This is the reason of having lower vegetation at the landward end. Vegetation is also present but not very developed in the zone between 2,800 to 3,100m, where it is generated but it doesn't manage to develop a lot due to higher inundation stresses.

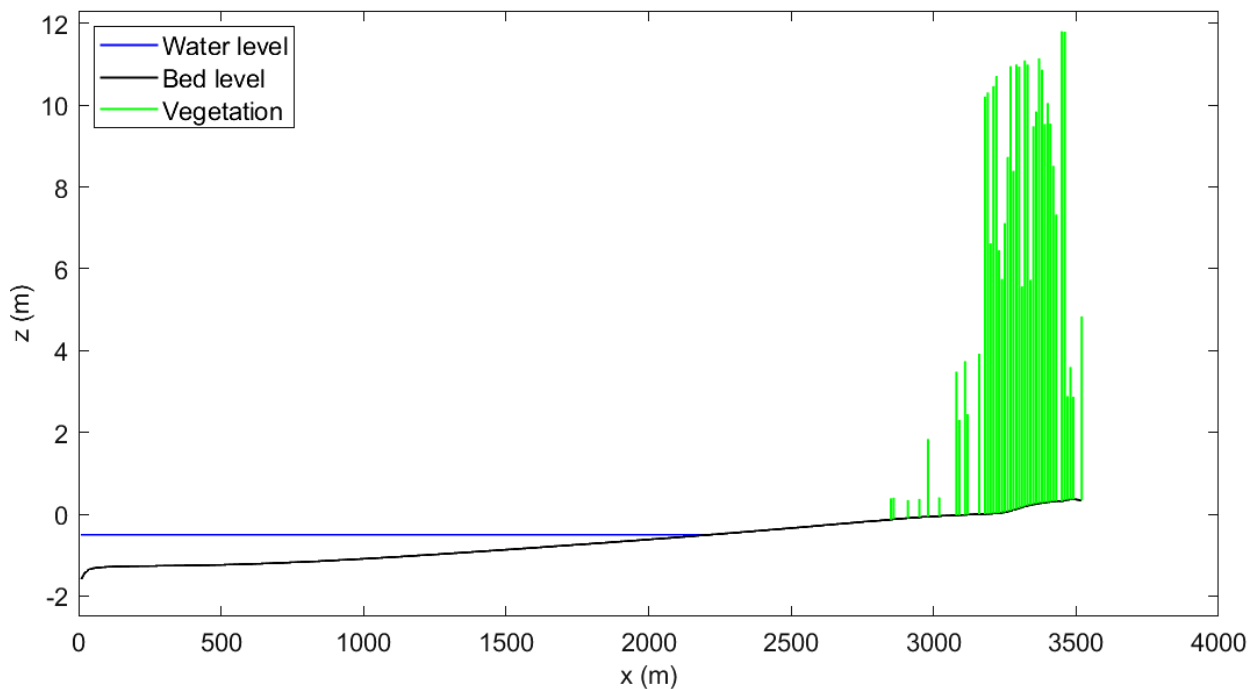


Figure 23 - Vegetation after 10 years of simulation. Green line indicated the position and the height of mangroves, while black line the bed level profile. Blue line indicated the water level (in the figure is at around Mean Sea Level).

This is a result very close to the field data, as the dense part of vegetation has indeed a width between 300m and 400m along the study area, while younger sparse vegetation is present up to a width of 800m indicating that vegetation has the tendency to develop further to the offshore.

The establishment of new vegetation as well as the gradual growth of it can be easily observed in Figure 24. Where vegetation is young, the number of plants per grid cell is high while with the gradual growth of vegetation, its diameter and its height are increasing and the number of plants is decreasing representing the natural process and being in accordance with literature.

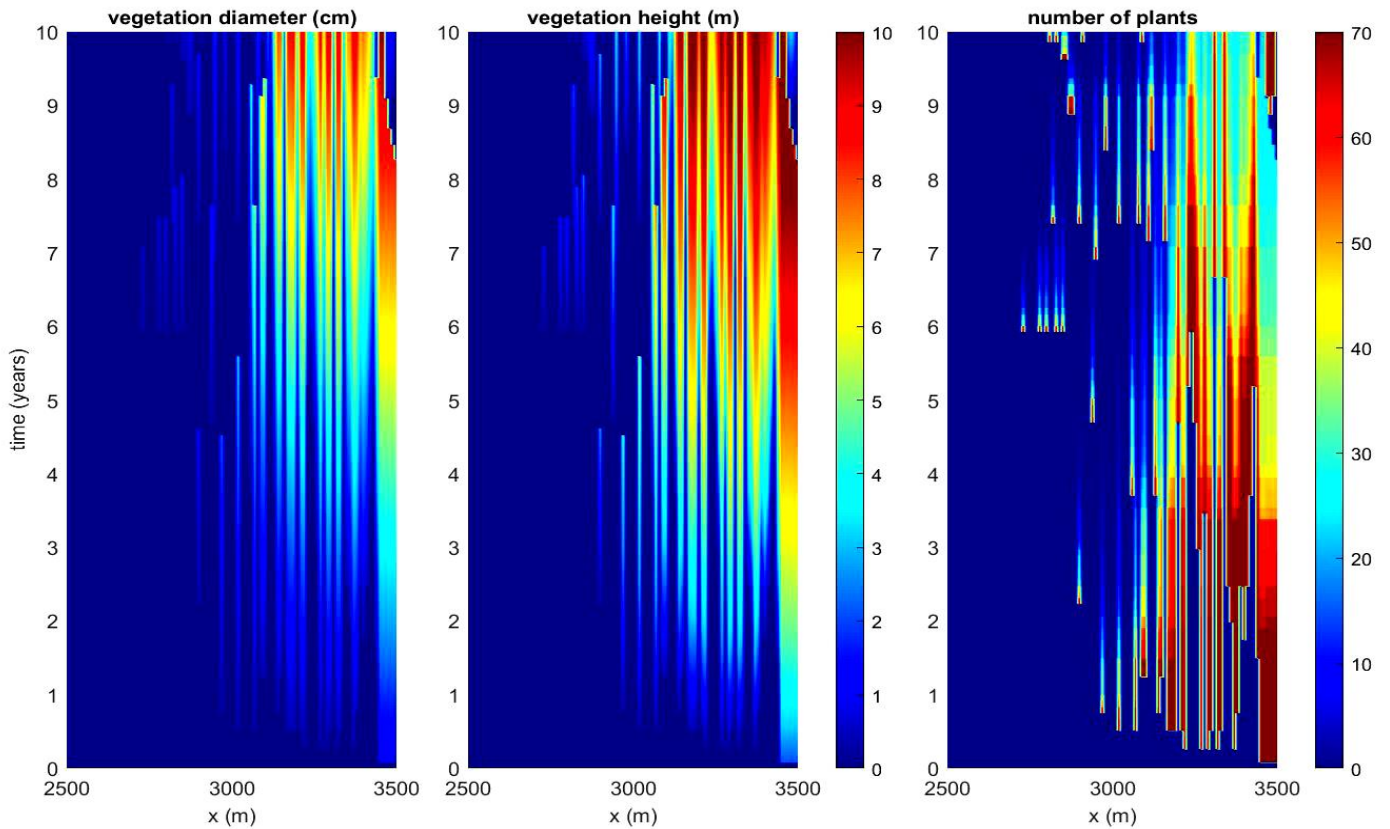


Figure 24 - Vegetation diameter in cm, vegetation height in m and number of plants per grid cell (10x10m) for the 10 years of simulation starting only with initial vegetation in the first 100m. The three pictures show only the last kilometer of the profile where vegetation is actually present. The color scale is the same for the first and the second picture.

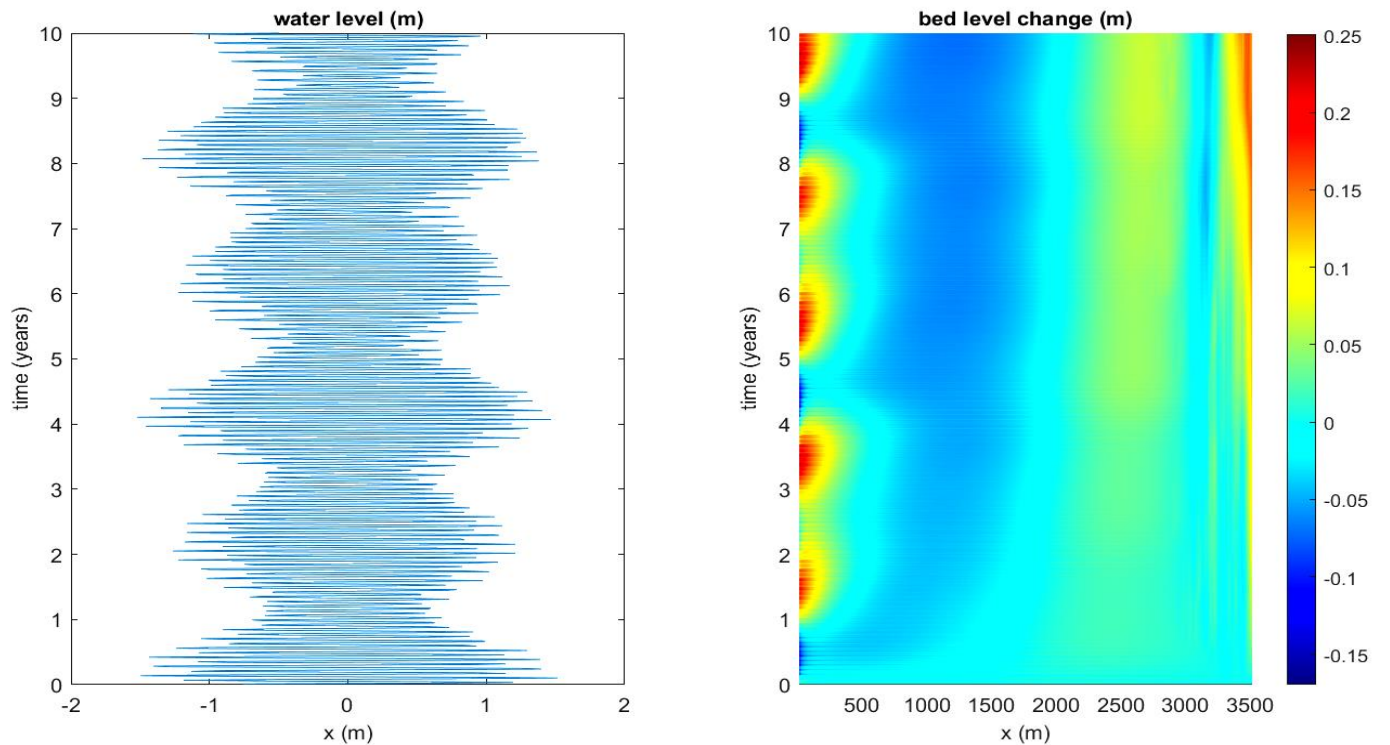


Figure 25 - Bed level evolution and tidal cycles of spring and neap tide. The model uses a morphological factor of 50, thus 10 years are represented by 2.4 months that correspond to 5 spring and 5 neap tides (as there are 2 spring and 2 neap tides during every month). Bed level oscillates at the seaward boundary, following the spring and neap tides. This is a boundary effect limited up to the first 500m of the profile. In the last 500m of the profile, accretion due to the presence of dense vegetation and erosion just in front of it is gradually occurring.

Bed level evolution during the 10 years of simulation is presented in Figure 25. The seaward boundary of the profile is sensitive to changes in tidal cycles but this sensitivity is limited only along the first 500m of the profile. At the landward part of the profile, for the last 500m where vegetation is densely developed, it is observed the gradual accretion in the vegetated part and the gradual erosion just in front of it, following the development of vegetation. This is an important output of the model, showing its ability to reproduce an expected natural behavior of the vegetated profile.

The difference between the vegetated and non-vegetated profile, after the 10 years of simulation period is shown in Figure 26. Where vegetation is not present, the two profiles are exactly the same. In front of the main part of vegetation there is erosion in the initial profile while in the main area of vegetation there is accretion, as expected, due to the dissipation of wave energy, the increase of critical shear stress and organic deposition.

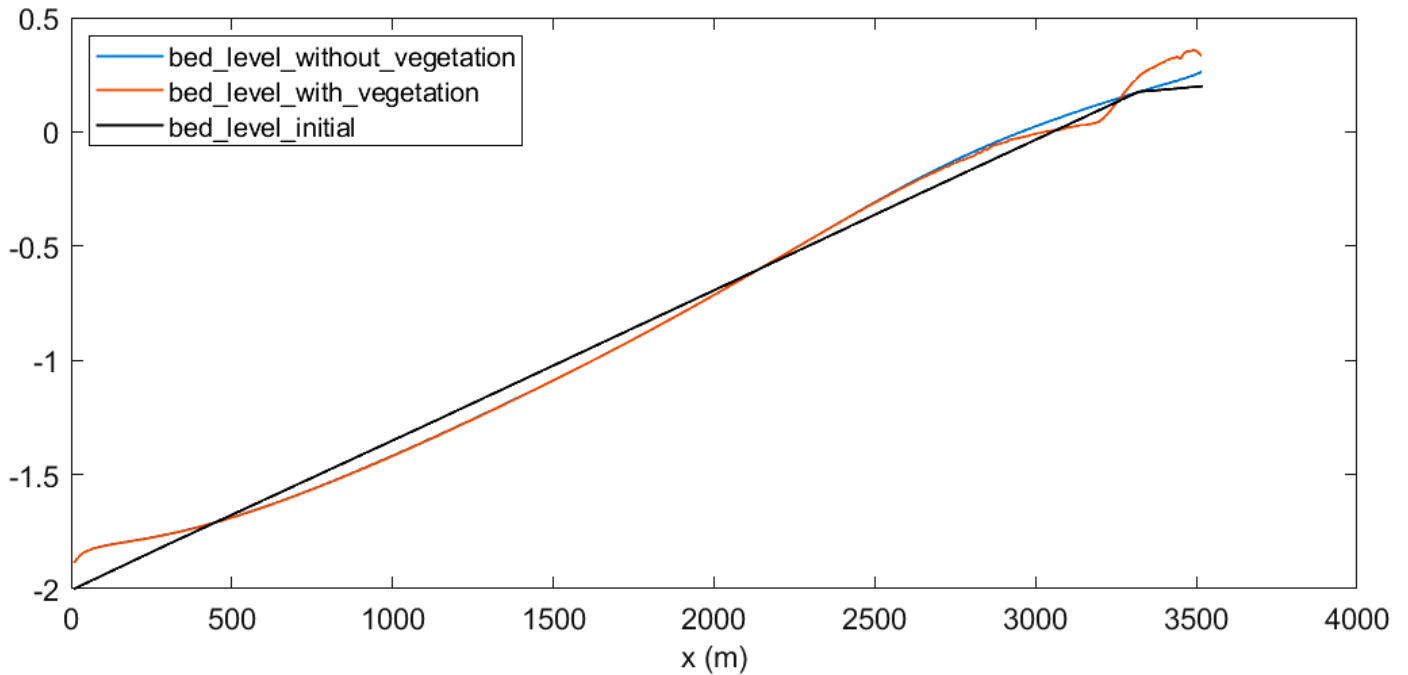


Figure 26 - 10 years of simulation with vegetation (red line) and without vegetation (blue line) compared with the initial profile (black line)

Other parameters of the simulation are presented in Figure 27 below, to give a sense of their range during a 12-hour tidal period at the end of the 10 years simulation period with vegetation. It can be observed the influence of vegetation on the response of the mudflat: From 2,800m and landward, the total shear stress drops more rapidly and sometimes with small steps, following also the behavior of the wave height. The reduction becomes larger landward, where vegetation is higher indicating also higher number of pneumatophores roots. This is a clear impact of vegetation at this part of the mudflat and differences can be observed by comparing Figure 27 with Figure 20 that represents the same hydrodynamic conditions without vegetation as explained.

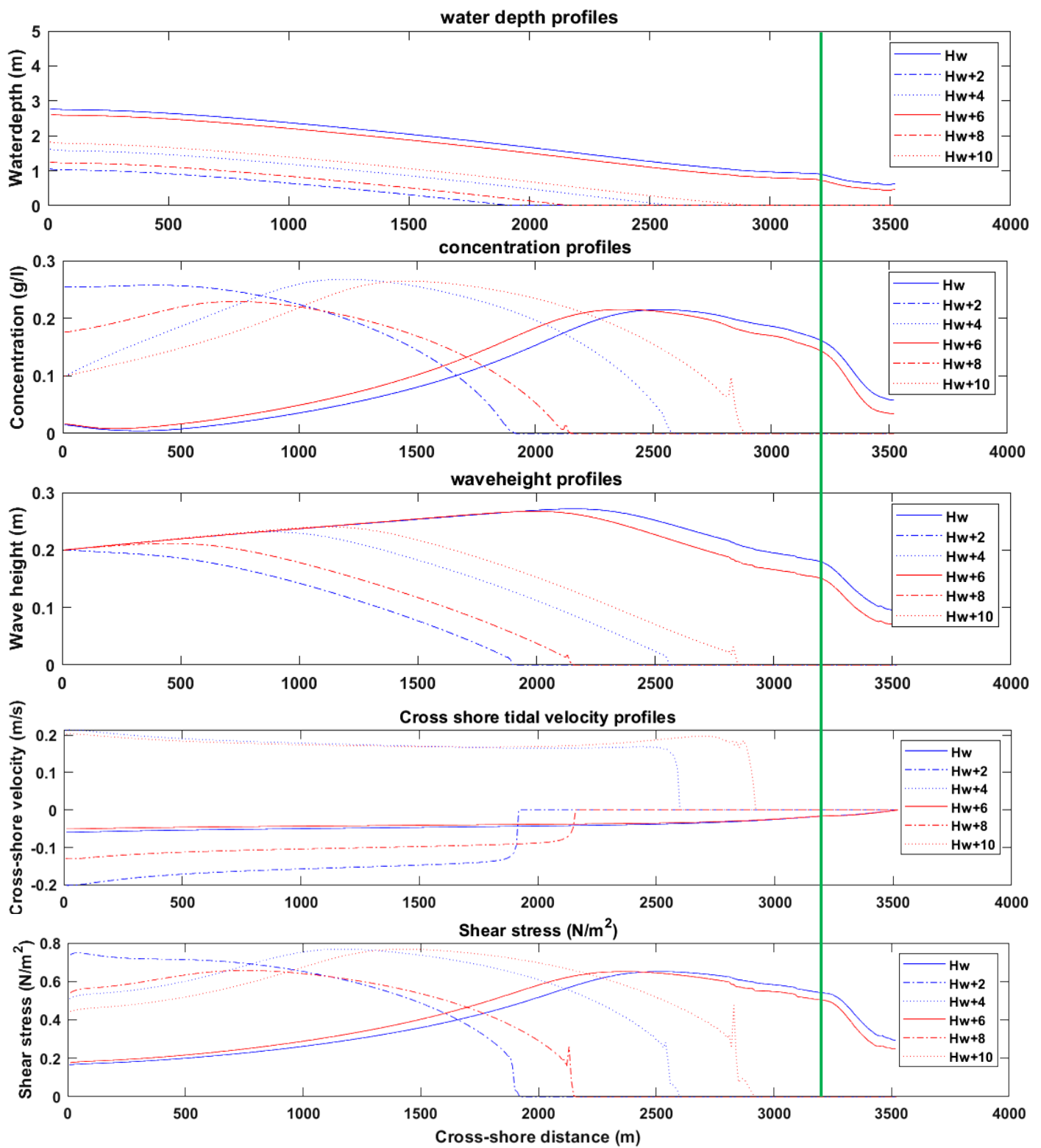


Figure 27 - The range of water depth, sediment concentration, wave height, cross-shore flow velocity and shear stresses during a 12-hour tidal period with 2-hours intervals at the end of the 10 years of simulation time with vegetation. The vertical green line shows the position where vegetation becomes denser, at 3200m.

The characteristics of vegetation, diameter & tree height and number of plants & tree height at the end of the 10 years of simulation, together with the average values from field measurements are presented in Figure 28 and in Figure 29 respectively.

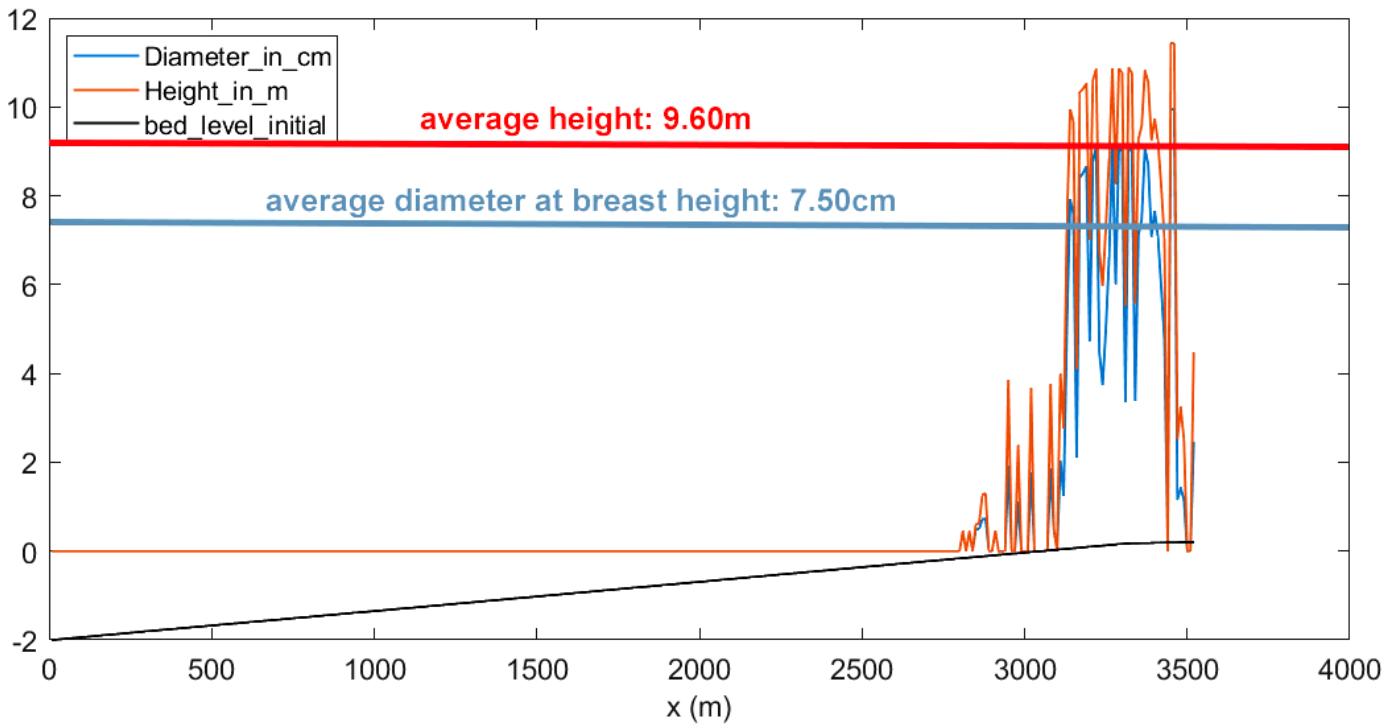


Figure 28 - Diameter in cm (blue line) and mangrove height in m (red line) after 10 years of simulation. Horizontal lines represent the average height (red line) and the average diameter (blue line) from field measurements. Black line shows the initial 1970 profile.

The average diameter at breast height from field data is 7.5cm and the maximum observed is 11.8cm. The average height is 9.6m with a maximum observed height of 12.3m. These findings are close to the results of simulation. It is not representative to compare the average from the model with the average from field measurements, as field measurements refer to already grown enough mangroves (the lower mangrove measured has a height of 2.7m) so the average is expected to be much higher.

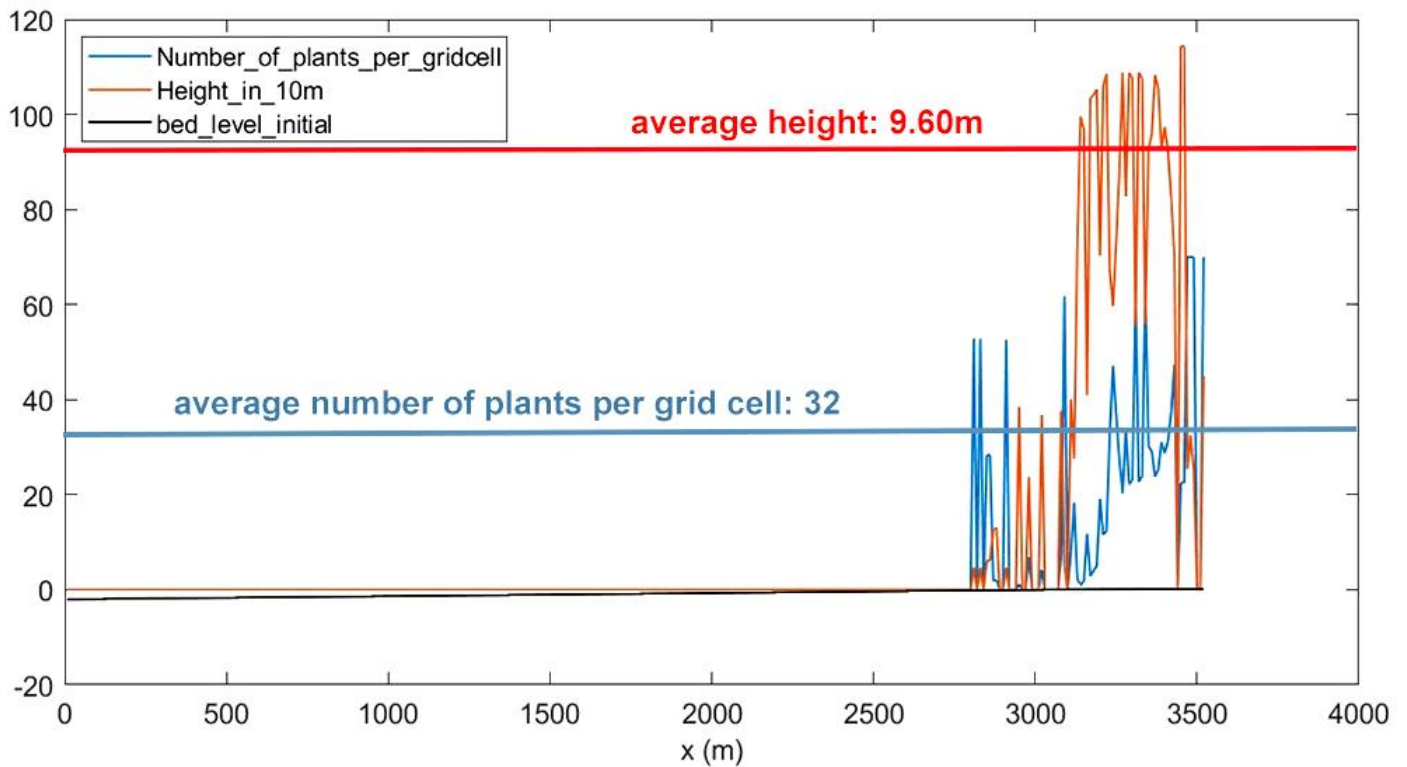


Figure 29 - Number of plants per grid cell (100m²) (blue line) and the height of plants in 10*m (red line). Black line represents the initial 1970 profile. Horizontal lines represent the average height (red line) and the average number of plants per grid cell (blue line) from field measurements.

The average number of plants per grid cell (100m²) from field measurements is 32 mangroves and the maximum is 70 mangroves. The maximum value of 70 is set as an input in the model, so it is impossible to be exceeded. The relation between the height and the number of plants (more plants for lower heights) is something that is visible by the results while the general behavior of the model is close to the observed relations between the density and the height of mangroves.

Equilibrium profile

In Figure 30 the evolution of the landward part of the profile for 10 years of vegetation is presented. It is shown only the last 500m of the profile as the rest appears to be stable through years where vegetation is not present, as expected due to the previous calibration for 40 years without vegetation. In the landward part where vegetation is present, there is a gradual accretion together with the gradual formation of the higher slope just in front of vegetation, as shown in Figure 25. The profile after 10 years of simulation is still under evolution and no equilibrium is visible yet.

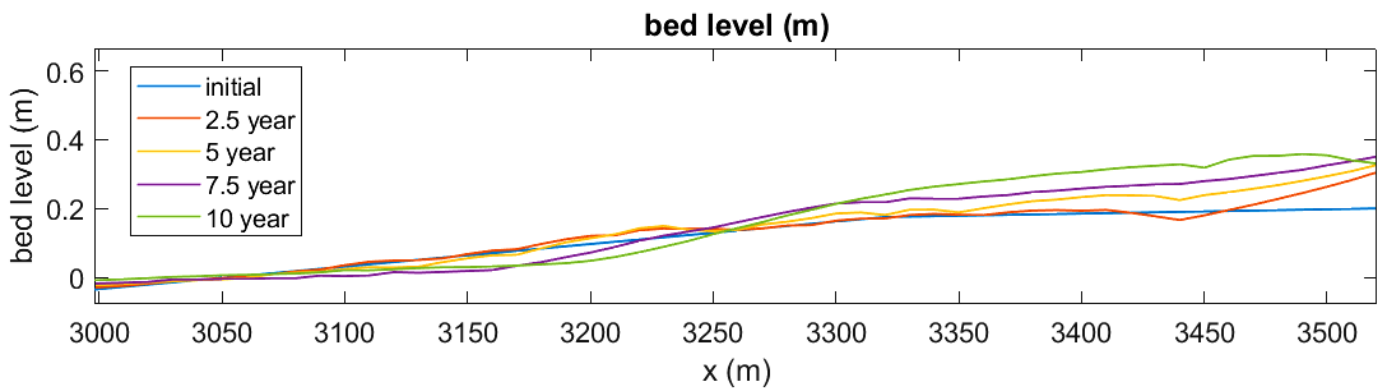


Figure 30 - Evolution of the profile through the years for 10 years of simulation with vegetation for the landward, densely vegetated part

Trying to reach an equilibrium profile with vegetation, a test simulation of 40 years is applied. The results are shown in Figure 31, zooming into the area of vegetation. The width of vegetation seems to be stable, as the dynamic part of the profile is between 2,800 and 3,500m through the 40 years of simulation. However, as vegetation grows, the processes that favor accretion (dissipation of wave energy, increase of critical shear stress, organic deposition) are intensified so there is further accretion at least for the first 30 years. The last 10 years of simulation, the bed level starts stabilizing as no remarkable difference is observed between the 30 and 40 years profile. So, it could be claimed that after 30 years the profile has reached equilibrium.

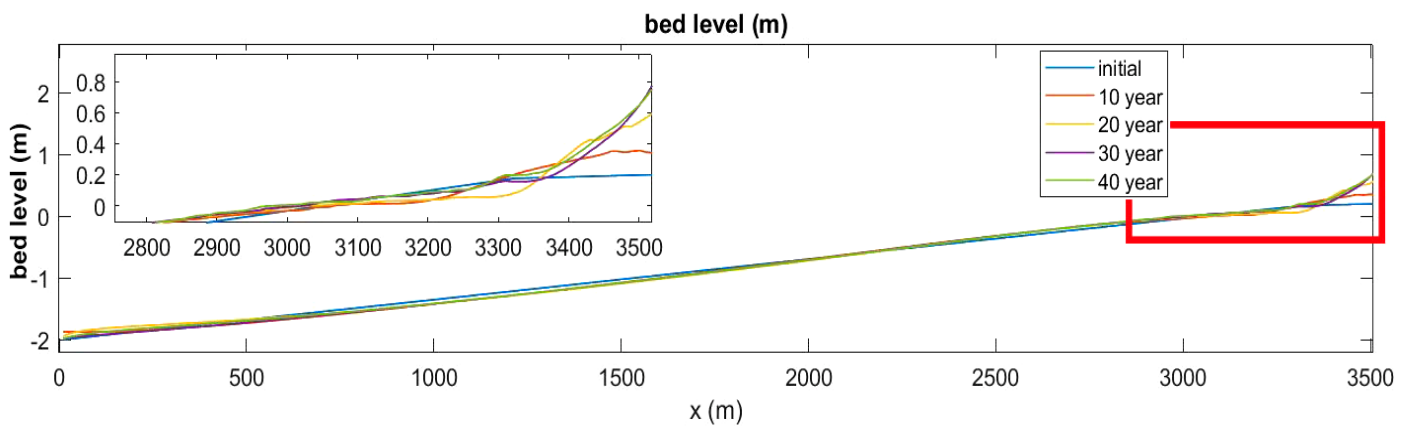


Figure 31 – The evolution of the profile through the decades for a 40 years simulation with a zooming into the vegetated area. Blue line represents the initial 1970 profile, while different colors refer to different decade of evolution.

Although the above argumentation about the equilibrium vegetated profile seems to be reasonable, there is a hidden point of attention: The calibration of the parameters used for vegetation growth (coefficients 'b₂' and 'b₃' for the height formula –Equation 3.1– and growth parameter 'G' –Equation 3.21–) as well as the parameter for the zone of influence of vegetation (coefficient 'α' –Equation 3.5–) is applied for 10 years of simulation using the available field data. The parameter setting, as explained above, gives a quite good matching between the computed and the observed vegetation characteristics (density, diameter, height, number of plants).

However, for a longer simulation, a different set of parameters is necessary for realistic results, as the vegetation characteristics are going to change differently and the results would be far from literature finding and from the expected ones. A characteristic example is that the height formula with the above calibrated parameters is not able to produce a tree higher than 15m. In literature findings mature *Avicennia Germinans* mangroves can easily reach 30m height and in reality it is expected a much higher tree than 15m, as in 10 years trees already can reach 12m. Thus, to be able to give an answer about if and when the vegetated profile can reach equilibrium, further research and modification of vegetation parameters is necessary.

4.4 Summary of calibration

The fact that Mflat model is able to simulate a profile in equilibrium by reproducing the initial input profile, while using reasonable values from literature and field observations about the hydrodynamic and sediment parameters is very important for continuing this study because it can prove that the model work for Guyana case and it is then possible to focus on the impact of only one parameter on the profile, as it is applied for the sensitivity analysis or on the impact of different hydrodynamic conditions, as it is the purpose of this study, by testing extreme events.

The ability of the model to reproduce, after the right calibration process, vegetation characteristics that are close to field observations and its ability to follow the development of vegetation together with morphodynamic evolution through the years gives one extra advantage keeping this study close to the real case for Guyana coast. This ability strengthens the expectation that the results of the model about the importance of vegetation on dissipating the wave energy and protecting the coast against extreme events are realistic and representative for the study area.

5 Sensitivity analysis

In this chapter, a sensitivity analysis is applied for the cross-shore flow case analyzed in chapter 4.2 for 40 years of simulation under normal hydrodynamic conditions and without vegetation. The purpose of this analysis is to understand deeper the behaviour of Mflat model and the importance of the choice of various parameters. It is applied only for the non-vegetated case, as vegetation characteristics are not expected to change during extreme hydrodynamic conditions. On the contrary, hydrodynamic and sediment characteristics are expected to be different because of the more dynamic environment.

It is chosen to test the sensitivity on basic sediment characteristics and on hydrodynamic forcing by waves, as other important parameters of the model are either quite certain (tide) or of less importance (wind) for the response of the non-vegetated profile. The parameters that are under sensitivity analysis are presented in Table 9.

Table 9 - The variation of sediment and hydrodynamic parameters to apply sensitivity analysis

Parameter	Explanation	Units	Range from literature	Final calibration	Sensitivity high	Sensitivity low
bcs	Sediment concentration at the sea boundary	kgr/m ³	~0.1 – 0.5 kgr/m ³	0.1	0.2	0.05
ww	Settling velocity of the sediment	m/sec	0.0001 - 0.0004 or in the order of 0.001 for some flocculation	0.0012	0.0024	0.0006
taucr	Critical shear stress for erosion	Pa	0.2±0.15 1±0.5 for consol. Mud	0.18	0.27	0.09
MM	Erosion factor	Kgr/m ² /sec	0.1·10 ⁻⁴ – 5·10 ⁻⁴	1·10 ⁻⁴	2·10 ⁻⁴	0.5·10 ⁻⁴
H_{rms}	Root mean square wave height	m	-	0.2	0.4	0.1
T_p	Peak wave period	sec	-	3	6	1.5
MF	Morphological Factor	-	100±	100	200 400	50

Critical shear stress

The critical shear stress determines the shear stress threshold above which erosion takes place. Higher critical shear stress makes erosion more difficult and the sediment that is deposited in low hydrodynamic conditions (during the tidal cycle) cannot be re-suspended, so it is expected a more elevated profile that is shown with the red line in Figure 32. On the contrary, lower critical shear stress allows more sediment to be in suspension. In the area of the mudflat that hydrodynamic conditions are very mild, more sediment settles and the very mild hydrodynamic conditions are not able to remove it resulting in accretion. In the area where hydrodynamic forcing is able to keep sediment in suspension there is erosion of the profile as shown by the green line in Figure 32.

The formula that describes erosion in Mflat model is shown in Equation 5.1:

Equation 5.1 - Erosion formula

$$ero = \begin{cases} 0 & \text{if } \tau \leq \tau_{cr} \\ M \cdot (\tau - \tau_{cr}) & \text{if } \tau > \tau_{cr} \end{cases}$$

'M' is the erosion factor, 'τ' the total shear stress due to current and wave action and 'τ_{cr}' the critical shear stress. When the total shear stress is below the critical one, there is no erosion, while when it is above the critical shear stress the erosion is the product of this subtraction with the erosion coefficient.

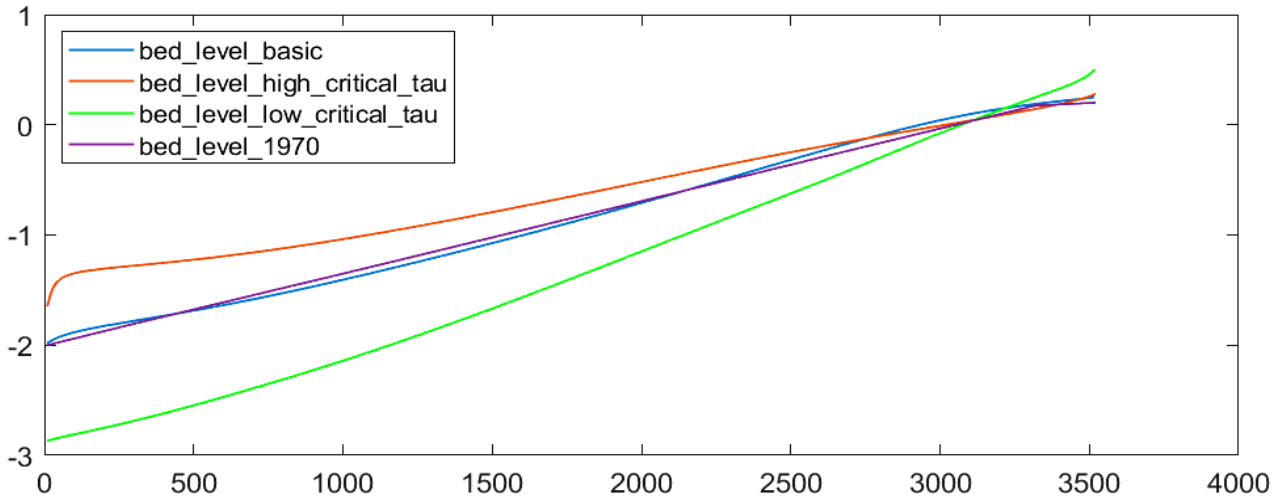


Figure 32 - Sensitivity on critical shear stress: The initial 1970 profile (purple line) together with the equilibrium profile after 40 years of simulation (blue line). Comparison with a profile with higher critical shear stress (red line – $\tau_{cr}=1.5 \cdot \tau_{crinitial}$) and with lower critical shear stress (green line – $\tau_{cr}=0.5 \cdot \tau_{crinitial}$). Horizontal axis: the length of the profile (m). Vertical axis: water depth (m).

Sediment boundary concentration

The sediment boundary concentration determines how much sediment is available at the offshore boundary of the model domain. Looking at the Figure 33, it seems initially strange why a higher boundary concentration results in erosion of the landward profile after 40 years of simulation while a lower concentration results in accretion.

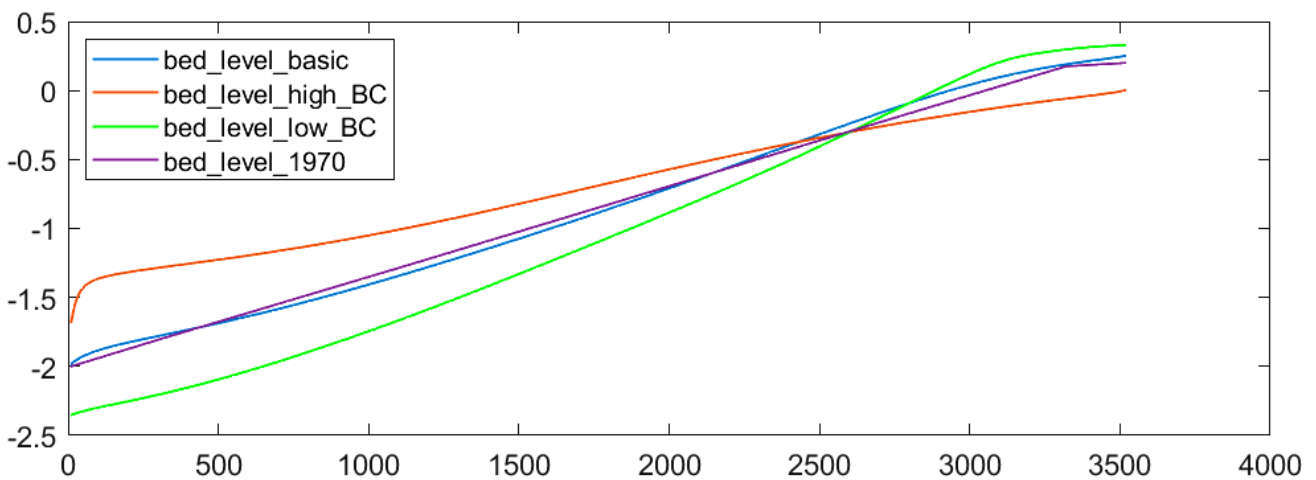


Figure 33 - Sensitivity on sediment boundary concentration: The initial 1970 profile (purple line) together with the equilibrium profile after 40 years of simulation (blue line). Comparison with a profile with higher boundary concentration (red line – $bc=2 \cdot bc_{initial}$) and with lower boundary concentration (green line – $bc=0.5 \cdot bc_{initial}$). Horizontal axis: the length of the profile (m). Vertical axis: water depth (m).

The explanation could be given by observing the evolution of the profile for the case of higher boundary concentration, as shown in Figure 34. The first response of the profile is a rapid accretion on the seaward side: sediment the first years settles as it enters the model domain. The rest of the profile remains stable. Then, the profile adjusts gradually to this first rapid change trying to find again an equilibrium stage: the seaward part remains almost stable and at the landward part there is gradual erosion resulting in a milder slope. The opposite phenomenon is happening in the case of lower sediment boundary concentration with rapid erosion the first years seaward and a gradual accretion the next decades landward. This behaviour may not be realistic, as in the real case accretion would be expected for higher sediment supply. It seems that the effect of the seaward boundary determines the behaviour of the whole domain for this case.

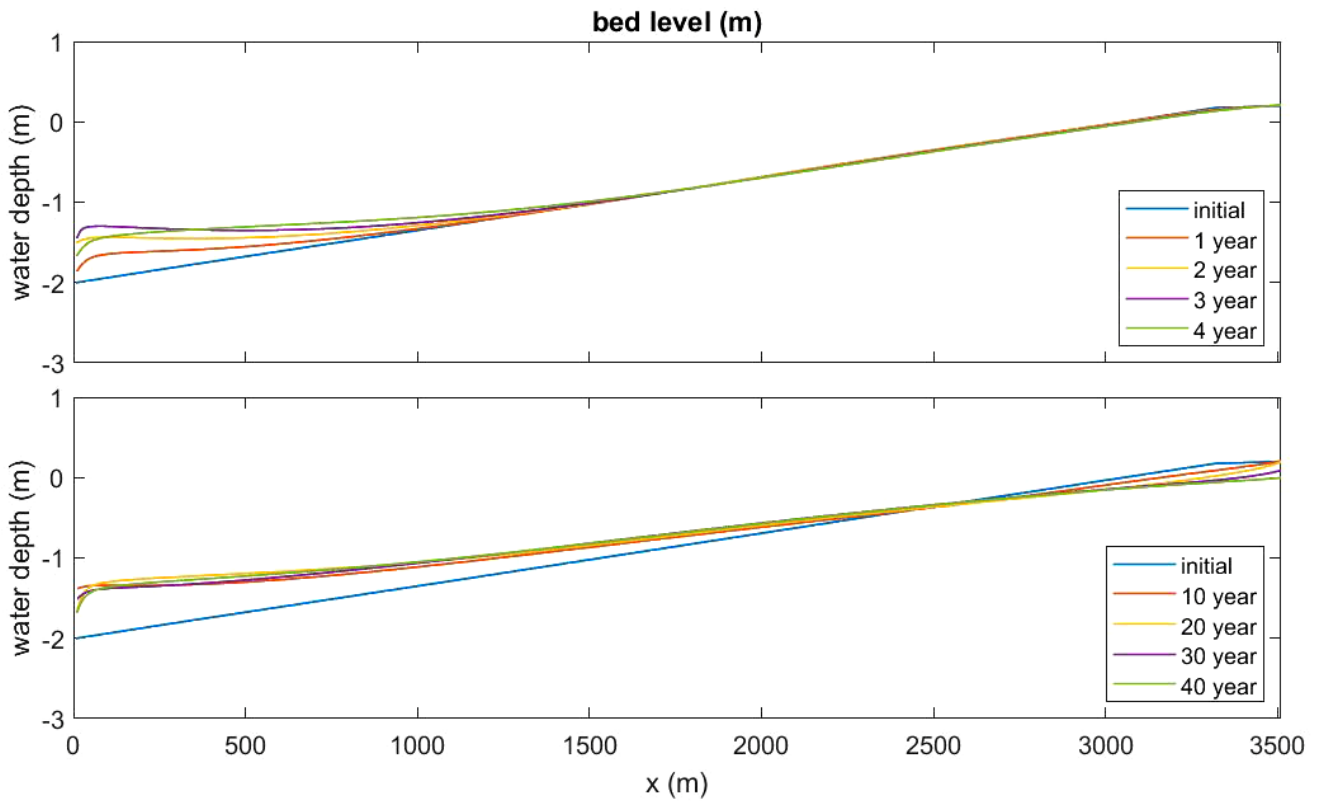


Figure 34 - Evolution of bed level profile for the case of increased (two times higher) sediment boundary concentration. In the upper figure the time step of plotting the profile is 1 year and in the second it is 10 years. With blue line it is the initial 1970 profile and with different color it is presented a different year (upper figure) or a different decade (lower figure).

Settling velocity

Settling velocity determines how fast sediment settles and is directly connected with deposition by the Equation 5.2:

Equation 5.2 - Deposition formula

$depo = ww \cdot c$, with 'ww' the settling velocity and 'c' the suspended sediment concentration.

It is observed in Figure 35 that higher settling velocity creates a milder slope for the profile. The reason is that higher settling velocity leads to higher deposition rates. Thus, less sediment is in suspension to reach the more landward part of the profile when tide allows water to flow in that area. So, there is a lower profile landward and a higher profile seaward as there is always water flow there and sediment settles faster. On the contrary, in case of lower settling velocity, more sediment is in suspension and can be transferred to settle landward when flood tide allows water with sediment to flow there.

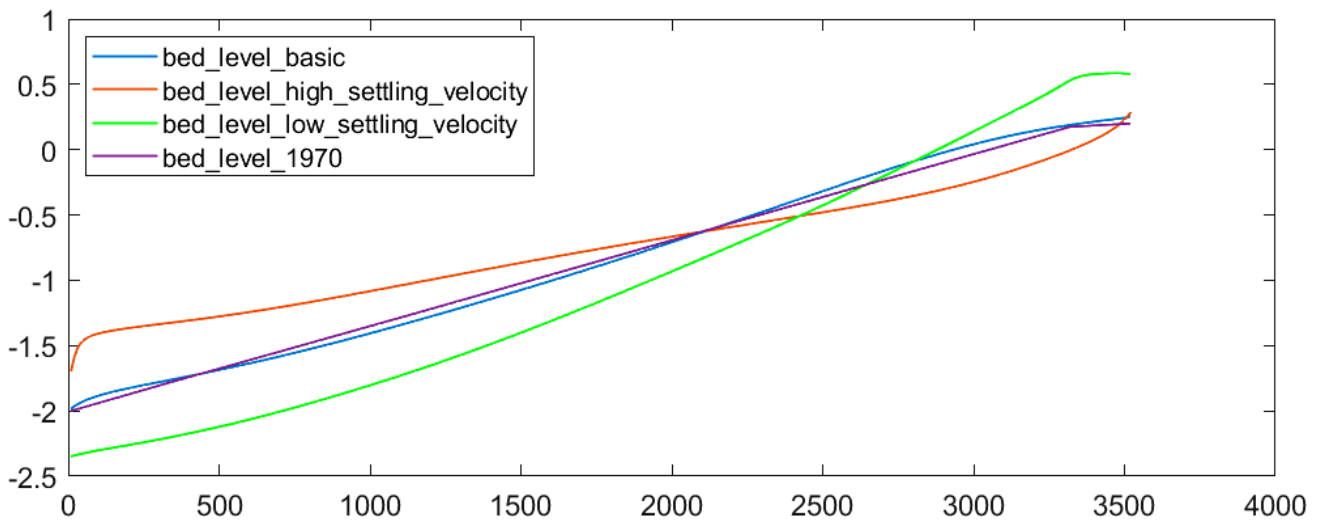


Figure 35 - Sensitivity analysis for settling velocity: The initial 1970 profile (purple line) together with the equilibrium profile after 40 years of simulation (blue line). Comparison with a profile with higher settling velocity (red line – $ww=2*ww_{initial}$) and with lower settling velocity (green line – $ww=0.5*ww_{initial}$). Horizontal axis: the length of the profile (m). Vertical axis: water depth (m).

Erosion Coefficient

The erosion coefficient is directly connected with the amount of erosion allowed as described by Equation 5.1 and the behaviour of the profile is similar with the one for the variation of critical shear stress shown in Figure 32: Higher erosion factor leads to more erosion almost to the whole profile and lower erosion factor allows for more accretion. The profiles are similar for all the cases landward as hydrodynamic conditions are milder there and erosion is limited by the very small difference between the total shear stress and the critical shear stress. Variations are larger for the seaward part where conditions are more dynamic, as shown in Figure 36.

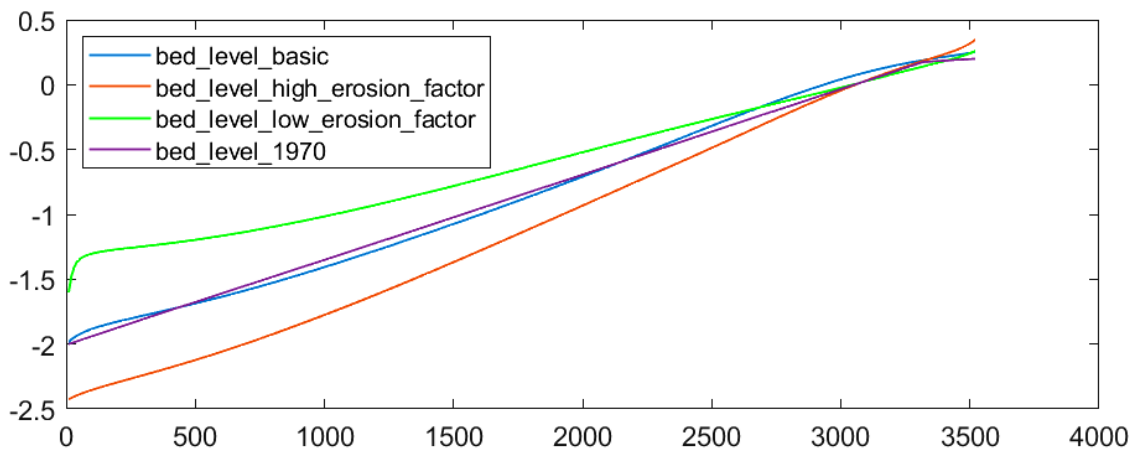


Figure 36 – Sensitivity for erosion factor: The initial 1970 profile (purple line) together with the equilibrium profile after 40 years of simulation (blue line). Comparison with a profile with higher erosion factor (red line – $MM=2*MM_{initial}$) and with lower erosion factor (green line – $MM=0.5*MM_{initial}$). Horizontal axis: the length of the profile (m). Vertical axis: water depth (m).

Wave height

The wave height is an important parameter as it can steer up sediment that is further transported by flood or ebb tide. In the model, the wave height can increase the total shear stress and lead to erosion. The impact of wave height on the profile is shown in Figure 37. Profiles for all the cases are similar landward as waves break and their height is depth restricted.

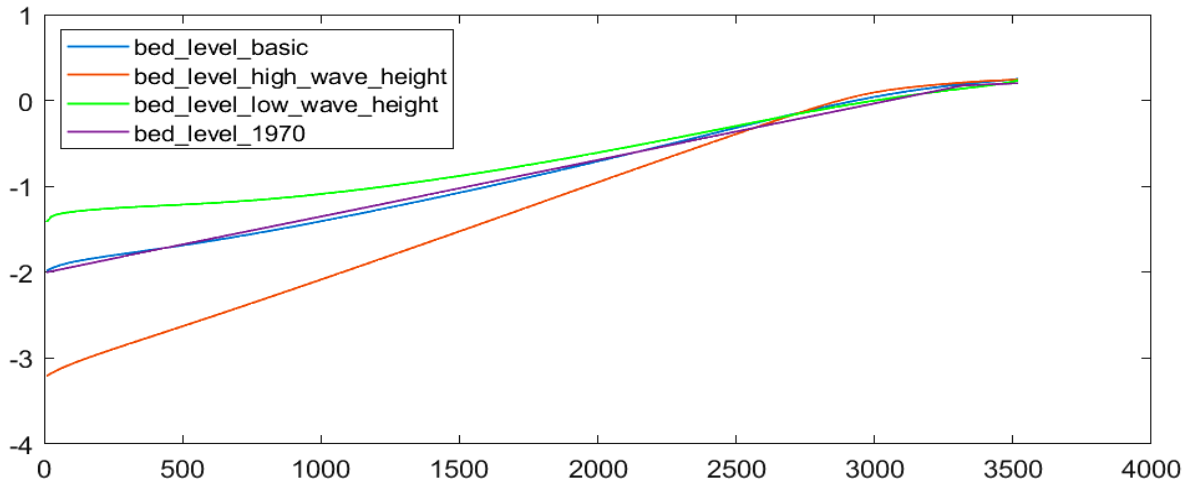


Figure 37 - Sensitivity for wave height: The initial 1970 profile (purple line) together with the equilibrium profile after 40 years of simulation (blue line). Comparison with a profile with higher wave height (red line – $H_{rms}=2*H_{rms_{initial}}$) and with lower wave height (green line – $H_{rms}=0.5*H_{rms_{initial}}$). Horizontal axis: the length of the profile (m). Vertical axis: water depth (m).

It is remarkable that for the lower wave height ($H_{rms}=0.1m$) the profile can reach an equilibrium through most of its length as shown in Figure 38. This is not the case for higher wave height for which erosion seaward and a very slight accretion landward is continuous, due to the transportation of high amount of suspended sediment.

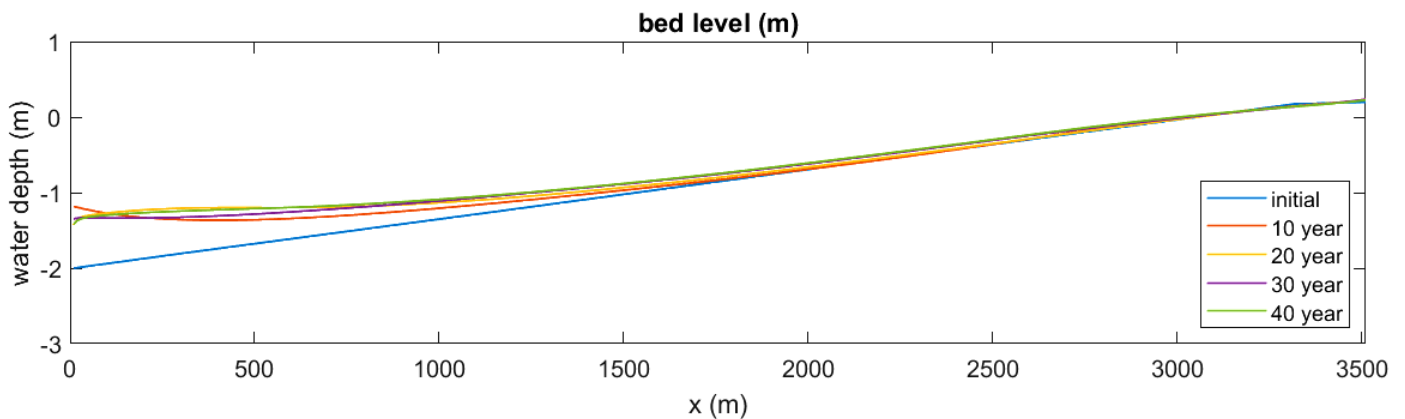


Figure 38 - The evolution of the bed level profile through decades for a 40 years of simulation with a wave height of $H_{rms} = 0.1m$, the half of the one used for the normal hydrodynamic conditions.

Wave period

The wave dissipation formulas that are used for the modelling are analyzed by van der Wegen et al. (2019). According to these formulas, wave period is connected with the dissipation of wave energy due to wave breaking and due to bed friction. Higher wave period results to less dissipation of energy. This is the reason why the profile with higher wave period is steeper, as more wave energy leads to more erosion where waves are more active and to more sediment transport landward resulting in accretion close to the inshore boundary, as shown in Figure 39.

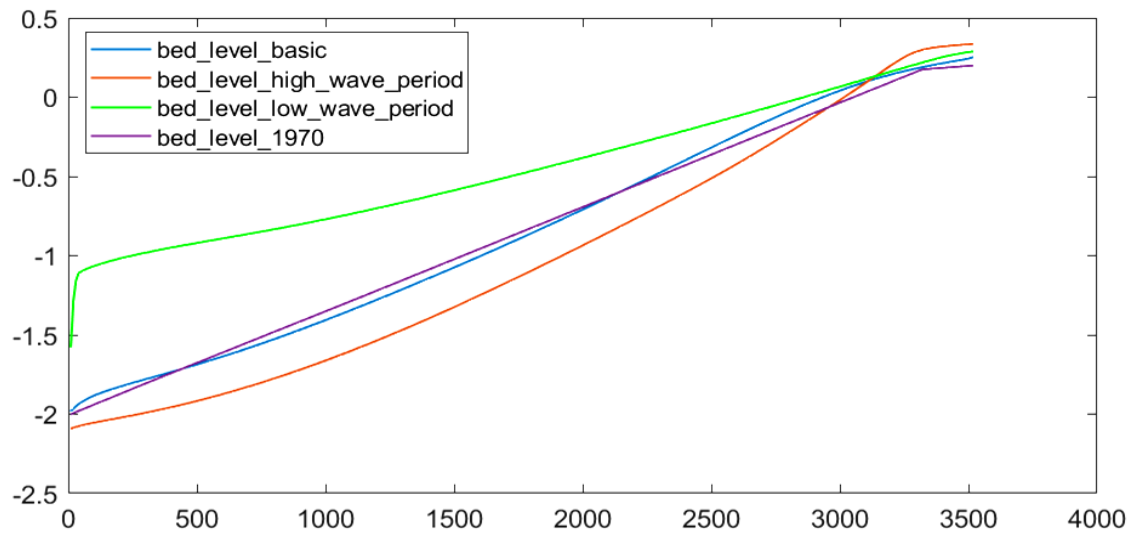


Figure 39 – Sensitivity for wave period: The initial 1970 profile (purple line) together with the equilibrium profile after 40 years of simulation (blue line). Comparison with a profile with higher wave period (red line – $T_p=2 \cdot T_{p_{initial}}$) and with lower wave period (green line – $T_p=0.5 \cdot T_{p_{initial}}$). Horizontal axis: the length of the profile (m). Vertical axis: water depth (m).

The dissipation of wave energy due to wave breaking is presented in Figure 40. It is observed that the case for lower wave period ($T_p=1.5\text{sec}$) has a strange, high dissipation of energy at the offshore boundary, probably caused by model instability there and further onshore almost no energy dissipation occurs. This profile it may not be representative of the real case with lower wave period, affected by the boundary, but it can indicate the trend of higher dissipation of wave energy resulting in more accretion on the initial bed profile.

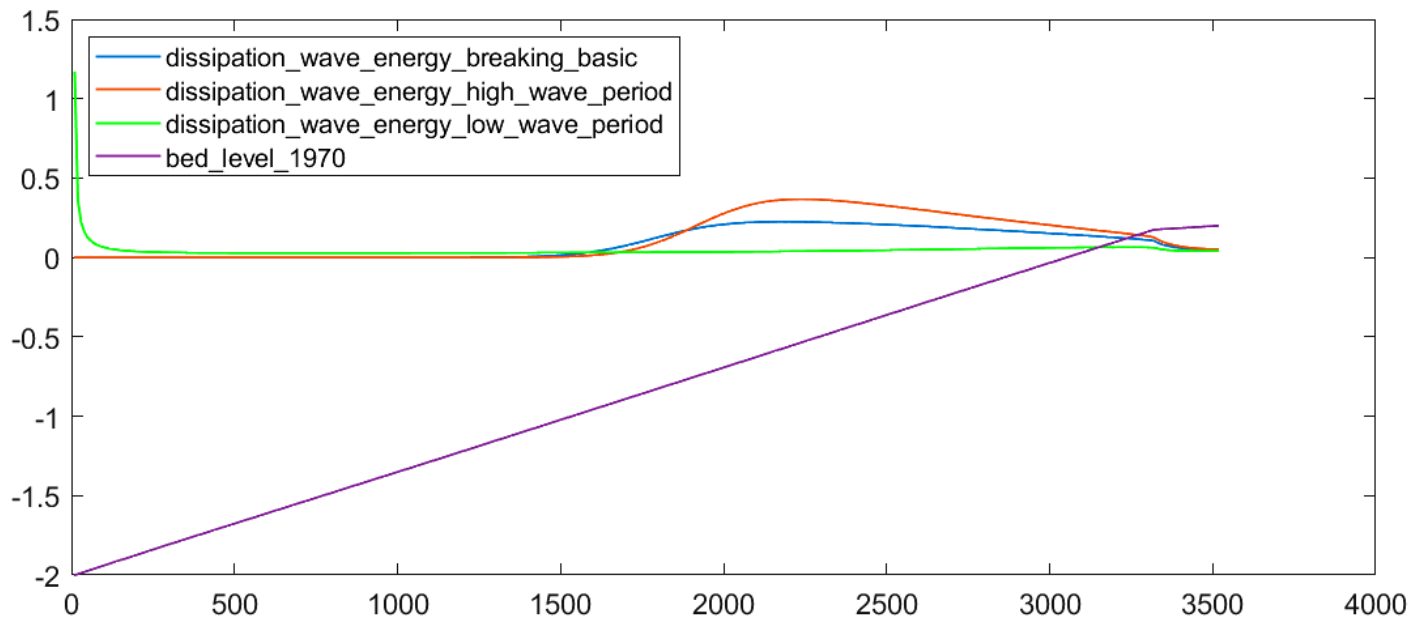


Figure 40 - Dissipation of wave energy ($\text{J/m}^2/\text{sec}$) due to wave breaking during flood tide at the beginning of the 40 years simulation. The initial 1970 profile (purple line) together with the distribution of wave energy dissipation during normal hydrodynamic conditions (blue line). Comparison with the dissipation using higher wave period (red line – $T_p=2 \cdot T_{p_{initial}}$) and lower wave period (green line – $T_p=0.5 \cdot T_{p_{initial}}$). Horizontal axis: the length of the profile (m). Vertical axis: dissipation of wave energy ($\text{J/m}^2/\text{sec}$).

Morphological factor

Morphological factor is a multiplier for the morphological processes accelerating the morphological changes with respect to the hydrodynamic processes and it is analyzed further in chapter 2.5. For this study a typical morphological factor of MF=100 is used for the 40 years simulation, a MF = 50 is used for the 10 years of simulation with vegetation and a MF=1 is used for the 5 days simulation of extreme events.

The higher morphological factor result to a shorter duration of simulation of a certain time period, so it is favourable to use it. However, a very high MF can cause differences with the normal expected behaviour and can produce unreliable results. So, it is important to know “how far we can go” with the increase of the morphological factor.

The morphological factor is used to accelerate the update of bed level changes according to Equation 5.3:

Equation 5.3 - Bed level update formula – equation 25 of van der Wegen et al. (2019)

$$\frac{\partial z}{\partial t} = MF \cdot \left[\frac{\partial uhc}{\partial x} - Dif \cdot \frac{\partial h \frac{\partial c}{\partial x}}{\partial x} + \frac{depo-ero}{\rho_b} \right]$$

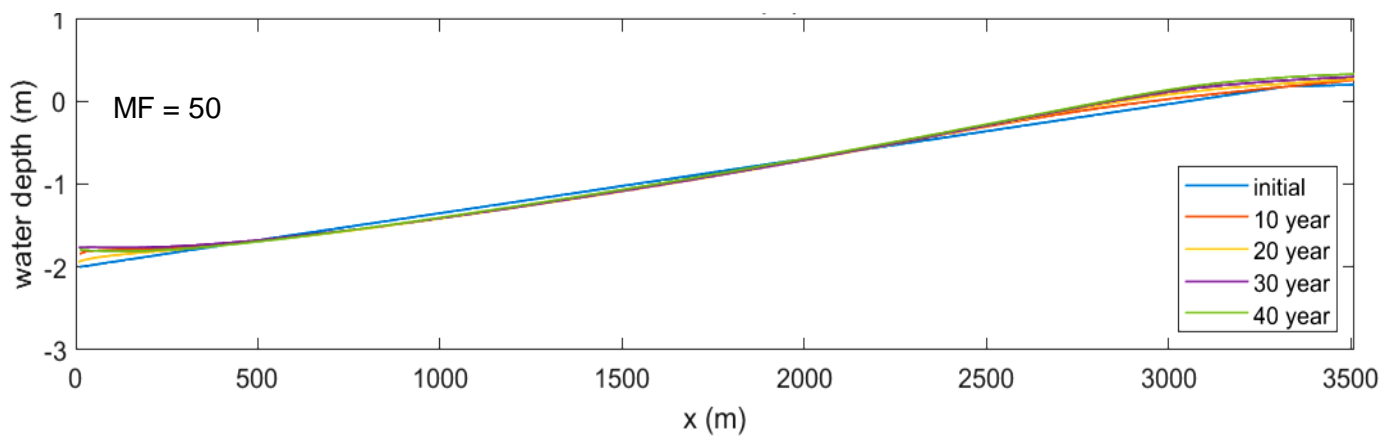


Figure 41 - Evolution of the profile through decades for the 40 years of simulation with a MF = 50

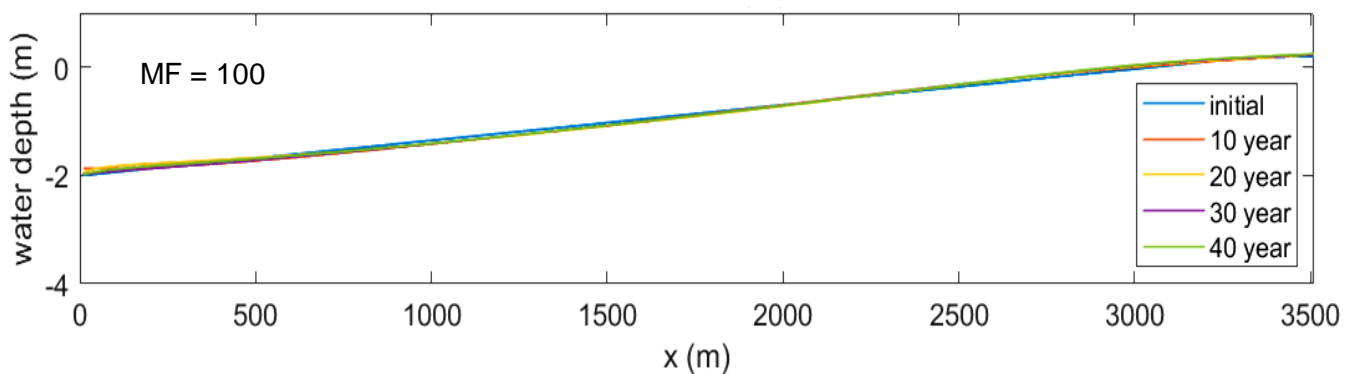


Figure 42 – Evolution of the profile through decades for the 40 years of simulation with a MF = 100 – the case that is used for this study

Looking at Figure 41 and Figure 42 there are very small differences of the profiles, in the order of maximum a few centimetres so it is a good choice to use MF = 100.

Looking at Figure 43, the simulation with MF = 200 gives a profile very close to the one with MF = 100 with differences in the order of maximum a few centimetres. It could be a good choice to use MF = 200, however the differences between MF = 50 and MF = 200 are larger, in the order of maximum 15 cm so this could be a deterrent to use such a high MF.

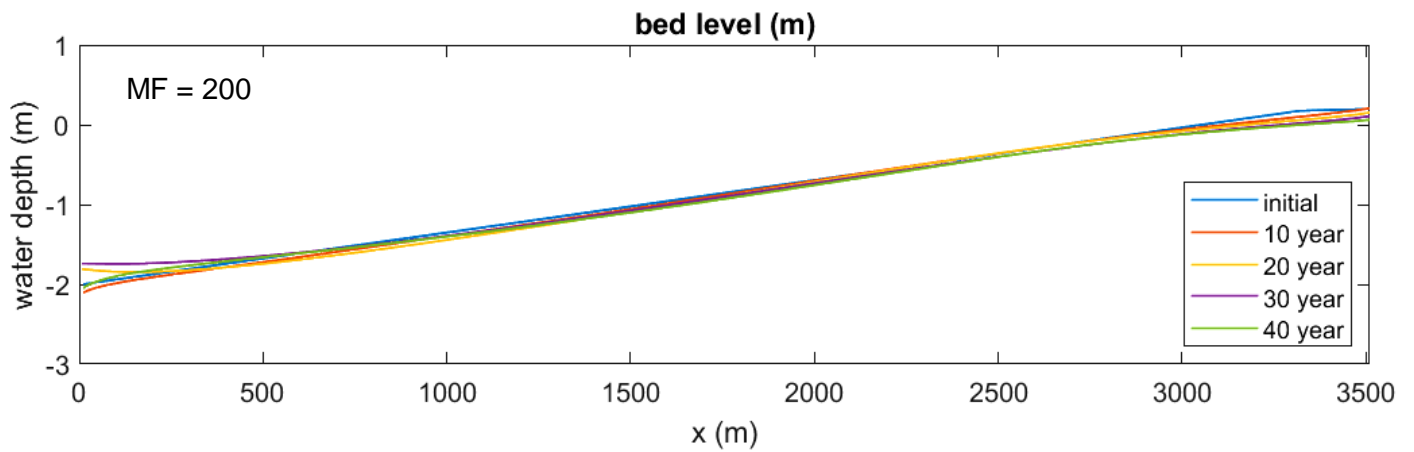


Figure 43 – Evolution of the profile through decades for the 40 years of simulation with a MF = 200

A last trial is applied with MF = 400. The differences in the landward part of the profile, as shown in Figure 44 are in the order of a few tens of centimetres compared to the profile with MF = 50, so a MF = 400 could be too high for a simulation with the characteristics chosen for Guyana coast.

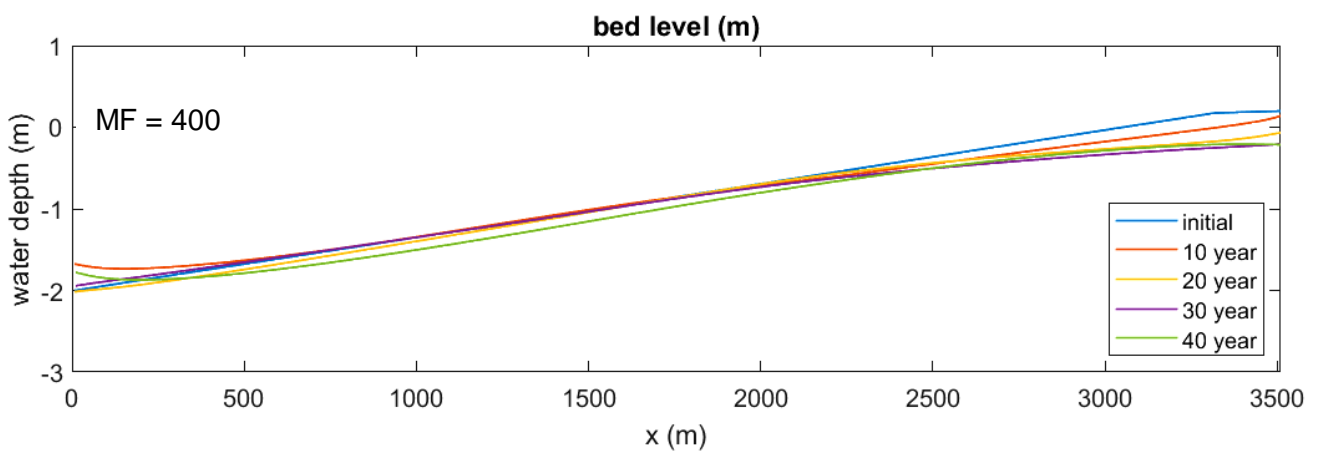


Figure 44 – Evolution of the profile through decades for the 40 years of simulation with a MF = 400

It is observed that lower morphological factor has similar effect with higher diffusion coefficient that keeps most of the profile the same, increasing the accretion landward, as shown in Figure 45. Thus, it could be claimed that a higher morphological factor results in a more diffusive behavior of the profile.

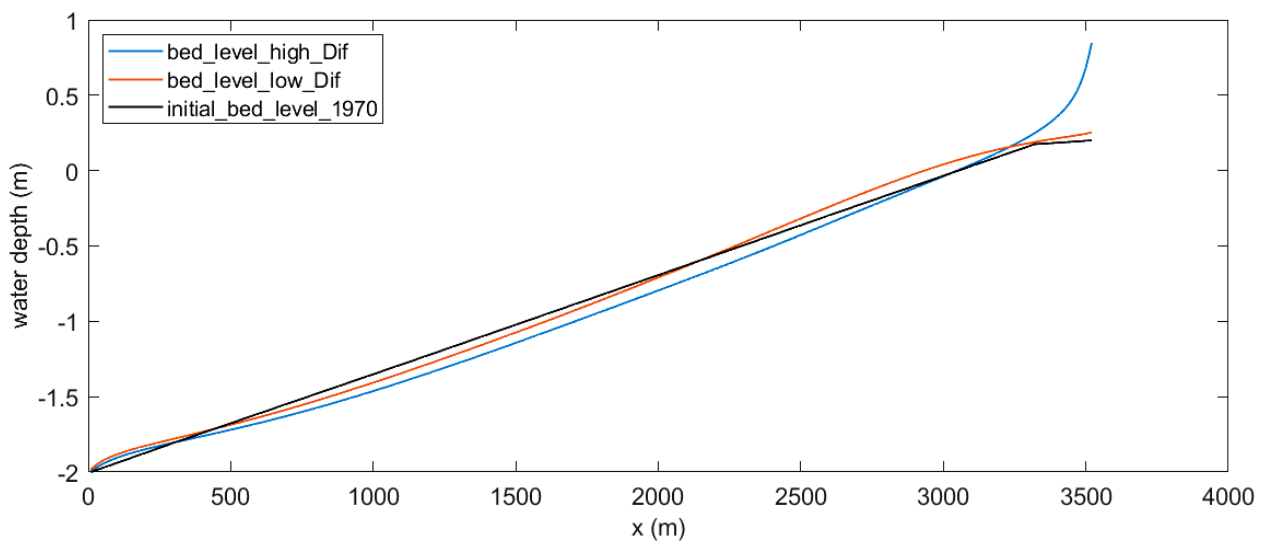


Figure 45 - Comparison between the equilibrium profile came out of calibration with diffusion coefficient Dif = 1.5 (red line), the case with much higher diffusion coefficient Dif = 5 (blue line) and the initial 1970 profile (black line).

The choice of a morphological factor of 100 is considered reasonable as it is proposed by literature for such cases (chapter 2.5) and results in a very stable profile with not large differences compared to the cases with lower morphological factors.

Summary of sensitivity analysis

The effect of variation of different sediment and hydrodynamic parameters on bed level profile after 40 years of simulation as presented in Table 9 is summarized in Table 10 below:

Table 10 – Description of the behavior of bed level profile for the tested cases of sensitivity analysis

Parameter	Explanation	Units	lower	higher
bcs	sediment concentration at the sea boundary	kgr/m ³	steeper slope with high erosion offshore and low accretion landward * boundary effect	milder slope, large accretion offshore, some erosion landward * boundary effect
ww	settling velocity of suspended sediment	m/sec	steeper slope more suspended sediment erosion seaward, accretion landward	milder slope less suspended sediment accretion seaward, erosion landward
taucr	critical shear stress for erosion	Pa	steeper slope more suspended sediment erosion	milder slope less suspended sediment accretion
MM	erosion factor	kgr/m ² /sec	milder slope less suspended sediment accretion	steeper slope more suspended sediment erosion
H_{rms}	root mean square wave height	m	milder slope, more accretion seaward landward end the same	steeper slope, more erosion seaward landward end the same
T_p	peak wave period	sec	higher wave energy dissipation, steeper profile *strange behavior of the model	lower wave energy dissipation, milder slope
MF	morphological factor	-	Accretion landward (less diffusive behavior)	Erosion landward (more diffusive behavior)

6 Results

The two extreme hydrodynamic conditions analyzed in chapter 2.3 are used as an input for the simulations with Mflat model to test the response of Guyana coast under the expected severe cases. Various plots are extracted by the model emphasizing on the impact of vegetation on the response of the mudflat, as this is the main subject of this study. Especially for the storm case, an extra sensitivity analysis is applied to understand better the processes under high hydrodynamics.

Both extreme cases are simulated using as an input for the vegetation parameters (diameter, height, number of plants) the output of the 10 years of simulations that is proved to be a representative condition close to the field data observations. These parameters are stable during the whole extreme case simulation, as its duration is too short (5 days) for new vegetation to be created or for existing vegetation to grow. The parameters for the death of vegetation as explained in chapter 3.7 are active. In addition, the starting point for bed level is the output of the 10 years of simulation with vegetation growth. Bed level is free to evolve under the extreme hydrodynamic conditions.

The parameters of the two cases of extreme events that are tested in this study are analyzed in chapter 2.3, while the general sediment and vegetation parameters are the result of calibration procedure analyzed in chapter 4. One extra simulation is applied for every case, the one of 5 days under normal hydrodynamic conditions, to be able to make comparisons with the extreme cases.

To be able to study the impact of vegetation on the response of the mudflat, one more case is simulated for both of the extreme events: the case without vegetation. For this hypothetical case, all the parameters are the same as for the corresponding extreme event case except of the diameter, height and the number of plants that are set to zero.

6.1 Extreme swell event

The extreme swell event differs from the normal hydrodynamic conditions by having a higher wave height, 0.5m instead of 0.2m, and a much higher wave period, 18sec instead of 3sec. All the other parameters are the same.

At the end of the 5 days of simulation, no remarkable bed level changes are observed, as shown in Figure 46. It seems that the bed level remains stable after the swell event.

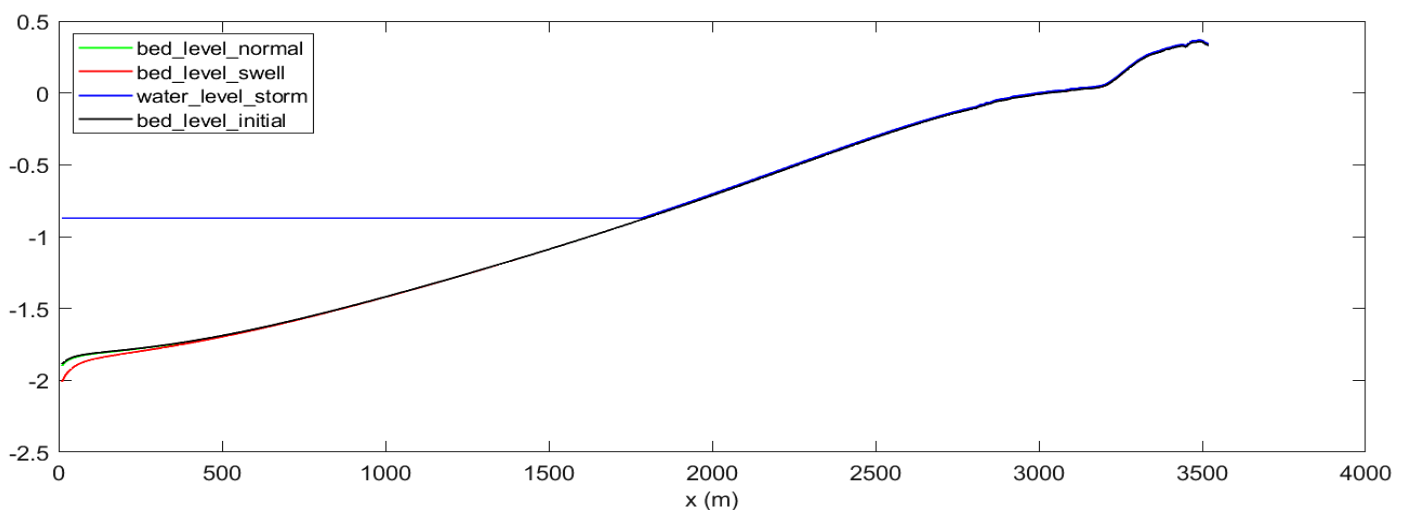


Figure 46 - Bed level profiles after 5 days of extreme swell event. The green line representing the case of normal hydrodynamic conditions is under the black one, representing the initial bed level profile. The red line represents the bed level after 5 days of extreme swell conditions and is almost the same with the other two, having only erosion in the order of 10cm at the very offshore boundary (boundary effect).

The wave height for high water – flood tide is shown in Figure 47. Wave height at the seaward boundary is the initially given one, remaining almost stable through the whole profile, before starting breaking landward.

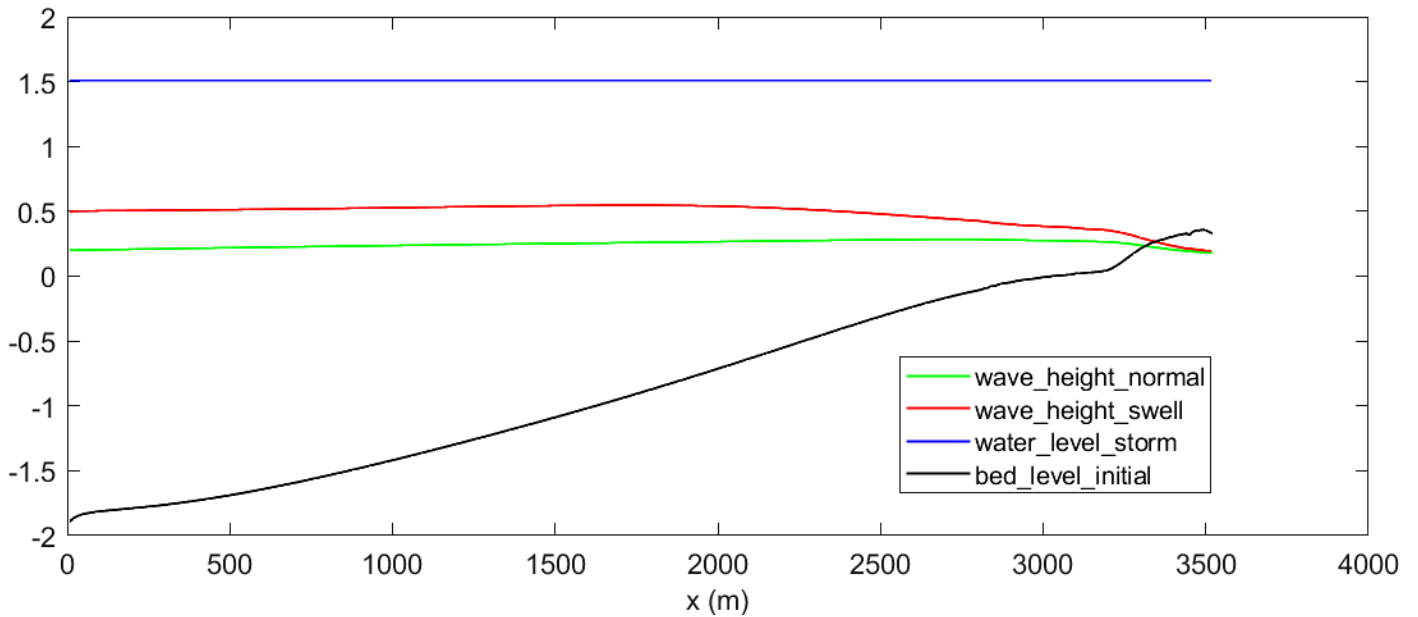


Figure 47 – Root mean square wave height (m) during flood tide – high water for normal hydrodynamic conditions (green line) and for extreme swell conditions (red line). The water level is shown by the blue line and the bed level by the black line.

The presence of vegetation reduces the wave energy as described in chapter 3.6, resulting in a wave height of 10cm at the landward boundary instead of 17cm for the hypothetical case without vegetation, as presented in Figure 48. This is a reduction of 41% on the wave height due to the presence of vegetation.

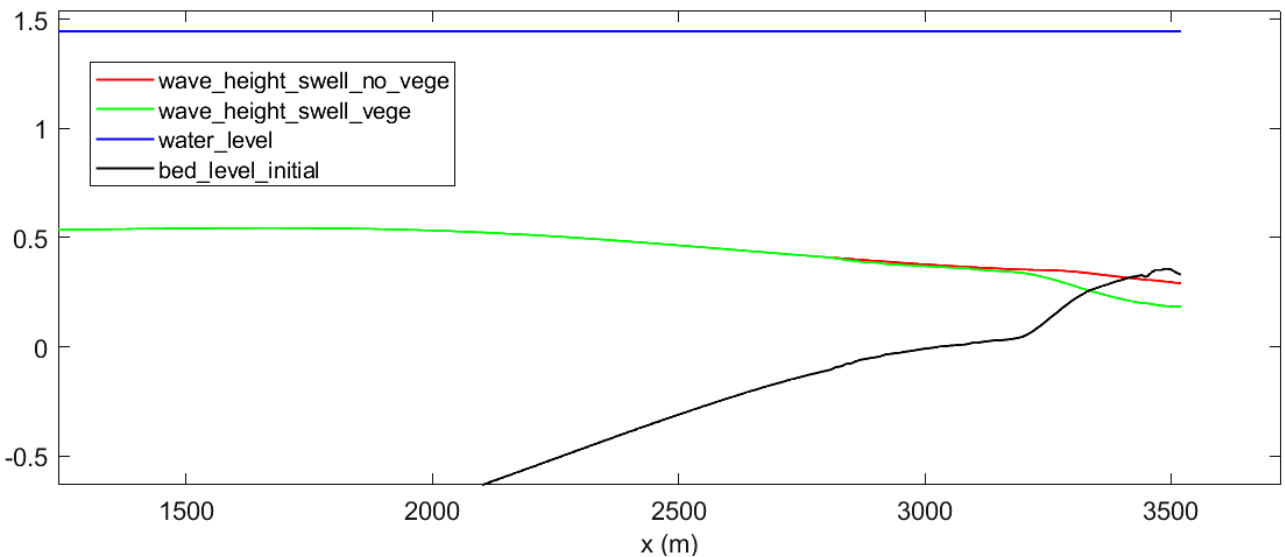


Figure 48 – Comparison of wave height (m) between the case of extreme swell event with vegetated mudflat (green line) and the hypothetical case of the same event occurring on the same mudflat without vegetation (red line) during flood tide – high water. The water level is shown by the blue line and the bed level by the black line. Only the landward half of the profile is presented as vegetation is only present landward.

Total shear stress variation for flood tide during the extreme swell event is presented in Figure 49. It is observed a higher shear stress along most of the profile because of the higher wave height compared to the normal hydrodynamic case. However, wave period is also important for the computation of wave induced shear stress, according to Equation 6.1, Equation 6.2, and Equation 6.3 below.

Equation 6.1 - Equation 22 by van der Wegen et al. (2019) for wave induced shear stress

$$\tau_w = 0.5 \cdot \rho \cdot f_w \cdot u_{orb}^2$$

Equation 6.2 - Equation 9.204 by Delft 3D Flow manual used in Mflat model about orbital velocity due to waves

$$u_{orb}^2 = \frac{1}{4} \cdot \sqrt{\pi} \cdot \frac{H_{rms} \cdot \omega}{\sinh(k \cdot h)}$$

Equation 6.3- Angular frequency of waves

$$\omega = \frac{2 \cdot \pi}{T}$$

Thus, higher wave period results to lower frequency and lower orbital velocity. Lower orbital velocity results in lower wave induced shear stress. This could explain why the shear stress during the extreme swell event is lower than during normal hydrodynamic conditions landward, where wave height is restricted by depth.

Total shear stress is lower only landward and, more precisely, landward of the breaking zone of swell waves, because the wave height for both of the cases in this area is the same due to breaking and water depth restriction. More to the offshore, the wave height for the swell event is higher and this dominates the shear stress formula causing higher shear stresses.

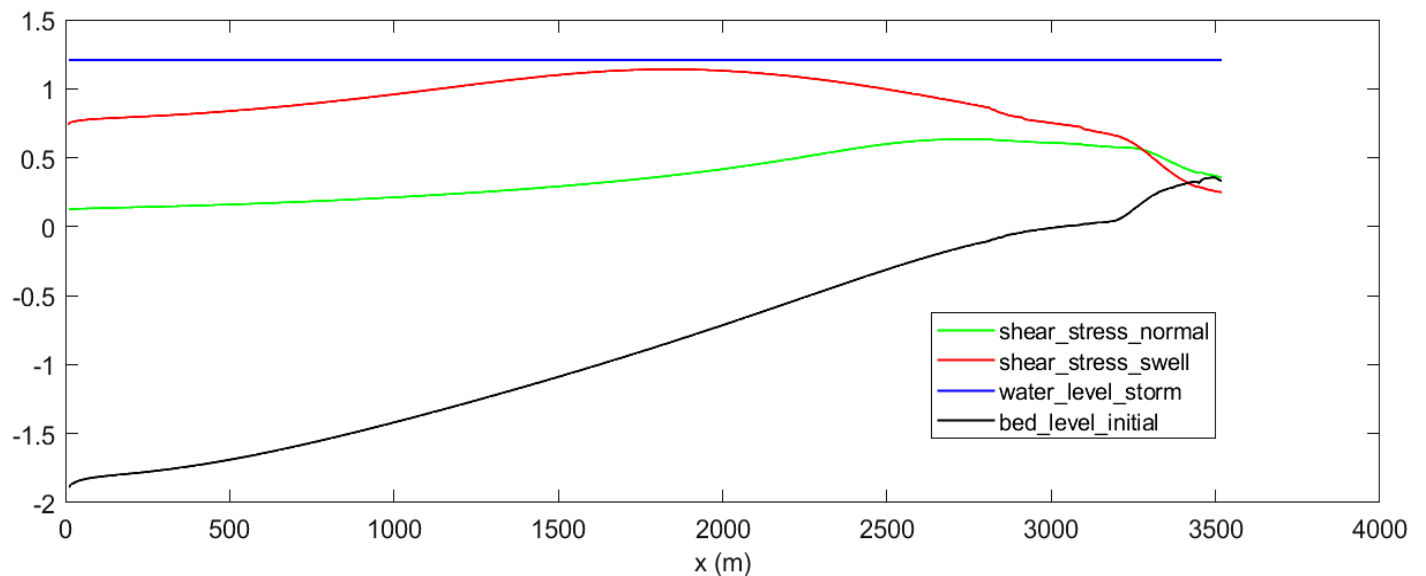


Figure 49 - Total shear stress profiles (Pa) for flood tide – high water during normal hydrodynamic conditions (green line) and during extreme swell conditions. The water level (m) is shown by the blue line and the bed level (m) by the black line.

The impact of vegetation on the shear stress is shown in Figure 50. The shear stress at the landward boundary is 0.34Pa instead of 0.72Pa for the hypothetical case without vegetation. This is a reduction of 53% due to the presence of vegetation.

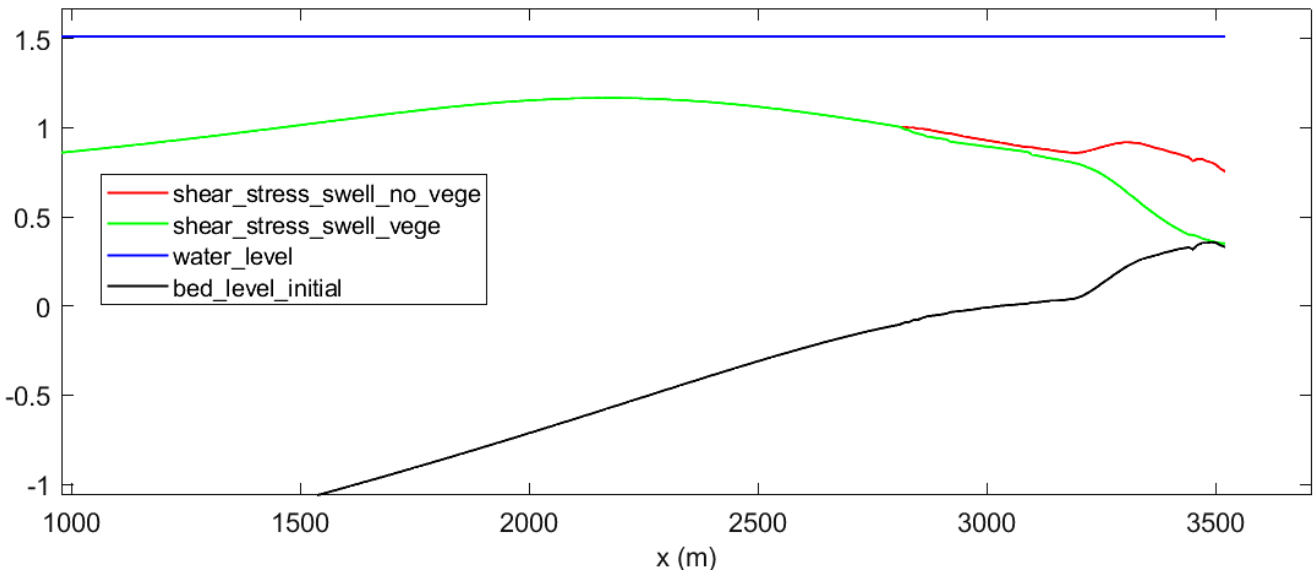


Figure 50 – Comparison of total shear stress (Pa) between the simulation for extreme swell event with vegetation (green line) and the hypothetical case of the same event occurring on the same mudflat without vegetation (red line) during flood tide – high water. The water level (m) is shown by the blue line and the bed level (m) by the black line. Only the landward half of the profile is presented as vegetation is present landward.

Sediment concentration profile, as shown in Figure 51 follows the behavior of total shear stress profile shown in Figure 49, as lower shear stress results in less erosion and lower suspended sediment concentration.

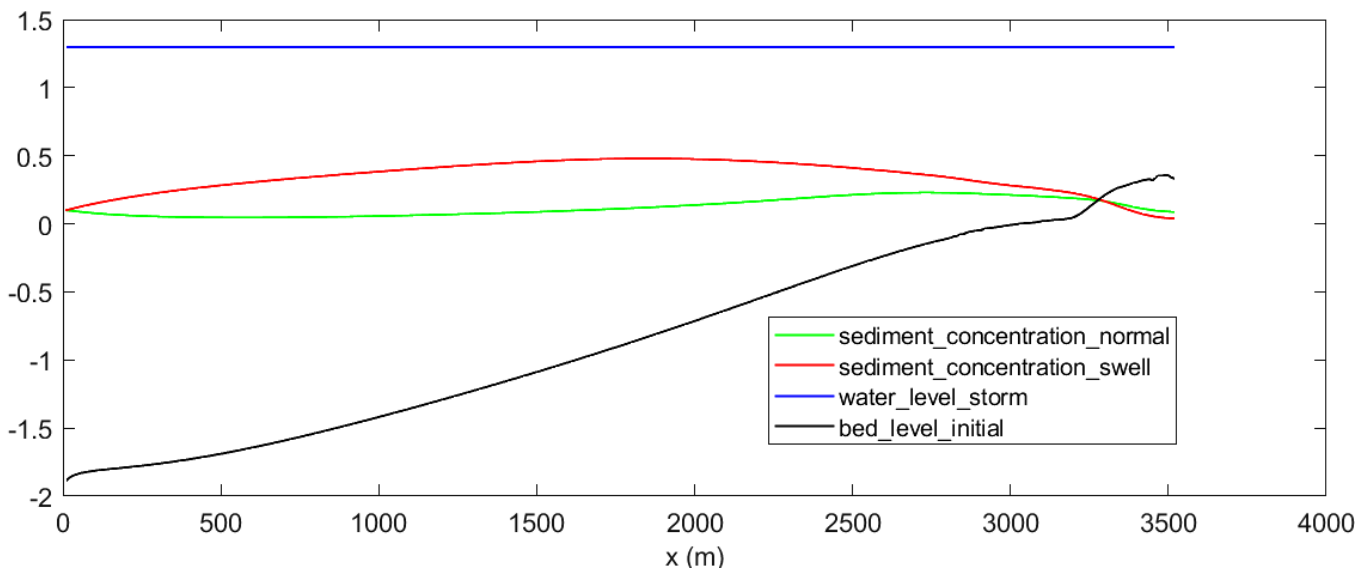


Figure 51 – Suspended sediment concentration (kgr/m^3) during flood tide – high water for normal conditions (green line) and for extreme swell conditions (red line). The water level (m) is shown by the blue line and the bed level (m) by the black line.

The presence of vegetation reduces the wave height, the total shear stress and consequently the suspended sediment concentration. From 0.20kgr/m^3 that is the concentration in the landward boundary to 0.035kgr/m^3 , resulting in a reduction of 82.5%, as shown in Figure 52.

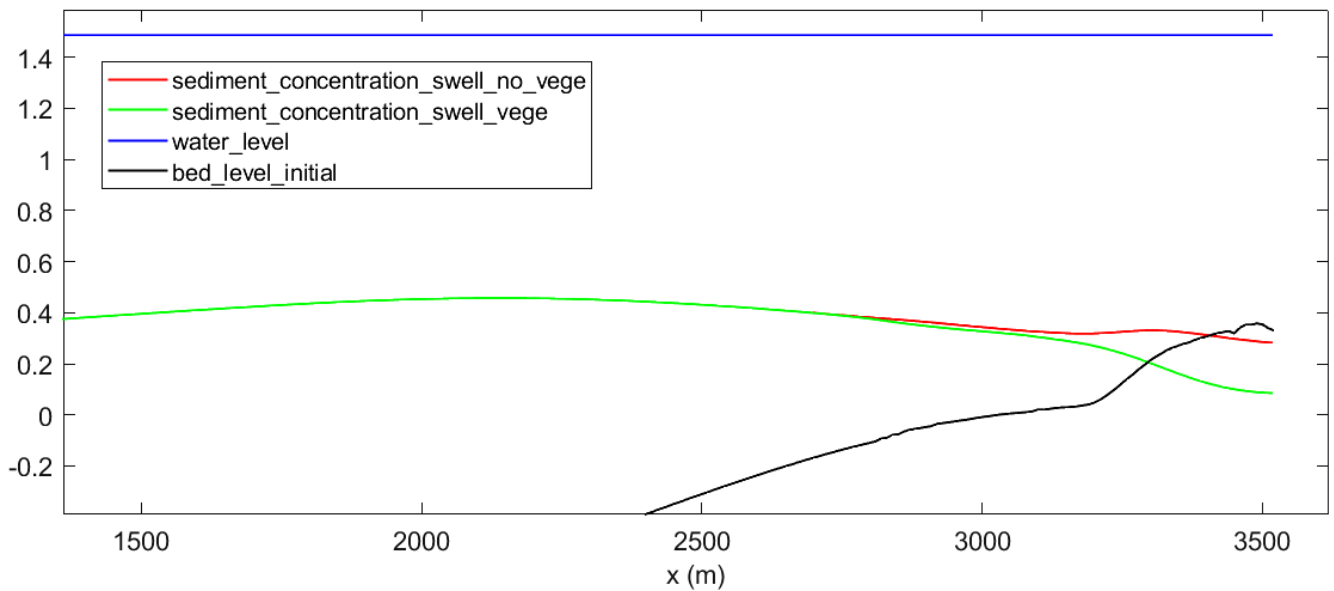


Figure 52 - Comparison of suspended sediment concentration (kg/m^3) between the case of extreme swell event with vegetated mudflat (green line) and the hypothetical case of the same event occurring on the same mudflat without vegetation (red line) during flood tide – high water. The water level (m) is shown by the blue line and the bed level (m) by the black line. Only the landward half of the profile is presented as vegetation is present landward.

Cross-shore velocity as computed by the model it is only depended on water level variation and not on the wave height or the wave period, as shown by Equation 6.4:

Equation 6.4 - Equation 1 by van der Wegen et al. (2019) about cross-shore velocity

$$u_i = \frac{dh_i}{dt} \cdot \frac{X_i}{h_i}, \text{ (} h_i \text{ represents the water depth and } X_i \text{ the distance from land boundary)}$$

Thus, in Figure 53, cross shore velocity profile for both of the cases of normal and extreme swell hydrodynamic conditions is the same.

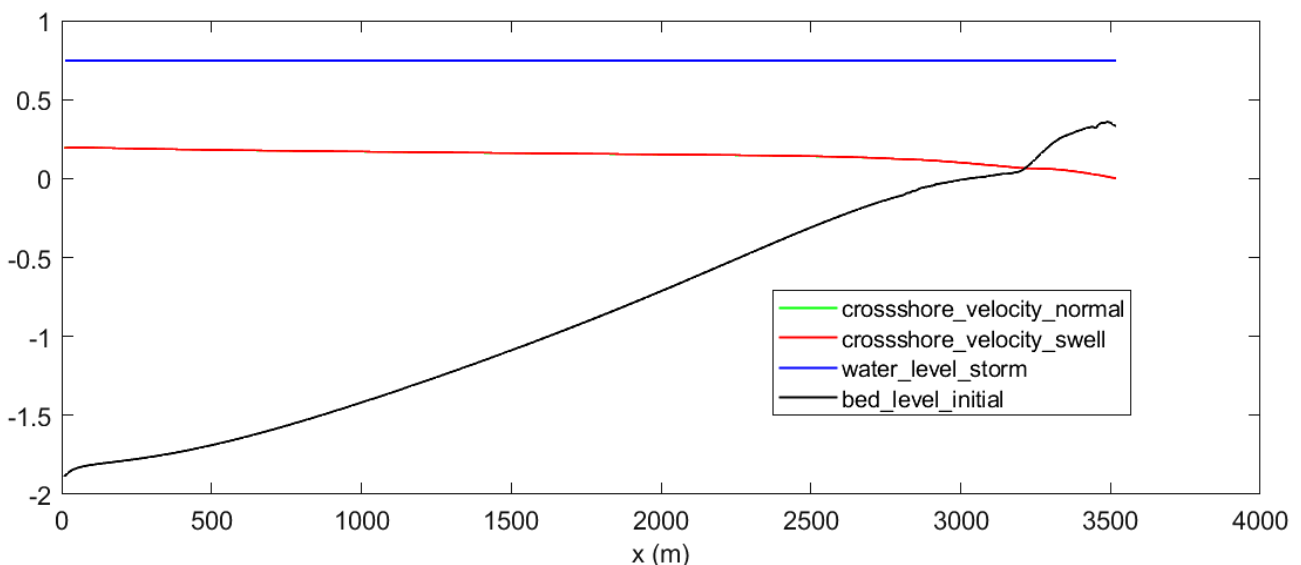


Figure 53 - Cross-shore flow velocity (m/sec) in case of extreme swell event and in case of normal hydrodynamic conditions during flood tide (both velocity profiles are on top of each other, represented by red line). The water level (m) is shown by the blue line and the bed level (m) by the black line.

Cross-shore velocity is also not affected by vegetation as there is no process included in the model to slightly reduce the water level due to the presence of vegetation as it could probably occur in reality, as analyzed in chapter 2.3, or to decrease directly the velocity due to the resistance of vegetation on the flow.

6.2 Extreme storm event

The extreme storm event differs from the normal hydrodynamic conditions by having a higher wave height, 1.0m instead of 0.2m, a higher wave period, 6sec instead of 3sec and a storm surge of 1.5m applied as a uniform increase of the water level through the whole model domain. All the other parameters are the same.

At the end of the 5 days of simulation, no remarkable bed level changes are observed, as shown in Figure 54. It seems that bed level remains the same during the storm event. This is something that is investigated further in this and in the next chapter.

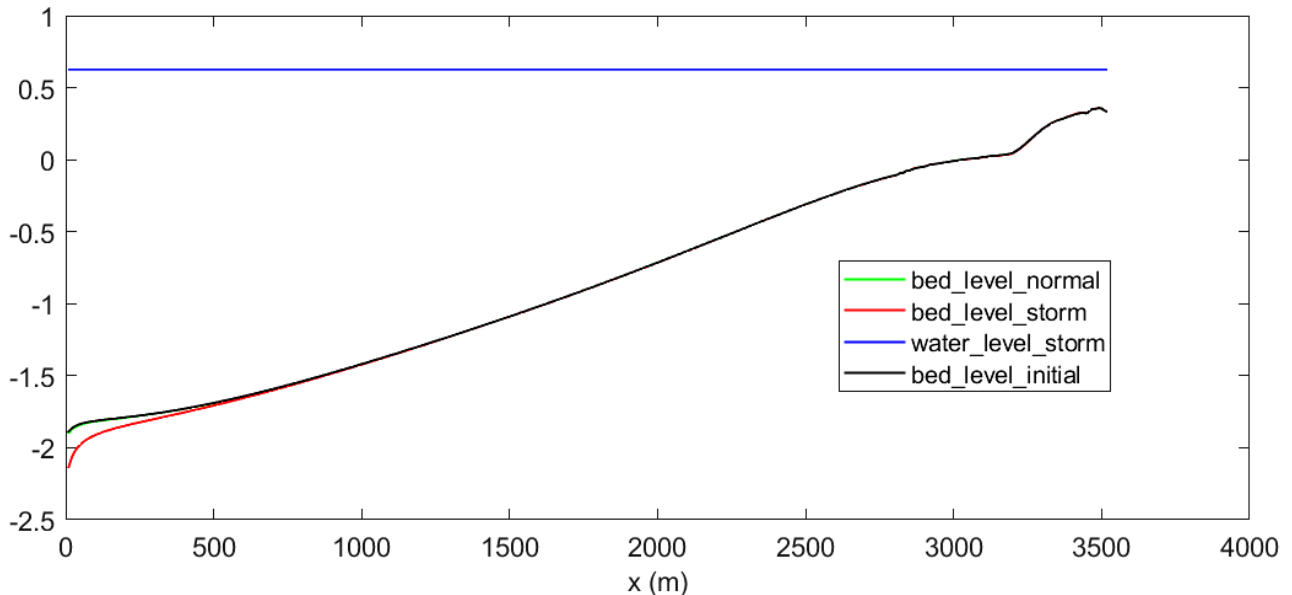


Figure 54 – Bed level profiles (m) after 5 days of extreme storm event. The green line representing the case of normal hydrodynamic conditions is under the black one, representing the initial bed level profile. The red line represents the bed level after 5 days of extreme storm conditions and is almost the same with the other two, having only erosion in the order of 10cm at the very offshore boundary (boundary effect).

The wave height for flood tide – high water is shown in Figure 55. It is higher in case of storm because of the higher initial wave height and of the higher water level due to storm surge that transfers the breaking zone more to the inshore and created higher water depths.

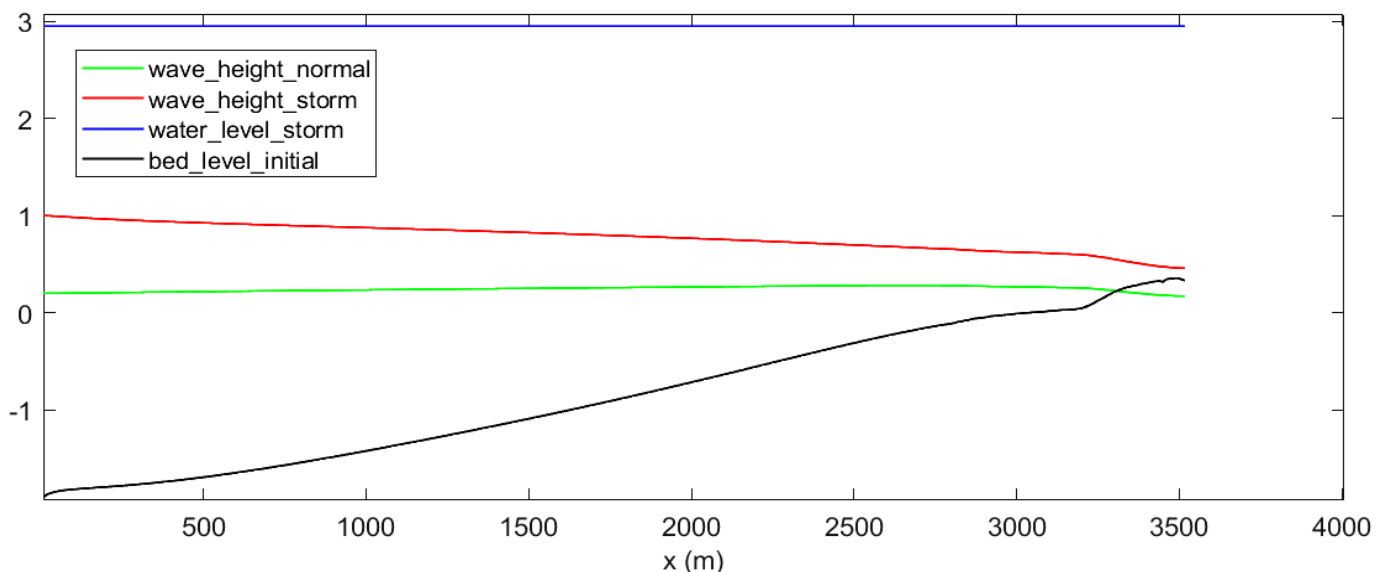


Figure 55 - Root mean square wave height (m) during flood tide – high water for normal hydrodynamic conditions (green line) and during extreme storm conditions (red line). The water level (m) during storm is shown by the blue line and the bed level (m) by the black line.

The presence of vegetation reduces the wave energy as described in chapter 3.6, resulting in a wave height of 47cm at the landward boundary instead of 57cm for the hypothetical case without vegetation, as shown in Figure 56. This is a reduction of 17.5% due to vegetation.

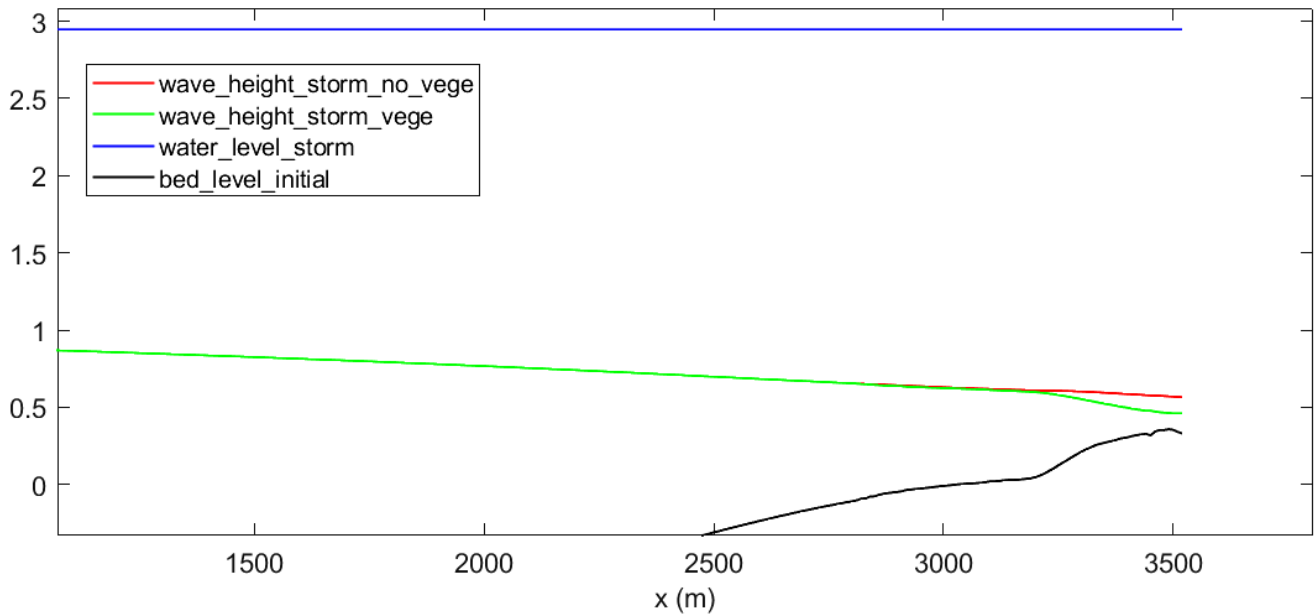


Figure 56 - Comparison of wave height (m) between the case of extreme storm event with vegetated mudflat (green line) and the hypothetical case of the same event occurring on the same mudflat without vegetation (red line) during flood tide – high water. The water level (m) is shown by the blue line and the bed level (m) by the black line. Only the landward half of the profile is presented as vegetation is present landward.

Total shear stress variation for flood tide - high water is presented in Figure 57. Total shear stress is higher through the whole model domain for the storm case, as expected, due to the much higher (five times) wave height.

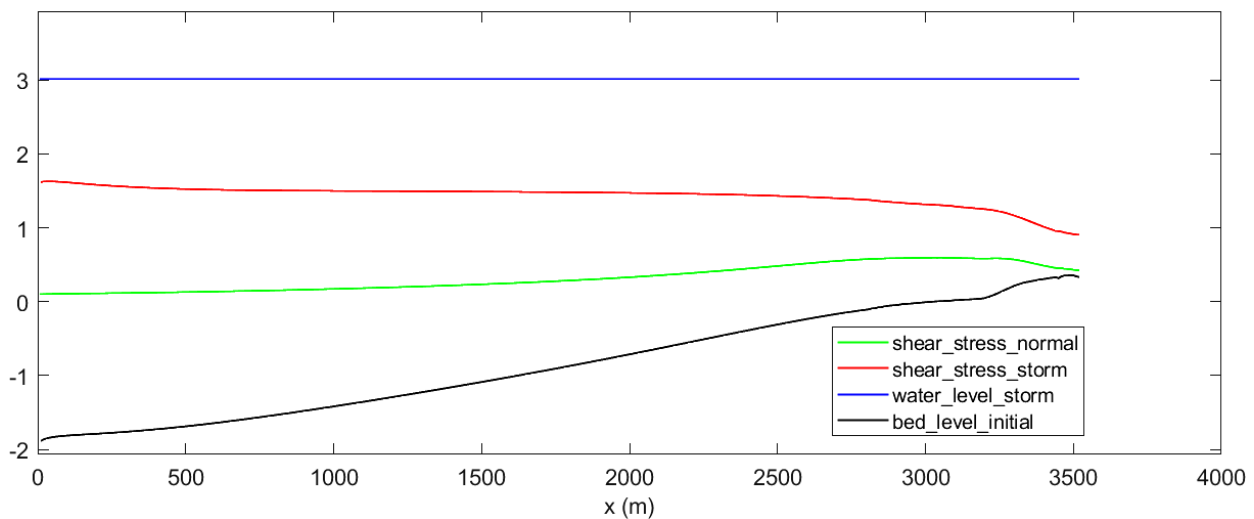


Figure 57 - Total shear stress profiles (Pa) during flood tide – high water for normal hydrodynamic conditions (green line) and during extreme storm conditions (red line). The water level (m) during storm is shown by the blue line and the bed level (m) by the black line.

The impact of vegetation on the shear stress is shown in Figure 58. The shear stress at the landward boundary is 0.90Pa instead of 1.27Pa for the hypothetical case without vegetation. This is a reduction of 29.1%. The dissipation of wave energy due to vegetation results to dissipation of the total shear stress too.

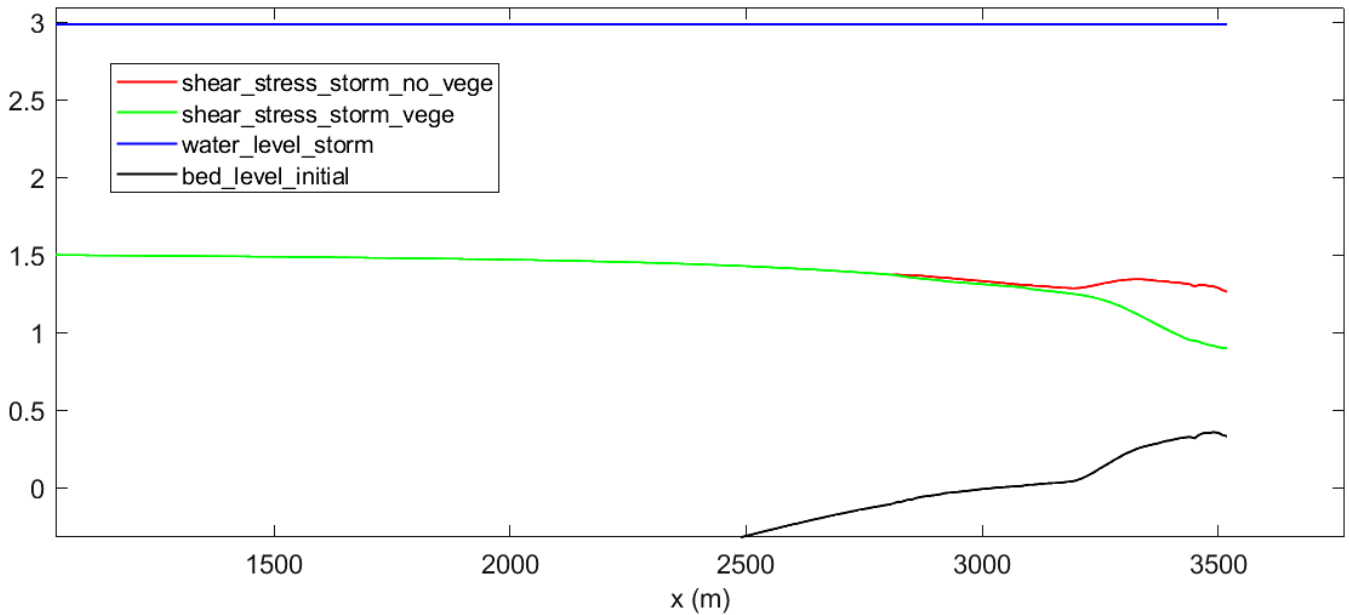


Figure 58 - Comparison of total shear stress (Pa) between the case of extreme storm event with vegetated mudflat (green line) and the hypothetical case of the same event occurring on the same mudflat without vegetation (red line) during flood tide – high water. The water level (m) is shown by the blue line and the bed level (m) by the black line. Only the landward half of the profile is presented as vegetation is present landward.

Sediment concentration follows the behavior of total shear stress profile shown in Figure 59, as lower shear stress results in less erosion and in lower suspended sediment concentration.

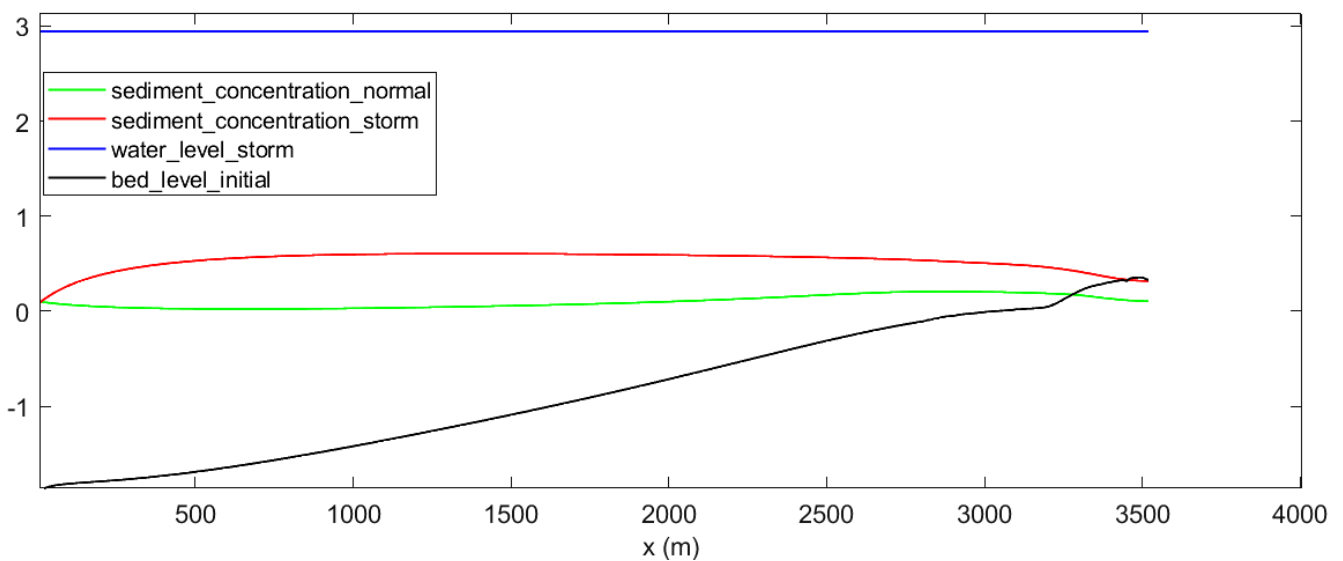


Figure 59 – Suspended sediment concentration (kg/m^3) during flood tide – high water for normal conditions (green line) and for extreme storm conditions (red line). The water level (m) during storm is shown by the blue line and the bed level (m) by the black line.

The impact of vegetation on the suspended sediment concentration is shown in Figure 60. The suspended sediment concentration at the landward boundary is $0.33\text{kg}/\text{m}^3$ instead of $0.50\text{kg}/\text{m}^3$ for the hypothetical case without vegetation. This is a reduction of 34.0% due to the presence of vegetation.

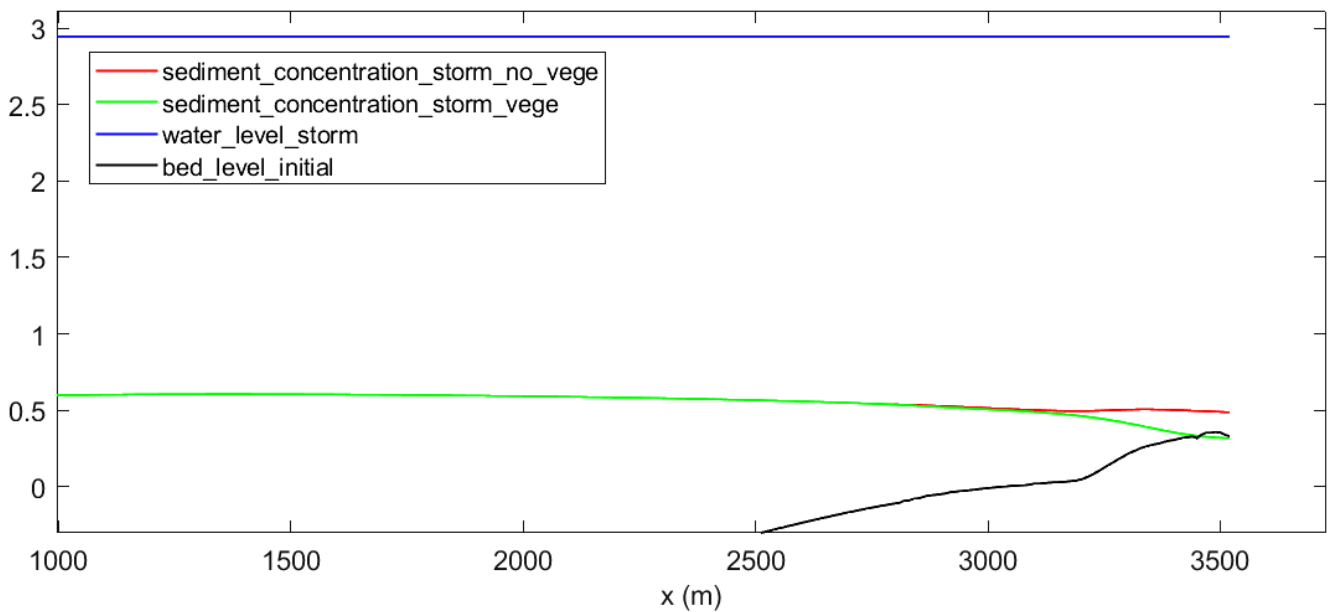


Figure 60 - Comparison of sediment concentration (kgr/m^3) between the case of extreme storm event with vegetated mudflat (green line) and the hypothetical case of the same event occurring on the same mudflat without vegetation (red line) during flood tide – high water. The water level (m) is shown by the blue line and the bed level (m) by the black line. Only the landward half of the profile is presented as vegetation is present landward.

Cross-shore velocity as simulated by the model it is only depended on water level variation and not on the wave height or the wave period, as explained for the swell case.

During normal hydrodynamic conditions, the variation of the water level is the same as in case of storm event (the astronomical tide variations), but the water level is lower, because of the absence of the storm surge. Thus, the same amount of water needs to move in a more swallow area, resulting in higher cross-shore velocity compared with the extreme storm case as shown in Figure 61. This explanation together with Figure 61 it may seems to be unrealistic for the storm case, as higher cross-shore velocities would be expected in the real storm case, but in the real case more hydrodynamic processes contribute to the cross-shore velocity than only the tide-induced water level change, as analyzed in chapter 7. So, taking into account how cross-shore velocity is simulated by the model, this result seems reasonable even if it is not realistic.

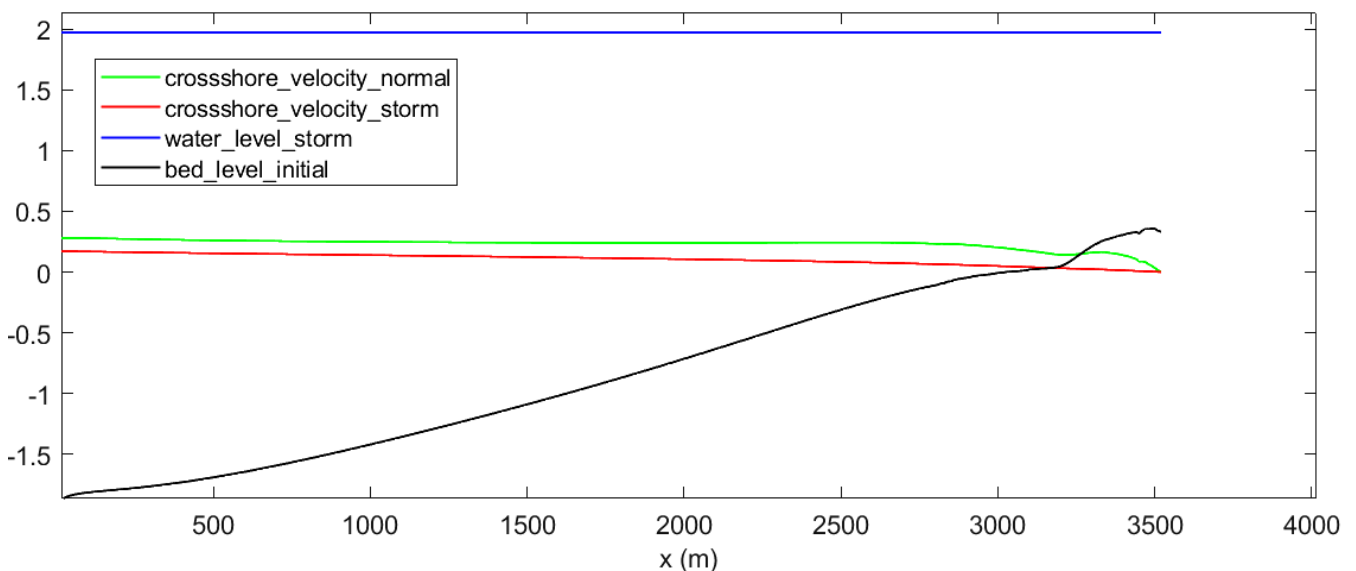


Figure 61 - Cross-shore flow velocity (m/sec) in case of extreme storm event (red line) and in case of normal hydrodynamic conditions (green line) during flood tide. The water level (m) during storm is shown by the blue line and the bed level (m) by the black line.

6.3 Sensitivity analysis for the storm case

It is observed that bed level does not have any remarkable change after five days of extreme storm conditions. To be able to investigate the reason why this is happening and understand if this is the case in reality or if something is missing from this analysis, further results and trials are presented in this chapter.

During the last tide of the five days of extreme storm simulation, bed level changes are shown in Figure 62. The bed level appears to be quite stable during the whole tidal period.

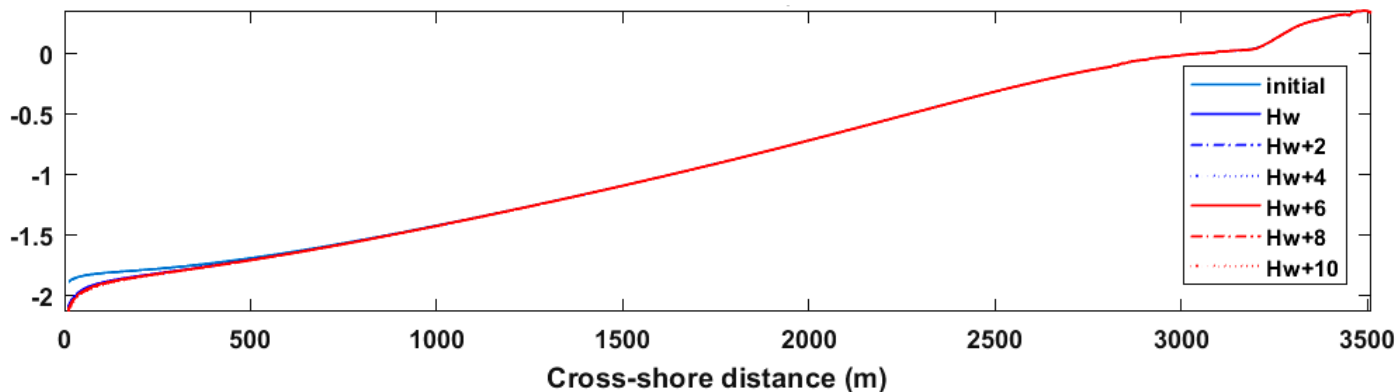


Figure 62 - Bed level profiles (m) for the last tide of the five days of extreme storm simulation. Profile plot for every 2 hours. Only in the seaward boundary the initial bed level is distinguished from the final one, while during the whole tidal period bed level remains stable.

The evolution of bed level during the whole period of 5 days of extreme storm is shown in Figure 63, together with the water level variation due to tide. Bed level is stable during the whole storm duration. There is only slight erosion at the seaward boundary, for the first 500m as boundary effect.

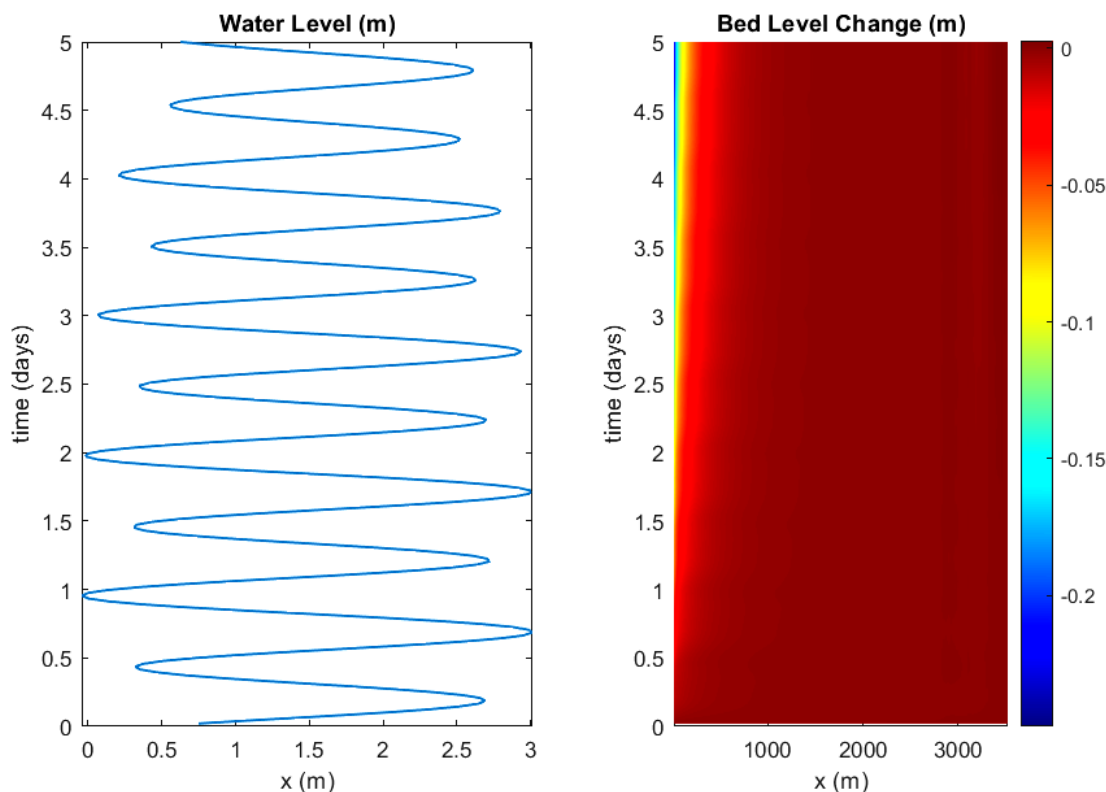


Figure 63 - Water level (m) and bed level (m) variation during the 5 days of storm conditions

The processes that cause the bed level changes are erosion and deposition. The cumulative erosion and deposition for each grid cell after the 5 days of simulation with a morphological factor of 1 for the normal hydrodynamic conditions and for the storm conditions are presented in Figure 64.

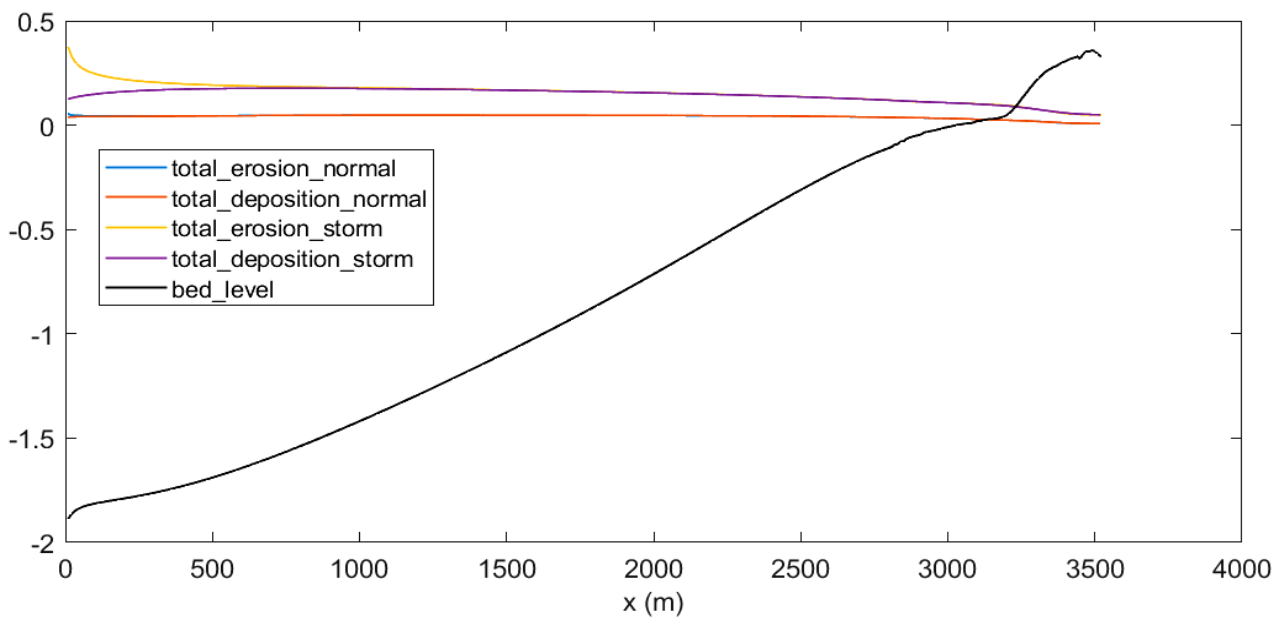


Figure 64 - Cumulative deposition (m) for normal conditions (red line), cumulative erosion for normal conditions (blue line, hidden behind the red one), cumulative deposition (m) for storm conditions (purple line) and cumulative erosion for storm conditions (orange line) through the model domain for 5 days of simulation. Bed level is shown by the black line.

It is observed that for both of the cases (normal and storm conditions), the cumulative erosion is equal with the cumulative deposition, except of the first 500m for storm conditions. This fact can explain the reason why there are no remarkable bed level changes. For the storm case, cumulative erosion and deposition are higher (almost double) compared with the case of normal hydrodynamic conditions, as expected for a more dynamic environment.

In an effort to understand which parameter of the model could be important for the equality of erosion and deposition, a sensitivity analysis is applied as analyzed in Table 11. The motive to test each case is explained as the “physical explanation” in the table. The “high” and “low” values are chosen to have large difference compared to the normal case, to be able to understand the behavior of the model.

Table 11 - The parameters of storm sensitivity analysis together with their physical explanation

Parameter	Normal	High	Low	Physical Explanation	Figure
settling velocity (m/sec)	0.0012	0.0048	0.0006	Higher velocity due to higher flocculation caused by higher concentration during storm conditions Lower velocity due to higher turbidity	Figure 65
diffusion coefficient	1.5	5	0.5	Diffusion coefficient drives the sediment concentration due to diffusion - an effort to check if different coefficient during storm, because of the different conditions, could affect the profile	Figure 66
critical shear stress (Pa)	0.18	-	0.05	Lower critical shear stress because of the soft mud layer on bed surface that could be eroded more easily	Figure 67
sediment boundary concentration (kg/m³)	0.1	0.2	-	Higher sediment boundary concentration because of the more severe hydrodynamic conditions and higher turbidity	Figure 68

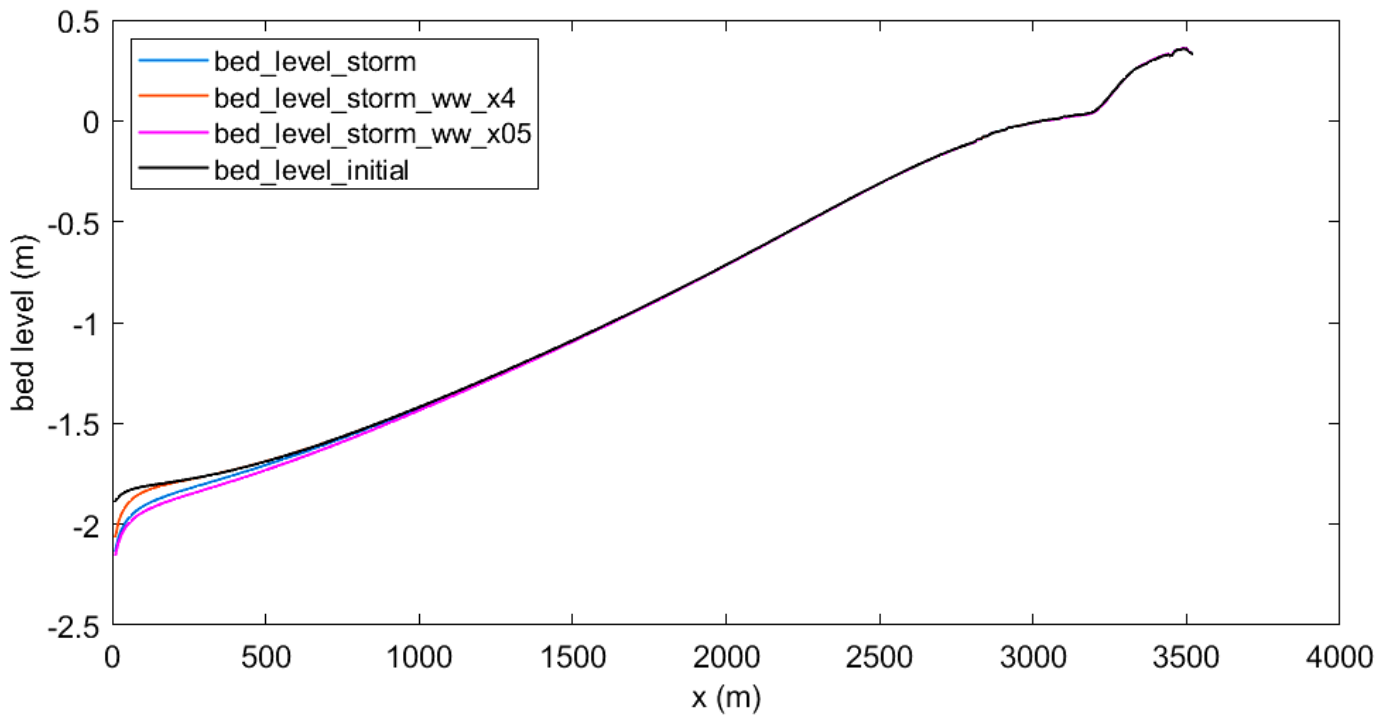


Figure 65 - Bed level profiles (m) after 5 days of storm conditions for the extreme storm (blue line), for the extreme storm using a four times higher settling velocity – $ww = 0.0048$ m/sec instead of $ww = 0.0012$ m/sec – (red line) and for the extreme storm using the half settling velocity – $ww = 0.0006$ m/sec instead of $ww = 0.0012$ m/sec – (magenta line)

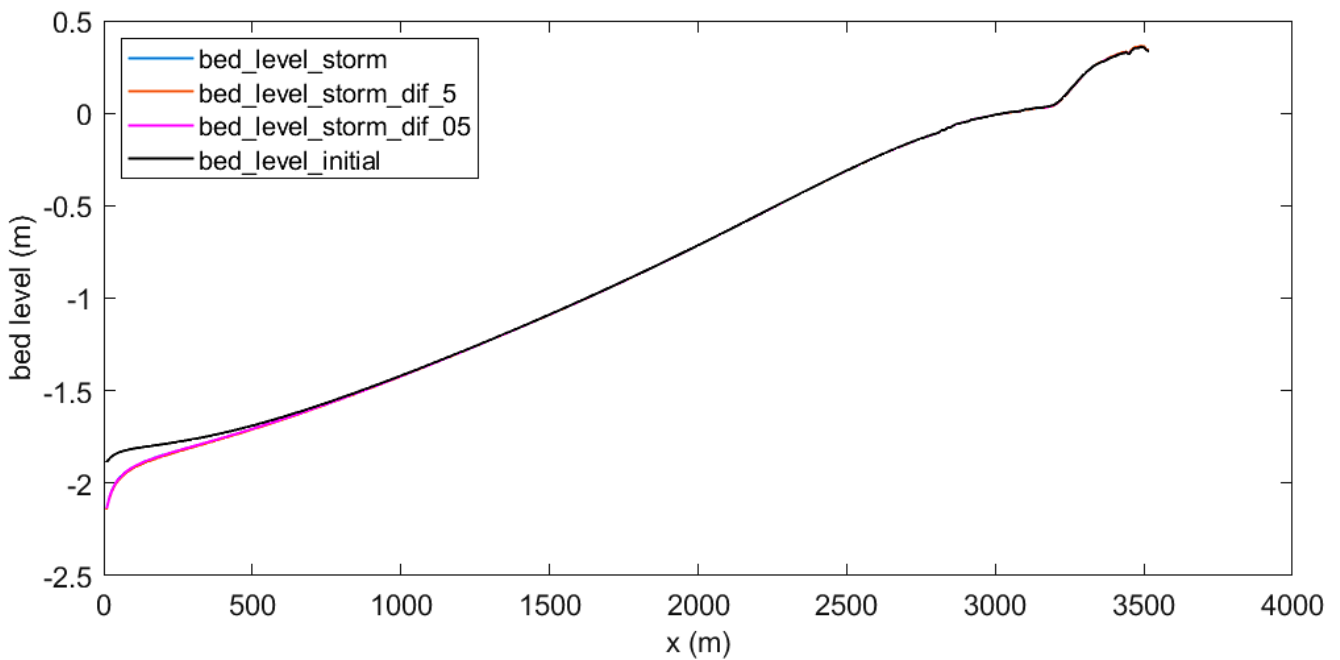


Figure 66 - Bed level profiles (m) after 5 days of storm conditions for the extreme storm (blue line), for the extreme storm using higher diffusion coefficient – $dif = 5$ instead of $dif = 1.5$ – (red line) and for the extreme storm using lower diffusion coefficient – $dif = 0.5$ instead of $dif = 1.5$ – (magenta line). All the profiles are on top of each other.

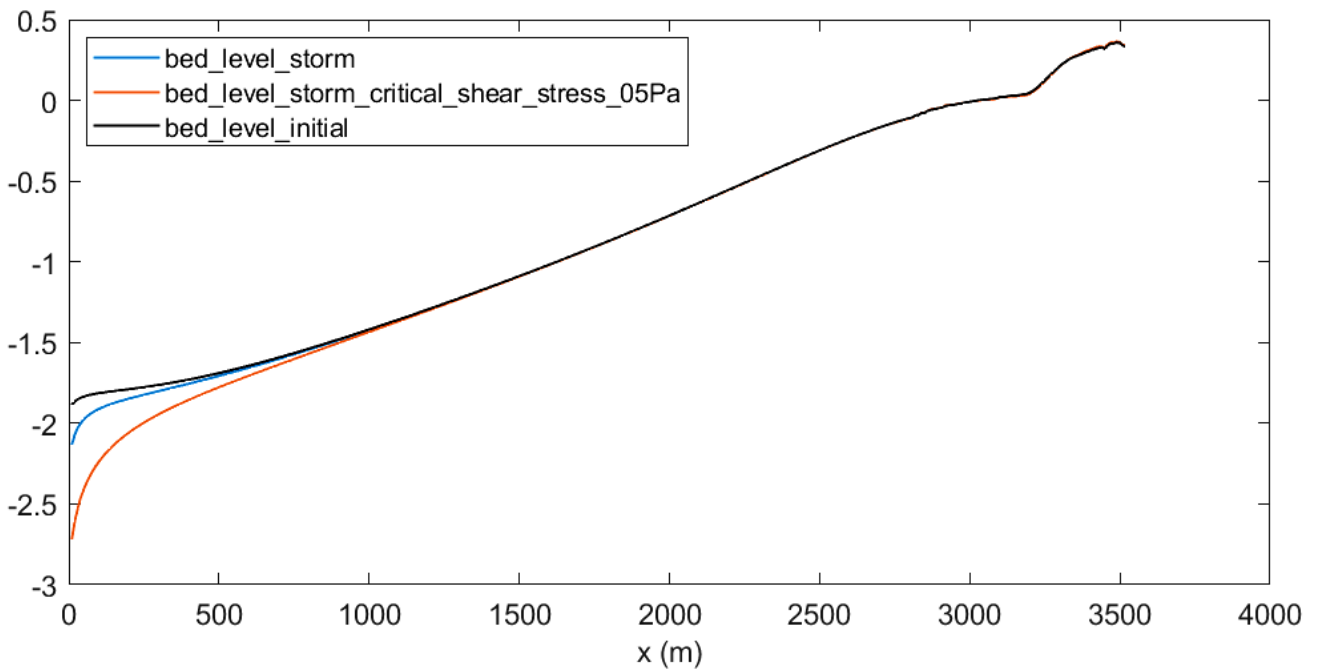


Figure 67 – Bed level profiles (m) after 5 days of storm conditions for the extreme storm (blue line) and for the extreme storm using lower critical shear stress – $\tau_{cr} = 0.05$ Pa instead of $\tau_{cr} = 0.18$ Pa – (red line). The initial bed level is shown by the black line.

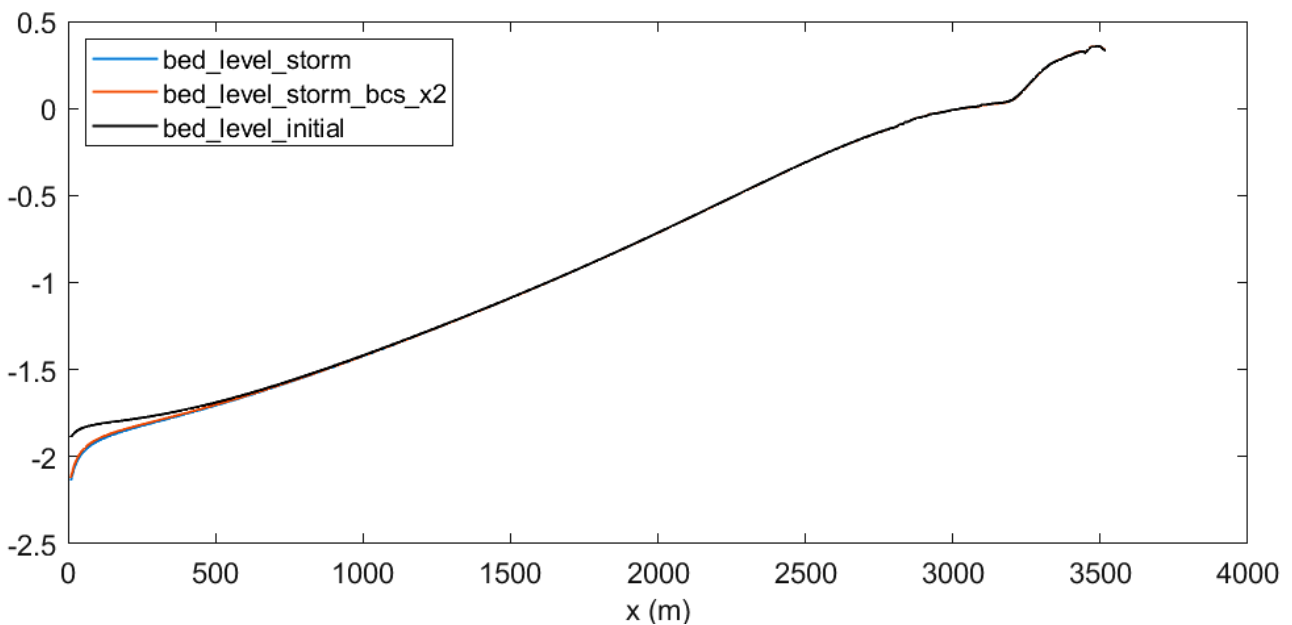


Figure 68 - Bed level profiles (m) after 5 days of storm conditions for the extreme storm (blue line) and for the extreme storm using higher boundary sediment concentration – $bcs = 0.2$ kg/m^3 instead of $bcs = 0.1$ kg/m^3 – (red line)

It is observed that for all the four cases of variation the bed level profile (except of the seaward boundary) remains stable despite of the changes in various parameters that are tested. In all the above cases, erosion is equal with deposition and the differences on bed level profile between the reference storm described in chapter 6.2 and the tested cases is in the order of 1mm to 3mm at the landward boundary.

Thus, it could be stated that the stability of the profile is not caused by the effect of one parameter of the model, but that the combination chosen by the calibration process to produce a long term profile in equilibrium, together with the very mild slope does not allow for short term bed level changes even under severe hydrodynamic conditions.

Another interesting finding is that the wave height is restricted by bed level and dissipation of energy: In the following case, a double wave height ($H_{rms} = 2\text{m}$ instead of 1m) is used and, as shown in Figure 69, the higher wave height is rapidly reduced and becomes equal with the normal one used for the storm case.

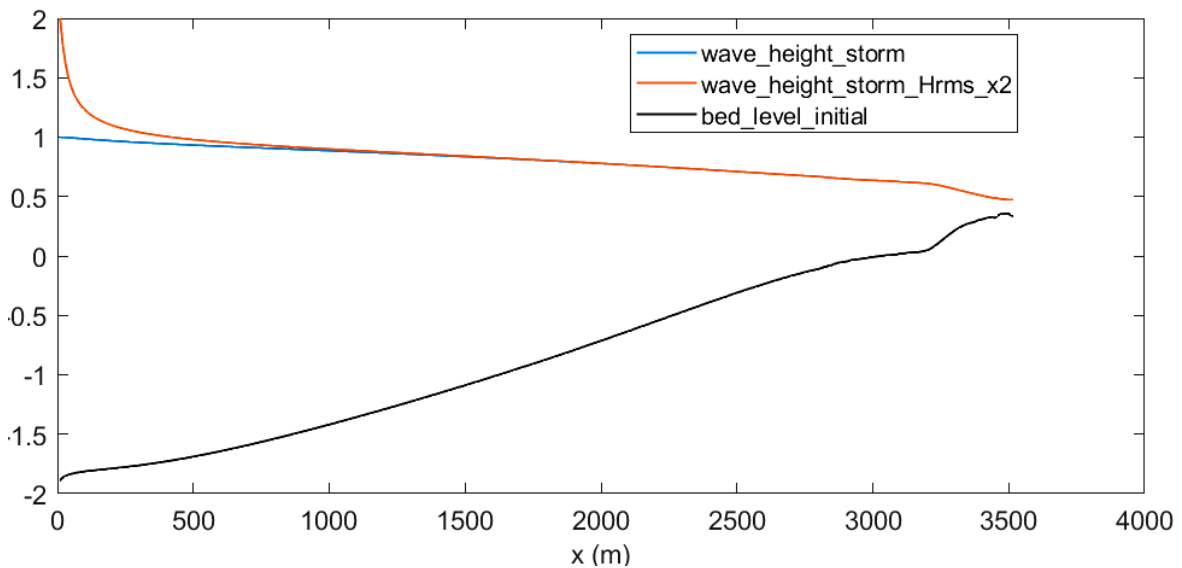


Figure 69 - Wave height profiles (m) for flood tide – high water during the 5 days of extreme storm simulation. Comparison between the normal storm conditions (blue line) and the conditions with a storm using double wave height (red line). Bed level is shown by the black line.

The slope effect

The slope of Guyana coastline is very mild, in the order of 1:1500, compared to other muddy coasts worldwide, so it is considered useful to check the impact of it on the response of bed level profile after the extreme storm event. To test this case, as a reference is used the initial 1970 profile, without vegetation, with the same characteristics as analyzed in chapter 4.2 that is under the extreme storm conditions assumed for Guyana as analyzed in chapter 2.3. The reason of this choice is the clear uniform slope of the profile. Vegetated bed level profiles, especially at the landward part, are quite complex making the study of the effect of the slope more difficult to apply and to be understood.

The steeper coast is consisted of exactly the same sediment and hydrodynamic parameters using 10 times steeper slope, i.e. 1:150 instead of 1:1500. The results are shown in Figure 70 and the bed level differences between the time moments right before and right after the storm for the two cases in Figure 71.

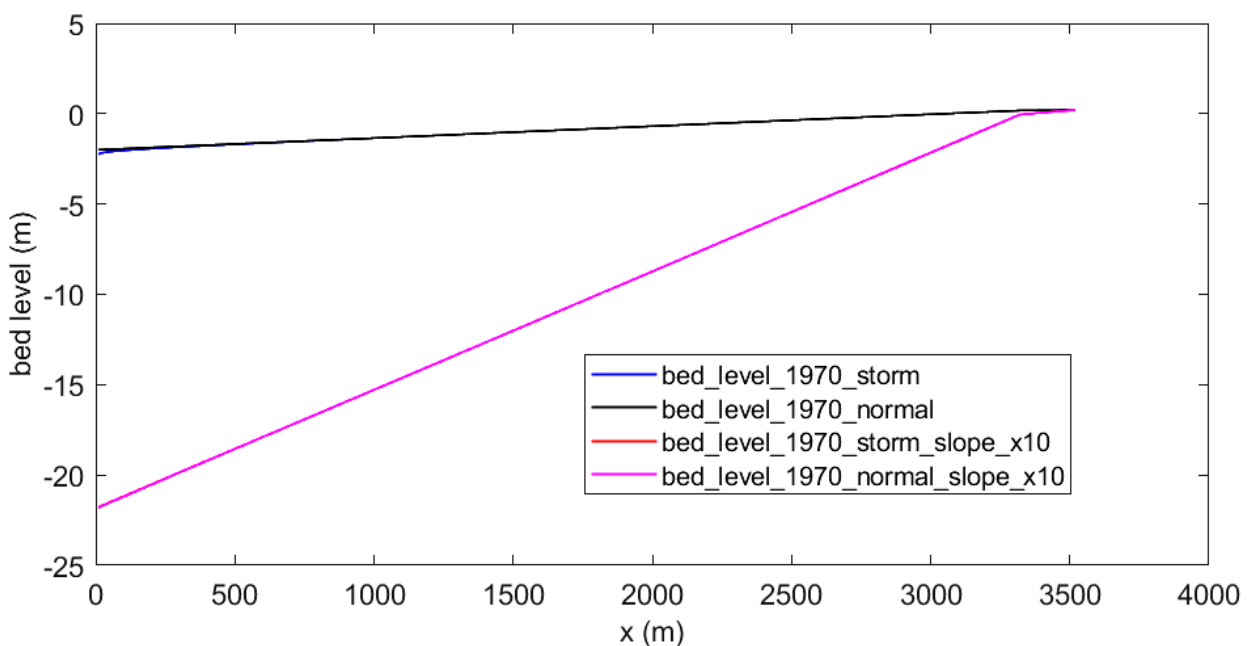


Figure 70 - Bed level profiles (m) for the case of Guyana coast slope (black line) and for the hypothetical case of 10 times steeper coast (magenta line). The differences after 5 days of storm conditions are not visible in the scale of water depth.

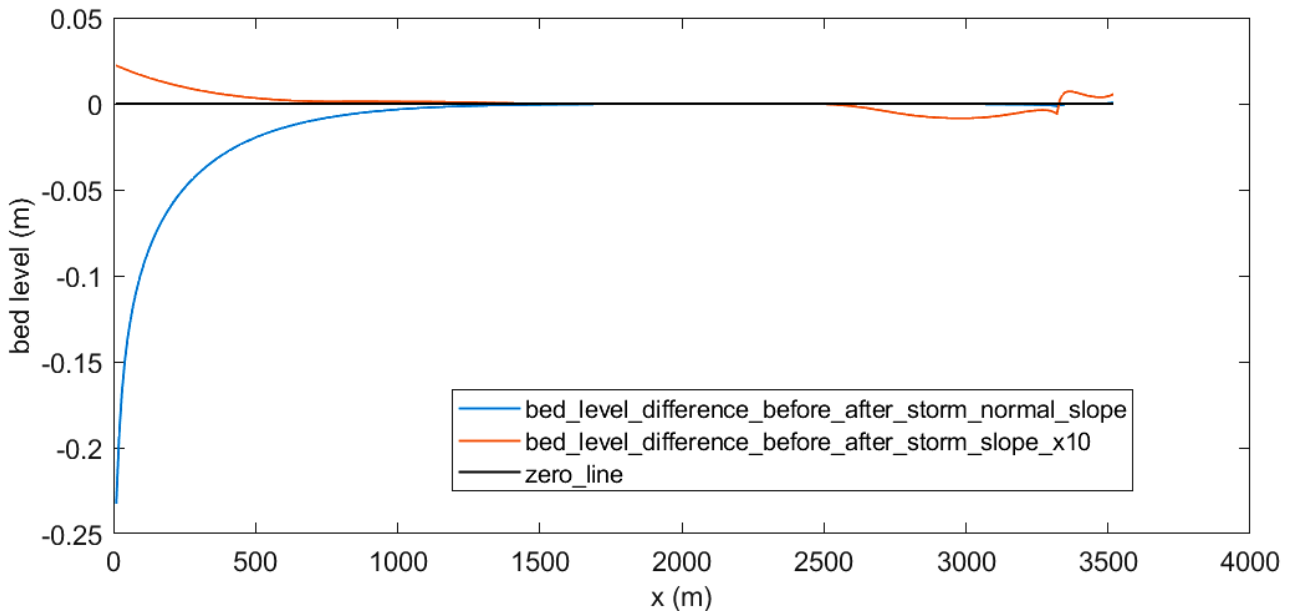


Figure 71 - Differences on bed level between the starting bed level and the final one after 5 days of storm conditions for Guyana coast (blue line) and for the hypothetical case of 10 times steeper coast (red line). With black line is represented the horizontal axis.

It is observed that the bed level changes, except of the seaward boundary are in the order of 0.5mm for the 1970 profile and in the order of 7mm for the steeper mudflat. Thus, an order of magnitude steeper slope results to an order of magnitude larger bed level change. A magnification of the landward part of the profile is shown in Figure 72. The point at 3310m where there is a jump from erosion to deposition is the point where the physical slope becomes milder by the definition of the profile (the last 200m of the profile have a slope of 1:8000m instead of 1:1500m for the 1970 profile of Guyana coast).

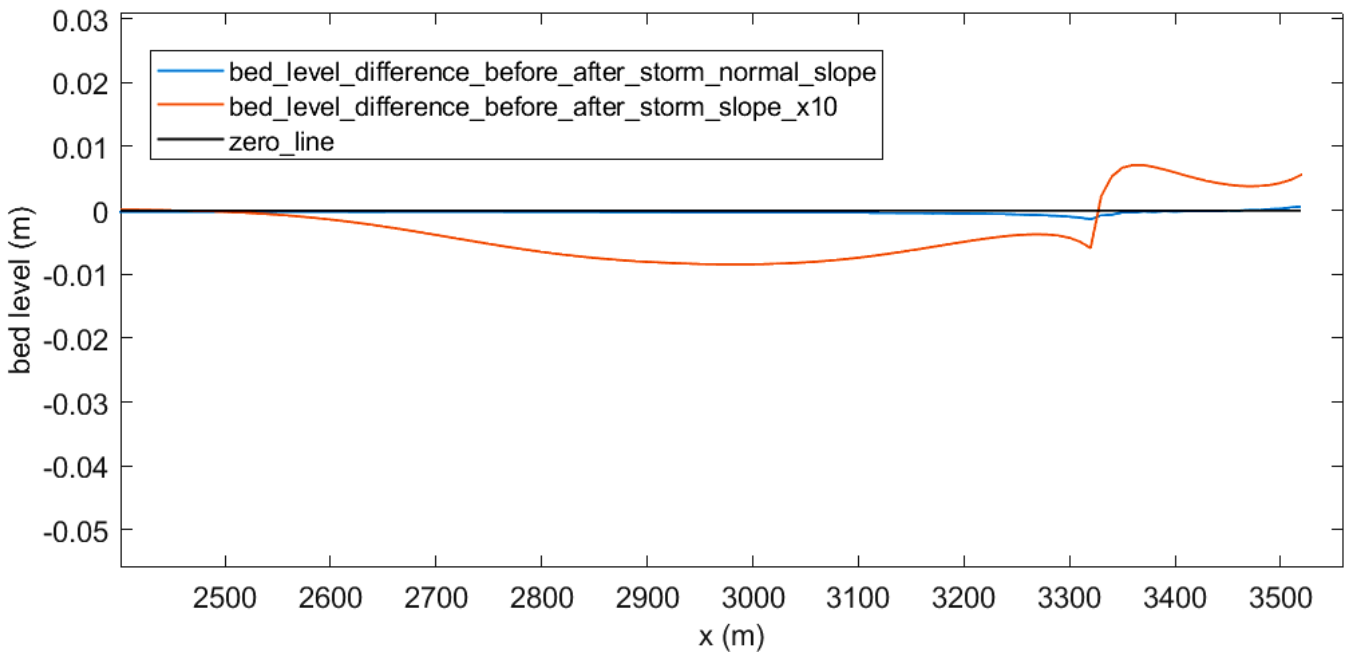


Figure 72 - Differences on bed level (m) between the starting bed level and the final one after 5 days of storm conditions for Guyana coast (blue line) and for the hypothetical case of 10 times steeper coast (red line). With black line is represented the horizontal axis. The figure shows a magnification into the landward part of the profile. The point (at 3310m) where the profile jumps from erosion to deposition is where the initial slope changes and becomes milder.

Forcing erosion

To understand how the model works for so mild slope and if it is possible to have more erosive conditions than for the storm case, a hypothetical case is tested intended to force the mudflat to erode. To succeed so, the critical shear stress is decreased (to increase erosion) from 0.18Pa to 0.05Pa and the settling velocity is also decreased (to avoid deposition) from 1.2mm/sec to 0.3mm/sec. Suspended sediment concentration is expected to be much higher and this sediment is expected to exit the model domain during ebb tide, so more erosion to be succeeded.

Indeed, as shown in Figure 73, during flood tide, suspended sediment concentration is much more increased for this case, compared to the reference one while during ebb tide, Figure 74, sediment concentration is very high at the seaward boundary indicating the export of sediment from the mudflat.

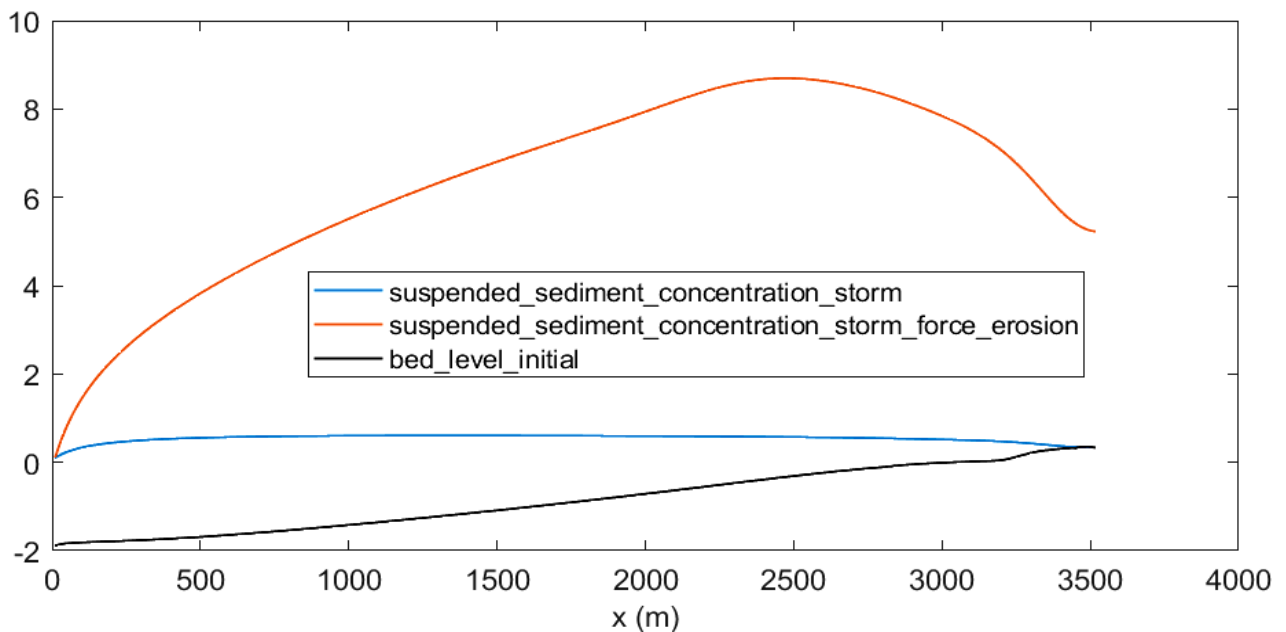


Figure 73 - Suspended sediment concentration (kg/m^3) for the normal storm case (blue line) and for the “forced erosion” storm case (red line) during flood tide – high water. With black line is shown the bed level (m) in the beginning of the storm.

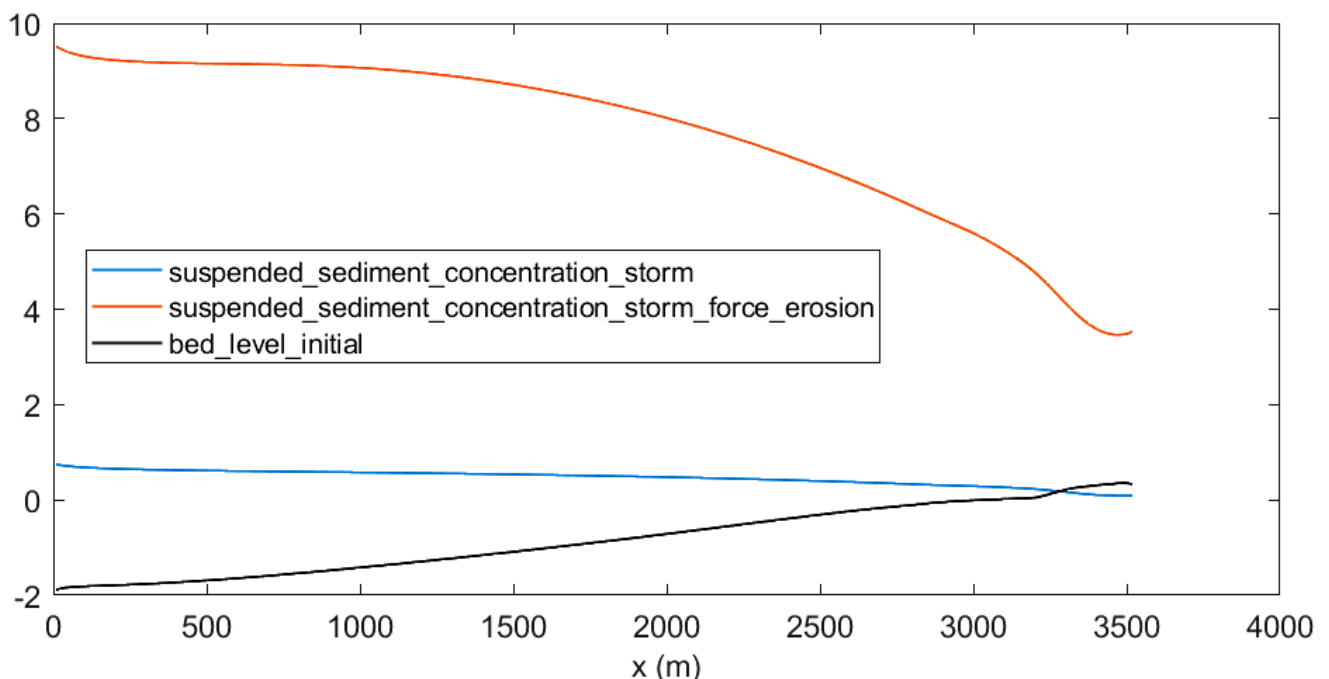


Figure 74 – Suspended sediment concentration (kg/m^3) for the normal storm case (blue line) and for the “forced erosion” case (red line) during ebb tide – high water + 4 hours. With black line is shown the bed level (m) in the beginning of the storm.

The erosion and deposition during flood and ebb tide for the normal storm case and for the “forced erosion” storm case are shown in Figure 75 and Figure 76. The magnitude of both erosion and deposition for the “forced erosion” case is 3 to 4 times higher compared with the normal storm case. It is also remarkable that for the “forced erosion” case, for flood tide, erosion is higher than deposition, while for all the other cases erosion equals deposition.

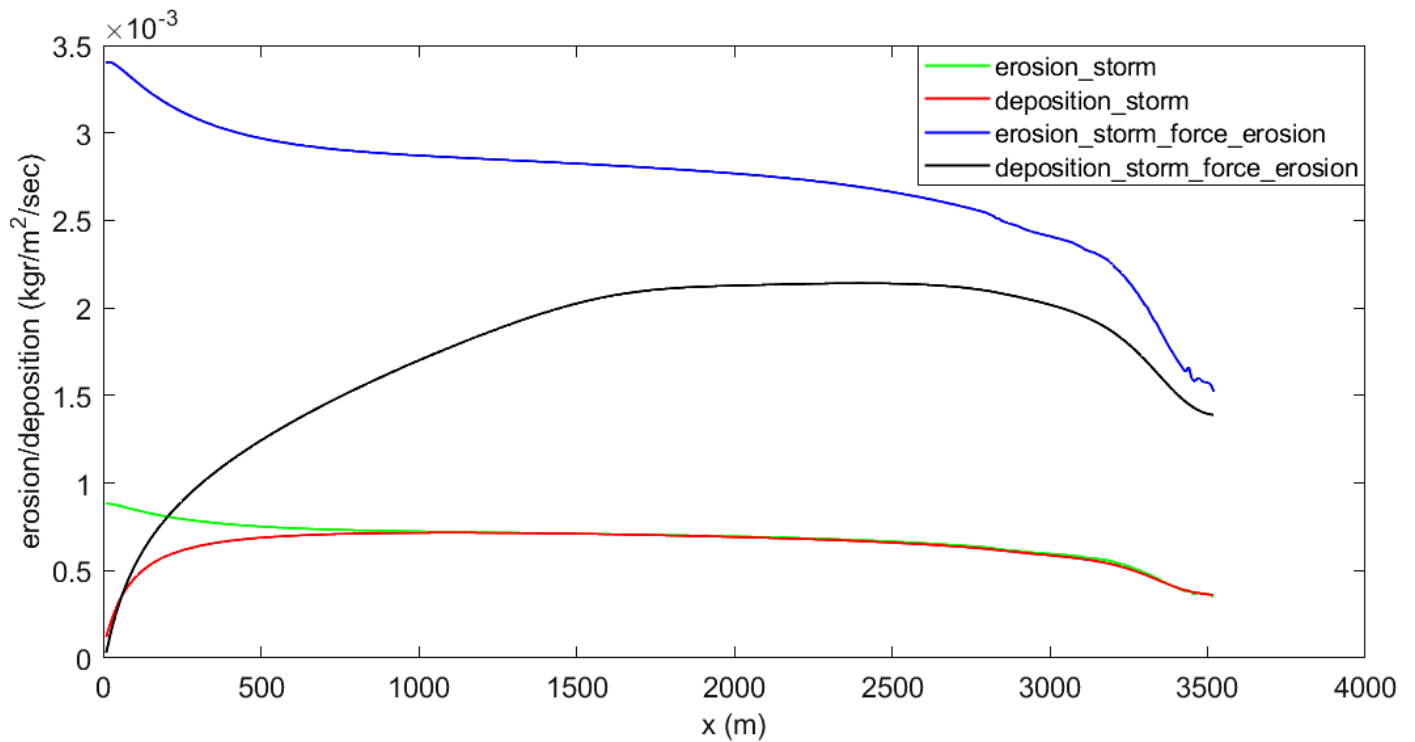


Figure 75 - Erosion and deposition (kgr/m²/sec) during flood tide – high water. Erosion for normal storm case (green line), deposition for normal storm case (red line), erosion for “forced erosion” storm case (blue line) and deposition for “forced erosion” storm case (black line).

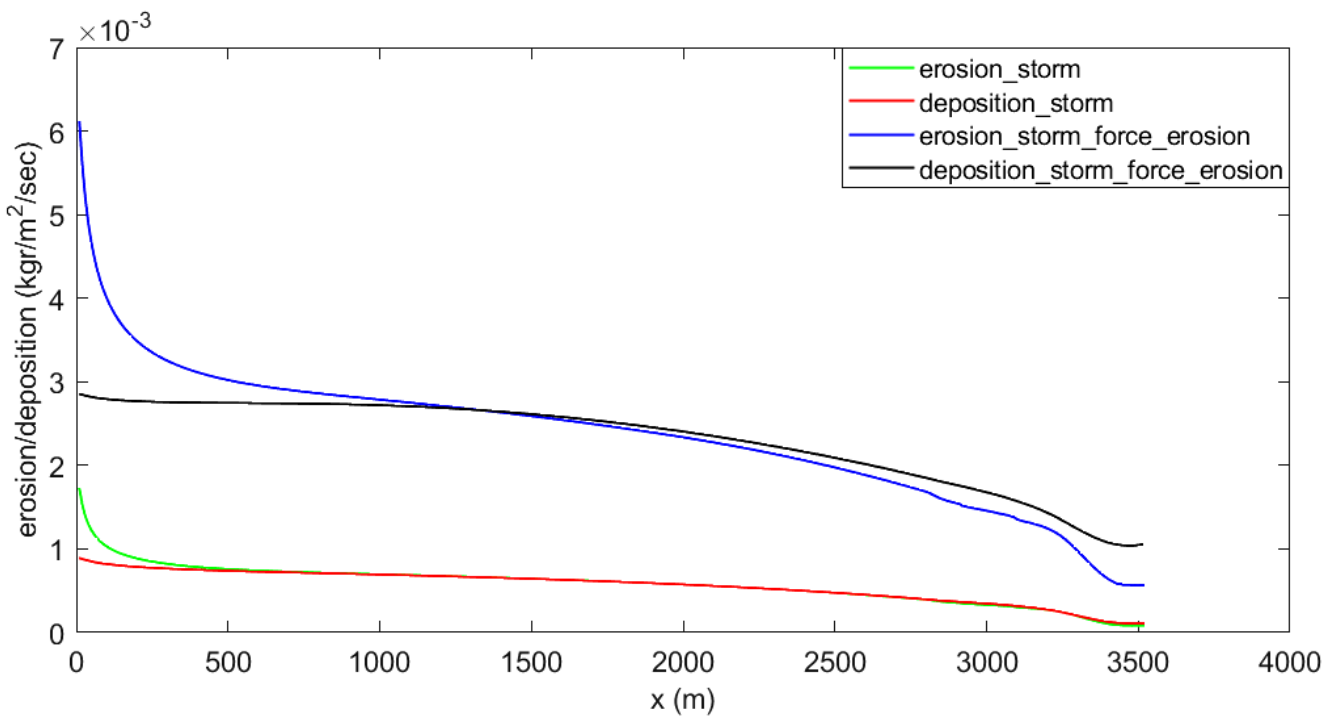


Figure 76 – Erosion and deposition (kgr/m²/sec) during ebb tide – high water + 4 hours. Erosion for normal storm case (green line), deposition for normal storm case (red line), erosion for “forced erosion” storm case (blue line) and deposition for “forced erosion” storm case (black line).

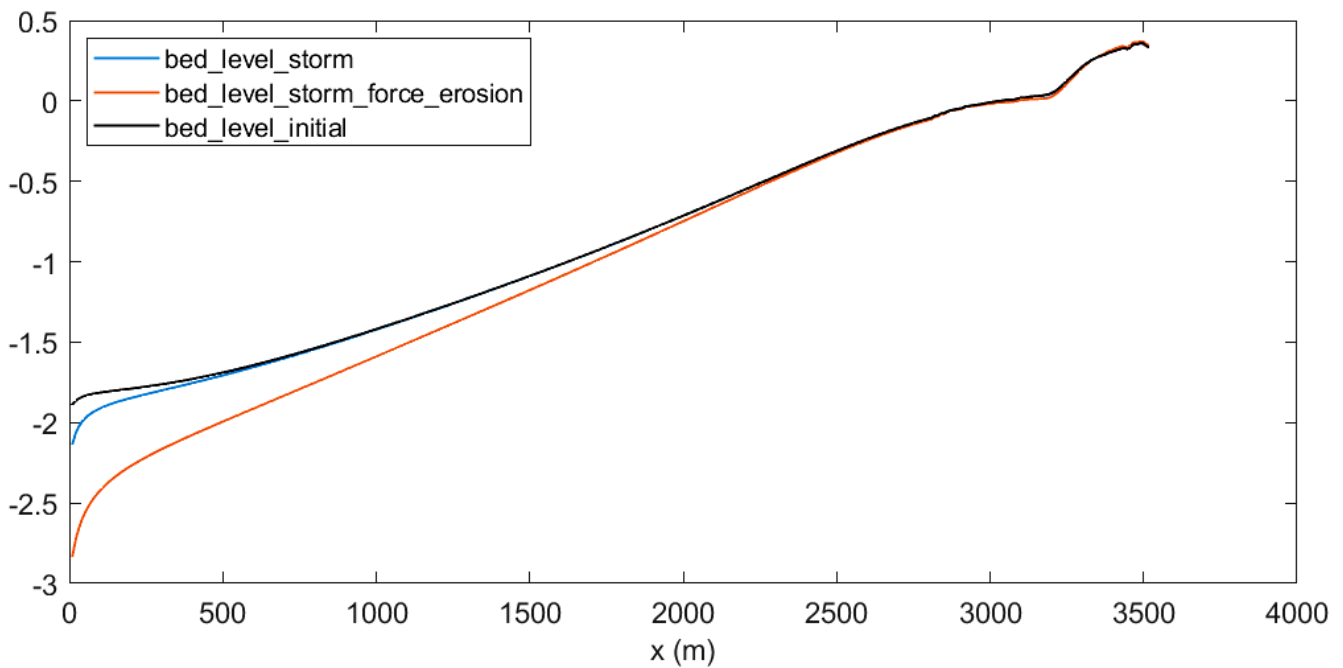


Figure 77 - Final bed level profiles (m): The initial profile (black line) and the profiles after 5 days of simulation under normal storm conditions (blue line) and under “forced erosion” storm conditions (red line).

As shown in Figure 77, there is more erosion in the seaward part of the profile, as expected because the case is set up so, but at the landward part of the bed level profile is almost stable, with accretion in the order of 1mm where vegetation is present, due to the much higher sediment concentration and the very mild hydrodynamic conditions in that part.

Despite of the effort to force the profile to erode in the above hypothetical case by the selection of appropriate initial sediment parameters, the landward part of the profile where hydrodynamic conditions are dissipated by bed level restriction appears to be again quite resilient in morphodynamic changes. However, other parameters like suspended sediment concentration, have the expected behavior, being much higher for the “forced erosion” case.

All the above investigation of the storm case creates the suspicion that the stability of bed level is not a result of model malfunction or of a wrong choice of sediment characteristics but is something that could be expected because of the very mild slope as it is further discussed in chapter 8.

6.4 Impact of extreme events on vegetation

Inside the model code, as described in chapter 3.7, the mortality of vegetation can be caused by the combination of high inundation and competition stresses over a period longer than a month, by high deposition rate (the limit is set to 15cm) and by high erosion rate (the limit is set to 50% of the current height of vegetation). Extreme event period is too short to cause the death due to the increased inundation stresses because of the storm surge, for the storm case. Furthermore, the stability of bed level profile as analysed above cannot justify any danger for vegetation as there is neither high erosion nor high deposition rate. It is then expected a stability on vegetation parameters.

Indeed, the results of the model according to the behaviour of vegetation during storm conditions show a stability of the number of plants that result in the same pattern of energy dissipation during the tidal cycles, as shown in Figure 78.

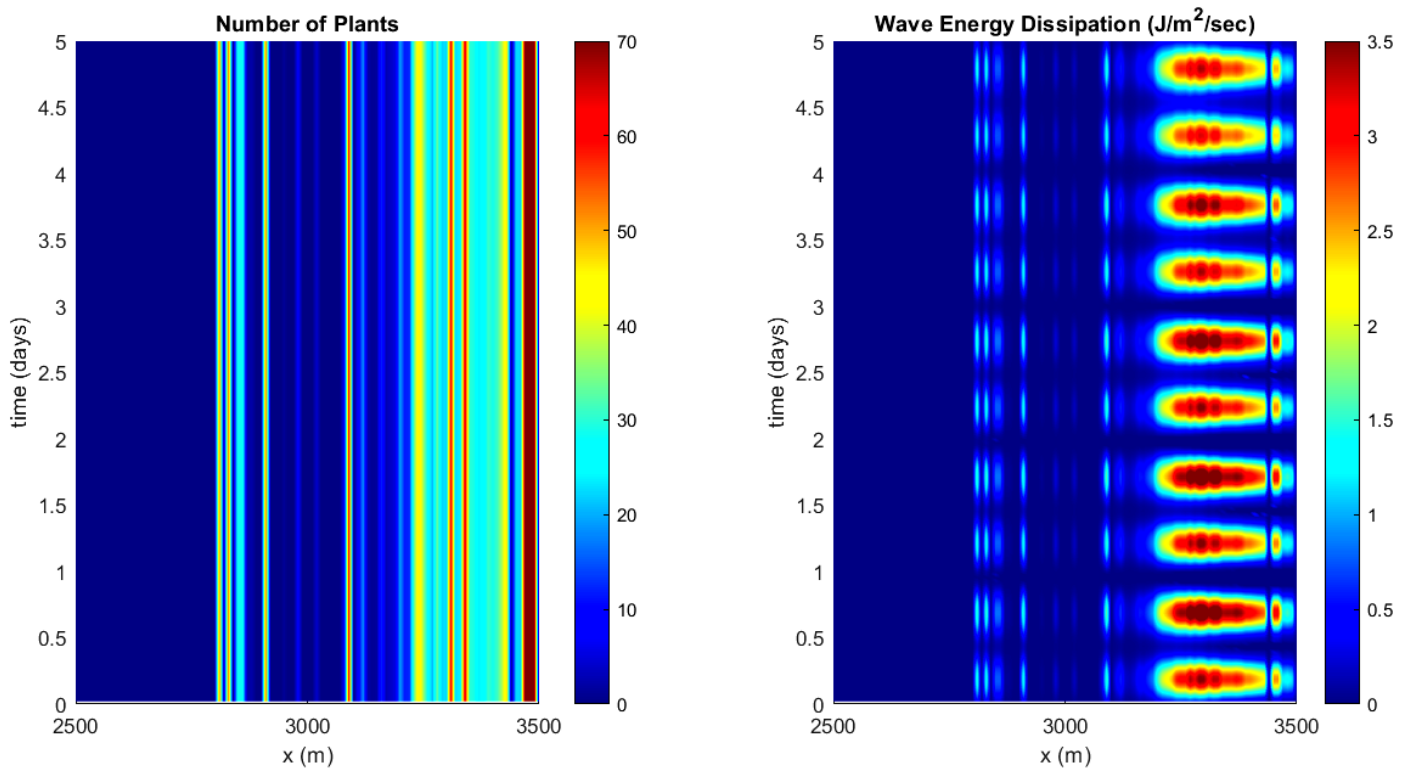


Figure 78 - Number of plants and wave energy dissipation for the last 1,000m of the profile, where vegetation is present during the 5 days of storm conditions

According to literature research and comparison with other cases worldwide analyzed in chapter 3.8, the extreme cases expected in Guyana coast as described in chapter 2.3 could not be characterized as severe for *Avicennia Germinans* mangroves that dominate vegetation in the study area.

7 Discussion

This study deals with different and complicated processes, like hydrodynamics, morphodynamics and vegetations dynamics in an effort to describe the behavior of a vegetated mudflat under extreme conditions. The effort starts with the interaction of sediment dynamics with hydrodynamics and morphodynamics finding a set of parameters that can produce an equilibrium profile. Then, vegetation is added to the model by describing the dynamics of generation, growth and death together with the influence of vegetation on flow and consequently on sediment dynamics and morphodynamics. All these processes are described and simulated by a 1-D process based model using assumptions and simplification resulting in a fast and, in some extend, complete way to describe all the basic processes. However, the realization of such an effort in the extend of a Master Thesis work is inevitable to generate uncertainties that in some of the cases tested above could be important.

The presence and migration of mudbanks

The scope of the hydrodynamic calibration is to derive a set of sediment parameters and coefficients that if used by the model, it is able to reproduce the real case. The profile chosen for this procedure is the 1970 profile and the effort of calibration is to produce a profile in equilibrium after 40 years of simulation. Then, by adding vegetation and by simulating hydrodynamics, sediment dynamics and vegetation dynamics for 10 more years there is an output profile that is used for testing the extreme cases. The final output profile after 50 years of total simulation, in the ideal case, should be similar with the 2020 profile available from the field measurements of last year, if all the physical processes could be simulated accurately by the model. The three profiles are presented in Figure 79.

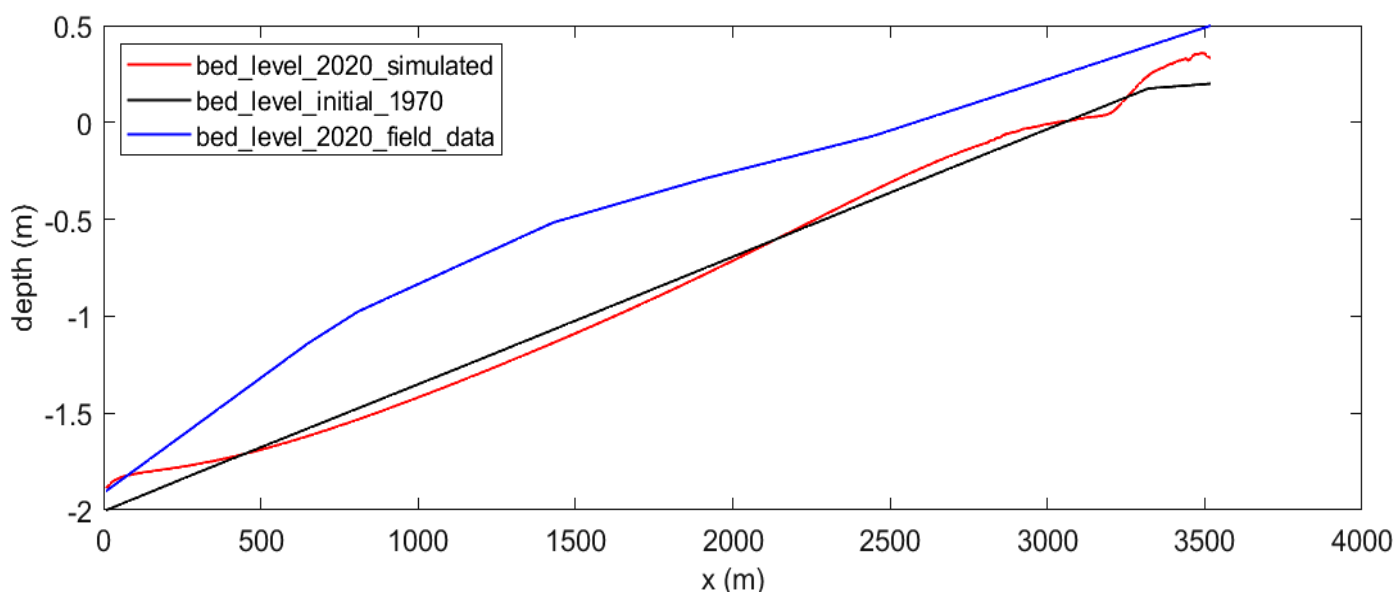


Figure 79 – The various profiles (m) used for this study: the measured 2020 profile (black line), the measured 1970 profile (red line), the simulated 2020 profile (blue line)

The two 2020 profiles are far from similar, but are accepted for this study. The reason, as explained in chapter 2.1, is the presence of a mudbank this period in front of the study area. The lack of field data through the decades for the bathymetry of this area does not allow for a reasonable assumption about when the mudbank appeared at the offshore of the study area or what is the difference caused according to suspended sediment concentration or the dissipation of wave energy. The 2008 profile as shown in Figure 5 could indicate the beginning of the effect of the mudbank or maybe this is the second mudbank passing through the study area after 1970, but again field data are quite poor to create a reliable input for the model. This is the reason why the presence of the mudbank is neglected and the calibration process is focused on reproducing the initial 1970 profile.

However, it is mentioned on literature that the periodicity of 20 to 30 years in the presence of the mudbank causes periodicity in erosion and accretion of the coast, thus in a next stage of research, when enough field data could be available, this phenomenon should be taken into account and be included in model simulations.

The hydrodynamic processes

The hydrodynamic processes taken into account by the model are limited in one wave condition (one route mean square wave height and one peak wave period in one direction) that should represent the full energy and direction spectrum of the real wave environment on the coast. However, even if the model could simulate the full wave spectrum, field data are not enough to produce a reliable spectrum for normal and for expected extreme conditions.

Furthermore, simplifications made by the model, like the one for the shallow water equation when neglecting inertia and friction effects, the exclusion of the wave induced alongshore flow and the exclusion of the tide induced alongshore flow to be able to reach an equilibrium profile could increase the uncertainty on how the final chosen set of parameters could produce an equilibrium profile in reality.

However, the ability of the model to produce an equilibrium profile, even if it excludes some hydrodynamic processes is important as it allows the researcher to focus on bed level changes caused by the test cases that are of his/her interest (presence of vegetation, changes in hydrodynamic conditions). Also, the simplicity of the model allows for fast calculations and gives the ability to test more cases in a restricted time period. It is remarkable that during this Thesis work, around 400 different cases were tested by the model.

Vegetation dynamics

Vegetation dynamics and their impact on the flow are analyzed in chapter 3 in which an effort to describe and quantify most of the relevant processes in the model is applied, using a wide range of literature and based on the work already done by Legay (2020). However, the worldwide research on vegetation and especially on quantifying its parameters is still in progress so this effort uses various simplifications and assumptions.

Vegetation in field has spatial heterogeneity even if it is consisted by a single species, which is usually not the case. For this study, it is assumed that in every grid cell of the model domain, i.e. in every 10x10m area, vegetation parameters, like the mangroves' diameter, height, number of pneumatophores, are the same. This is not the case in nature but grouping is necessary for every effort of simulation. Furthermore, there are parameters like the height and the diameter of pneumatophores that are assumed the same for the whole model domain, while it is known by literature that these parameters could vary even for the roots of the same tree. Also, the number of pneumatophores and the influence of a tree in its zone of influence are considered stable, while in reality closer to the stem it is expected higher number of roots and stronger influence than closer to the limits of the zone of influence.

Despite of the simplifications and assumptions in building up the model code for vegetation, it is remarkable that after calibrating various parameters, like the ' α ' parameter for the zone of influence and the growth coefficient ' G ', the model is able to reproduce, after 10 years of simulations, vegetation characteristics that are close to the field observations.

To compute the influence of vegetation on the flow, various coefficients are used, like the ' K_{cr} ' to increase the critical shear stress, ' e ' to increase the drag coefficient, ' K_{org} ' for the organic deposition, ' C_D ' for the dissipation of wave energy. All these coefficients are difficult to be calibrated as there are no field data about the real influence of vegetation on the flow so these parameters are kept the same as proposed by literature. In simulations, vegetation does influences the flow mainly by decreasing significantly the wave height and there is an observable change in behavior of the profile, however further research on this field with lab or field experiments could be able to specify better the way that the above various coefficient should be used.

The storm case

The first uncertainty on the storm case is generated by the lack of field data about the extreme events for Guyana coast: poor data on hydrodynamic conditions and no historical records on water level result in assumptions based on literature for the severity of the expected extreme storm and for the height of the corresponding expected storm surge.

Furthermore, concerning the simulation itself, there are a lot of processes that are not included in the model that may become more important during storm conditions as wind and waves dominate the hydrodynamic conditions instead of the tide and non-linear phenomena are stronger (J.Bosboom, 2015):

- Wind induced currents can be important in case of strong winds. They are created on the water surface by the wind induced shear stress on the water and have the direction of the wind (usually landward). They may create circulation currents in the opposite direction (deeper and seaward) to keep the water mass balance. Depending on the case, they may have significant impact on sediment transport.
- Cross-shore wave induced currents as expressed by the net mass flux above wave through (Stoke's drift) can be significant in case of high shallow waves (the storm case) and could result in a return current near bed (undertow) that compensates the onshore surface mass flux. Because of the higher sediment concentration near bed, these wave induced cross-shore currents could result in a net sediment transport to the offshore during storm conditions. To calculate these currents it is necessary to solve the horizontal momentum equation.
- Alongshore currents: Even if it is assumed that the wind and the waves reach the coast perpendicularly (which may not be exactly the case), the topographic variation of the coast could create alongshore currents in the breaking zone. The presence of alongshore currents can also create rip currents and then the hydrodynamic and morphodynamic processes in the breaking zone become highly non-linear and difficult to be modeled even by more sophisticated 3D models. These processes may not be dominant in case of mean normal hydrodynamic conditions but they could dominate the response of the profile in case of a storm, when the wave height and thus the wave energy is much higher. For Guyana case, the storm wave height is five times higher than the "normal" wave height and thus the wave energy in case of a storm is 25 times higher. However, the way that waves are breaking (spilling breaking waves) in combination with the very mild slope create a very wide breaking zone (in extend of some kilometers) and consequently the expected velocity of alongshore currents is not high and the dynamics of this zone may not be enough to create rip currents.
- Turbidity because of the high wave energy is able to stir up sediment. The increased suspended sediment concentration can create larger sediment fluxes at the cross-shore and alongshore direction.
- The formulas used in the model for the description of wave behavior (wave energy dissipation, wave induced shear stress) are based on linear wave theory. Increased wave height (storm case) increases also non-linear phenomena that can impose uncertainties on the validity of the formulas used.
- In the model only one harmonic wave is used to represent the whole wave energy and direction spectrum that is present in real conditions. This may work for the long-term simulations with mild wave conditions or in swell case for which waves are more regular and in a narrow energy band, but for the storm case for high wind generated waves it may be a quite rough simplification.
- "During stormy conditions wave action increases considerably and becomes the dominant process in sediment transport. This results in severe erosion of the mudflat", Brigit Janssen-Stelder, 2000. This notion highlights the importance of waves on understanding and simulating storm conditions compared with normal hydrodynamic condition for which tide is dominant for Guyana case.

Hydrodynamic and sediment dynamic parameters, like suspended sediment concentration, total shear stress, etc. are simulated by the model with reasonable results as analyzed in chapter 6.2. The effort through the sensitivity analysis to understand if there is a parameter that has an important influence on bed level shows that the stability of the profile is a combined result of the whole set of parameters. However, all the above listed processes, when added together could result in different behavior of the mudflat profile.

Furthermore, for the case of extreme storm, additional reduction of the wave height due to vegetation, more than the 17.5% computed by the model it is expected. The reason is that the elevated water level due to storm surge is capable of reaching mangrove canopy and thus the projected to the flow area is much larger than only the stem and the pneumatophores. Larger projected area is directly connected with higher wave energy dissipation (Equation 3.16). This is difficult to be modeled due to the complexity of canopy and due to the uncertainty on the height of the canopy that would be submerged in case of a storm but it could have a remarkable result on the final effect of vegetation on wave reduction. Further research on this issue could quantify the impact of canopy on the waves and give a more clear result about the effectiveness of mangroves on coastal defense.

Expected bed level changes

The next question arising from the above discussion about the storm case is if the behavior of the bed level profile in the real case is expected to be similar with the outcome of the model. To be able to answer to this interesting question, as no field records from previous storm events are available for the study area, further literature research on similar cases is necessary.

Unfortunately, all the relevant literature found about storm impact on mudflats (de Vet et al. 2020, Daidu et al. 2006, Yaoshen et al. 2020, Stelder 2000) concerns mudflats of estuaries and not mudflats purely exposed on sea (ocean) environment. In all relevant literature found, there is some erosion on mudflat after storm in the order of a few centimeters, depending on the case and on the location on the mudflat. The main difference between literature and Guyana case, except of the estuarine environment of literature findings and the oceanic environment of study area, is that the slope of Guyana coast is very mild, 1:1500, compared with other cases that have slope even one order of magnitude steeper (1:150). To reach the 20m isobaths it is necessary to extend the domain to 25 to 35km offshore, depending on the specific location along Guyana coast.

According to de Vet et al. (2020), milder slope and more shallow water can result in decreased bed level dynamics. This could be in accordance with the model results, as bed level changes are one order of magnitude smaller (in the order of a few millimeters) following the difference of the slope that is also one order of magnitude smaller compared to literature findings. Even when testing a slope 10 times steeper than the actual one, bed level changes are still very small. It is worth mentioning that according to the classification of Dyer et al. (2000), mudflats of slope < 0.04 are classified as low slope mudflats. The ten times higher slope chosen for comparison is 1:150, i.e. $0.0067 < 0.04$, so still low for a mudflat.

Thus, in that sense, and taking into account the extremity of the storm that is not so severe (wind velocity of 14m/sec – 50.4km/hour) compared with other storms, the observed erosion by model results could be stated that is close to what expected by literature research and in reality.

Another interesting result is that, as shown in Figure 69, the mudflat is so flat that it can dissipate the wave energy during the propagation of the waves through it, forming a depth restricted wave height profile at least for the last 2km onshore that makes the final waves reaching the landward part of the profile independent of the initially assume wave height for the storm. Off course a more severe storm, except of higher waves can introduce higher storm surge and this can allow waves to penetrate more into the mudflat because of the increased water level. In that sense, it is more important a right assumption on the storm surge than on the wave height.

Finally, a “forced erosion” storm case is tested in an effort to force the mudflat to erode. Even if the parameters chosen for this simulation, i.e. the combination of very low critical shear stress and very low settling velocity, are not representative of the real case, this test can show the ability of a mudflat with very mild slope to resist in bed level changes. This case enhances the argument that for the real case, mudflats like the one of Guyana coast could be resilient against rapid changes during extreme events.

The swell case

For the extreme swell case, the study is based on the work of van Ledden et al. (2009) who analyzed the extreme swell event of October 2005 in Guyana coast. Because of the lack of other literature sources, the most severe of the records of van Ledden is used as an input in the model. Thus, hydrodynamic conditions are clear for this case.

The profile has the same behavior with the storm case: Remains stable. The difference in the swell case is that the hydrodynamic conditions are quite milder compared to the storm, so the stability doesn't cause such questioning on the results. However, the hydrodynamic and sediment dynamic processes listed above that dominate the storm case could also affect in some extent the swell case, because the waves are still quite larger (2.5 times higher) compared to the normal hydrodynamic conditions.

The damages by the swell events recorded by van Ledden et al. (2009) are caused by the extreme run-up and overtopping due to surging waves with high peak period. The interesting result from the model for this case is that vegetation is able to reduce significantly the wave height, thus the final run-up is expected to be quite lower. This could be important for the sea defense as, no matter if there is a bit different behavior of the mudflat profile in front of sea walls compared with the model output, the final waves that reach the landward end of the mudflat would be expected to be highly dissipated by vegetation.

The impact of extreme events on vegetation

As analyzed in chapter 6.4, there are not yet enough available field data and corresponding formulas to be able to quantify the effect of the combined action of strong winds and high waves on vegetation. The ability of the model to compute vegetation death based on erosion or deposition on mangrove roots is also based on assumptions about the amount of erosion or deposition that is able to cause the death of vegetation and finally appears to be inactive because of the stability of the bed profile during the simulation.

Literature research and comparison with other cases worldwide with mangrove vegetation under the impact of extreme events appears to be the only way to derive some conclusions about how vegetation could be affected by a storm or a swell event. However, the difference in the severity of the expected events in Guyana compared to a mild hurricane or other studied cases could give a reasonable certainty that vegetation would not be affected remarkably by extreme events expected in Guyana. Maybe a higher threat for vegetation could be the migration of the mudbank that in some years will move north-westwards providing less protection from waves in normal conditions and less sediment supply, but this could be a subject of another study when more data would be available about the exact impact of mudbanks on the dynamics of mudflats along the Guyana coast.

8 Conclusion

A large range of processes is handled in this study in the effort to simulate the response of a vegetated mudflat under extreme conditions. The model is able to produce a stable equilibrium profile under normal hydrodynamic conditions using reasonable assumptions for the sediment parameters and calibration coefficients. It is also able to produce vegetation characteristics close to field measurements and simulate effectively vegetation dynamics. The influence of vegetation on the flow is also simulated by the model giving reasonable results, but this process is more difficult to be calibrated. The successful calibration process ends up with a fully developed bio-geomorphological model for Guyana coast.

For the highly dynamic conditions of a storm, some of the processes that are not included in the model may become dominant and the response of the mudflat could be less representative of the real case, however vegetation interacts with hydrodynamics giving reasonable results on wave dissipation. Furthermore, the extremely mild slope of Guyana mudflat, after an extended sensitivity analysis for storm case, gives the answer for the stability of bed level profile.

The response of vegetated mudflat on extreme events

During the extreme hydrodynamic events tested for the Guyana case, vegetation has beneficial effect on reducing the wave energy, the total shear stress and the sediment concentration at the landward part of the mudflat where it is present. The reduction of these parameters due to vegetation is presented in Table 12 for both of the cases. The reduction appears to be milder for the storm case, compared with the swell case, mainly because of the storm surge expected that increases the water level through the whole mudflat and allows for higher waves to penetrate through vegetation. However the model does not count for the impact of canopy on wave energy dissipation, so the dissipation for the storm case in real conditions is higher.

Table 12 - Reduction of various parameters at the landward end of the model domain for a random flood tide – high water during the 5 days of extreme event simulation, compared with the same simulation using normal hydrodynamic conditions

Parameter	Swell case	Storm case
bed level changes	negligible	
wave height	41.0%	17.5%
total shear stress	53.0%	29.1%
sediment concentration	82.5%	34.0%

Thus, vegetation does affect beneficially the response of the mudflat in the case of extreme events, by reducing the hydrodynamic forcing that reach the landward end. This can be further beneficially for the sea defence of Guyana, as lower waves can cause less damage to the sea walls and can result in less (or no) overtopping and flooding.

The impact of extreme events on the mangrove-mudflat system

Very mild slope can act as a stabilising parameter for a mudflat's bed level. This is the case for the study area, where no remarkable bed level changes are expected, even when neglecting vegetation, as the mudflat by itself, due to its slope, is able to resist on morphodynamic changes.

The impact of extreme events on vegetation is not quantified: the lack of literature findings makes it very uncertain to model and quantify breaking or uprooting of mangroves. However, the intensity of the extreme events for Guyana case is much milder than the intensity of tropical hurricanes for which there is field research available. Mangroves, especially *Avicennia Germinans*, are quite resilient in more severe hydrodynamic conditions than the ones that can occur in Guyana, so it is expected that vegetation can withstand such extreme events without significant damage. Vegetation would be able to recover possible minor damages in short period (in the order of a year).

References

- Anthony Edward J., Antoine Gardel, Nicolas Gratiot, "Fluvial sediment supply, mud banks, cheniers and the morphodynamics of the coast of South America between the Amazon and Orinoco river mouths", Geological Society, London, Special Publications, 2013
- Berger Uta, Hanno Hildenbrandt, "A new approach to spatially explicit modelling of forest dynamics: Spacing, ageing and neighbourhood competition of mangrove trees", *Ecological Modelling* 132 (2000) 287 – 302
- Bosboom Judith, Marcel J. F. Stive, "Coastal Dynamics I" version 0.5, 2015, ISBN 978-90-6562-3720
- Deltares, Delft-3D FLOW User Manual, version 3.15, 2 December 2020.
- de Vet P.L.M., B.C. van Prooijen, I.Colosimo, N.Steiner, T.Ysebaert, P.M.J. Herman, Z.B.Wang, "Variations in storm-induced bed level dynamics across intertidal flats", *Scientific Reports*, 10:12877 (2020), <https://doi.org/10.1038/s41598-020-69444-7>
- De Vos Willem-Jan, "Wave attenuation in mangrove wetlands", MSc Thesis at TU Delft, 2004
- Dyer K.R., M.C. Christie, E.W. Wright, "The classification of intertidal mudflats", *Continental Shelf Research* 20 (2000) 1039-1060
- Ellison Joanna C., "Impacts of Sediment Burial on Mangroves", *Marine Pollution Bulletin* Vol. 37, Nos.8-12, pp 420-426, 1998
- Fan Daidu, Yanxia Guo, Ping Wang, John Z. Shi, "Cross-shore variations in morphodynamic process of an open-coast mudflat in the Changjiang Delta, China: With an emphasis on storm impacts", *Continental Shelf Research* 26 (2006) 517-538
- Fan Yaoshen, Shenliang Chen, Shunqi Pan, Shentang Dou, "Storm – induced hydrodynamic changes and seabed erosion in the littoral area of Yellow River Delta: A model-guided mechanism study", *Continental Shelf Research* 205 (2020) 104171
- Farid Dahdouh-Guebas, James G. Kairo, Ruth de Bondt, Nico Koedam, "Pneumatophore height and density in relation to microtopography in the gray mangrove *Avicennia Marina*", 2007, *Belg.J.Bot.* 140 (2): 213-221 (2007)
- Feller Ilka C., Marsha Sitnik, "Mangrove ecology, workshop manual", Smithsonian Institution, 1996
- Froidefond J.M., M. Pujos, X. Andre, "Migration of mud banks and changing coastline in French Guiana", *Marine Geology*, 84: 19-30, 1988
- Fromard F., H.Puig, E.Mougin, G.Marty, J.L.Betoulle, L.Cadamuro, "Structure, above-ground biomass and dynamics of mangrove ecosystems: new data from French Guiana", *Oecologia* (1998) 115:39-53
- Friedrichs Carl. "Tidal Flat Morphodynamics", 2011. doi:10.1016/B978-0-12-374711-2.00307-7.
- Hashim Ahmad Mustafa, Sim Mong Pheng Catherine, Husna Takaijudin, "Effectiveness of Mangrove Forests in Surface Wave Attenuation: A Review", *Research Journal of Applied Sciences, Engineering and Technology* 5 (18): 4483-4488, 2013
- Healy T.R. (2005) Muddy Coasts. In: Schwartz M.L. (eds) *Encyclopedia of Coastal Science*. Encyclopedia of Earth Science Series. Springer, Dordrecht. https://doi.org/10.1007/1-4020-3880-1_220
- Hill Mary C., "Methods and guidelines for effective model calibration", U.S. Geological Survey, Water – Resources Investigations Report 98-4005, 1998

- Holman R.A., A.H. Sallenger, "Setup and Swash on a Natural Beach", *Journal of geophysical research*, vol. 90, No C1, Pages 945-953, 1985
- Jun Tang, Shaodong Shen, Hui Wang, "Numerical model for coastal wave propagation through mild slope zone in the presence of rigid vegetation", *Coastal Engineering* 97 (2015) 53-59
- Krauss Ken W., Michael J. Osland, "Tropical cyclones and the organization of mangrove forests: a review", *Annals of Botany* 125: 213-234, 2020
- Kuznetsov Sergey, Yana Saprykina, "Depth – induced wave breaking criteria in dependence on wave nonlinearity in coastal zone", *Coastal Dynamics* 2017, Paper No. 093
- Legay Alexandre, "Mudflat Simulation: Adding the vegetation influence and its dynamics to an existing Matlab model", IHE & ESPCI internship report, 2020
- Le Hir P., W. Roberts, O. Cazaillet, M. Christie, P. Bassoullet, C. Bacher, "Characterization of intertidal flat hydrodynamics", *Continental Shelf Research* 20 (2000) 1433 – 1459
- Lesser G.R., J.A. Roelvink, J.A.T.M. van Kester, G.S. Stelling, "Development and validation of a three-dimensional morphological model", *Coastal Engineering* 51 (2004) 883-915
- Mariotti Giulio, Sergio Fagherazzi, "A numerical model for the coupled long-term evolution of salt marshes and tidal flats", *Journal of Geophysical Research*, Vol. 115. G01004, doi:10.1029/2009JG001326, 2010
- Mazda Yoshihiro, Eric Wolanski, Brian King, Akira Sase, Daisuke Ohtsuka, Michimasa Magi, "Drag force due to vegetation in mangrove swamps", *Mangroves and Salt Marshes* 1: 193-199, 1997, Kluwer Academic Publishers.
- Mclvor Anna L., Iris Möller, Tom Spencer, Mark Spalding, "Reduction of Wind and Swell Waves by Mangroves", *Natural Coastal Protection Series* ISSN 2050-7941, 2012.
<http://resolver.tudelft.nl/uuid:79fe752e-ce52-4bf6-a45c-2847bead07ab>
- Mclvor Anna L., Tom Spencer, Iris Möller, Mark Spalding, "Storm Surge Reduction by Mangroves", *Natural Coastal Protection Series* ISSN 2050-7941, 2012
- Murray Nicholas J., Stuart R. Phinn, Michael DeWitt, Renata Ferrari, Renee Johnston, Mitchell B. Lyons, Nicholas Clinton, David Thau & Richard A. Fuller, "The global distribution and trajectory of tidal flats", *Nature* 565, 222-225 (2019)
- NOAA, National Oceanic and Atmospheric Administration, US Department of Commerce. Retrieved 05/05/2021, 2021, from: https://tidesandcurrents.noaa.gov/about_harmonic_constituents.html
- Petti Marco, Sara Pascolo, Silvia Bosa, Annelore Bezzi, Giorgio Fontolan, "Tidal Flats Morphodynamics: A new Conceptual Model to Predict Their Evolution over a Medium-Long Period", *Water* 2019, 11, 1176; doi:10.3390/w11061176
- Pritchard D., and A. J. Hogg, Cross-shore sediment transport and the equilibrium morphology of mudflats under tidal currents, *J. Geophys. Res.*, 108(C10), 3313, doi:10.1029/2002JC001570, 2003
- Resio Donald T., Val R. Swail, Robert E. Jensen, Vincent J. Cardone, "Wind Speed Scaling in Fully Developed Seas", *Journal of physical oceanography*, 1999, Volume 29, 1801-1811
[https://doi.org/10.1175/1520-0485\(1999\)029<1801:WSSIFD>2.0.CO;2](https://doi.org/10.1175/1520-0485(1999)029<1801:WSSIFD>2.0.CO;2)
- Roelvink Dano J.A., Dirk-Jan Walstra, "Keeping it simple by using complex models", *Advances in Hydro-Science and Engineering*, Volume VI, 2005

Rogers W.E., J.M. Kaihatu, H.A.H. Petit, N. Booij, L.H. Holthuijsen, "Diffusion reduction in an arbitrary scale third generation wind wave model", *Ocean Engineering* 29 (2002) 1357-1390

s.R.L., Navionics (2021). "Nautical Chart Viewer." Retrieved 05/05/2021, 2021, from: https://webapp.navionics.com/#boating@7&key=_bzh%40~d_aJ

Servino Ricardo Nogueira, Luiz Eduardo de Oliveira Gomes, Angelo Fraga Bernardino, "Extreme weather impacts on tropical mangrove forests in Eastern Brazil Marine Ecoregion", *Science of the Total Environment* 628 – 629 (2018) 233 – 240

Smith Thomas J. III, Gordon H. Anderson, Karen Balentine, Ginger Tiling, Greg A. Ward, Kevin R. T. Whelan, "Cumulative impacts of hurricanes on Florida mangrove ecosystems: Sediment deposition, storm surges and vegetation", *Wetlands*, Vol. 29, No. 1, March 2009, pp. 24-34

Spalding M., McIvor A., Tonneijck F.H., Tol S., P. van Eijk, "Mangroves for coastal defence – Guidelines for coastal managers & policy makers", *Wetlands International and The Nature Conservancy*, 2014

Stelder Janssen Brigit, "The effect of different hydrodynamic conditions on the morphodynamics of a tidal mudflat in the Dutch Wadden Sea", *Continental Shelf Research* 20 (2000) 1461 – 1478

Toorman E.A. et al. (2018) "Interaction of Mangroves, Coastal Hydrodynamics, and Morphodynamics Along the Coastal Fringes of the Guianas". In: Makowski C., Finkl C. (eds) *Threats to Mangrove Forests*. Coastal Research Library, vol 25. Springer, Cham. https://doi.org/10.1007/978-3-319-73016-5_20

van der Wegen M., J.A. Roelvink, B.E. Jaffe, "Morphodynamics Resilience of Intertidal Mudflats on a Seasonal Time Scale", *JGR Oceans*, 2019

van Ledden Mathijs, Geoffrey Vaughn, Joost Lanser, Frank Wiershman, Mewburn Amsterdam, "Extreme wave event along the Guyana coastline in October 2005", *Continental Shelf Research* 29 (2009) 352-361

van Maanen B, Coco G, Bryan KR., "On the ecogeomorphological feedbacks that control tidal channel network evolution in a sandy mangrove setting." , 2015, *Proc. R. Soc. A* 471: 20150115. <http://dx.doi.org/10.1098/rspa.2015.0115>

van Rijn Leo C., "Erodibility of mud – sand mixtures", <https://www.leovanrijn-sediment.com/papers/Reporterodibilitymud-sand2018.pdf>, 2018

van Rijn Leo C., "Literature review of critical bed-shear stresses for mud-sand mixtures", <https://www.leovanrijn-sediment.com>, August 2020

van Rijn Leo C., "Settling velocity and equivalent size of mud", <https://www.leovanrijn-sediment.com>, May 2020

van Rooijen A.A., J.S.M. van Thiel de Vries, R.T. McCall, A.R. van Dongeren, J.A. Roelvink, A.J.H.M. Reniers, "Modeling of wave attenuation by vegetation with XBeach", *IAHR*, 2015

van Wesenbeeck Bregje K., Wiebe de Boer, Siddharth Narayan, Wouter R. L. van der Star, Mindert B. de Vries, "Coastal and riverine ecosystems as adaptive flood defences under a changing climate", *Mitigation and Adaptation Strategies for Global Change*, 2016

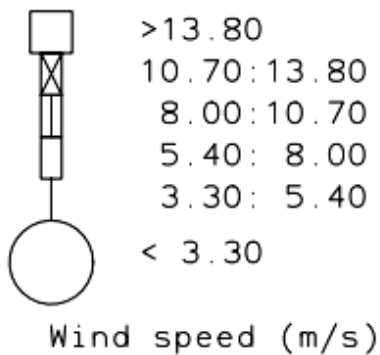
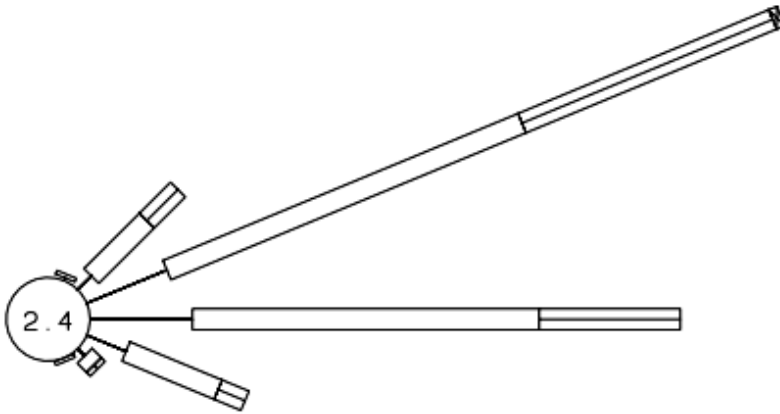
Winterwerp, J. C., W. G. M. van Kesteren, B. van Prooijen, and W. Jacobs (2012), "A conceptual framework for shear flow–induced erosion of soft cohesive sediment beds", *J. Geophys. Res.*, 117, C10020, doi:10.1029/2012JC008072.

Winterwerp J.C., R.F. de Graaff, J. Groeneveg, A.P. Luijendijk, "Modeling of wave damping at Guyana mud coast", *Coastal Engineering* 54 (2007) 249-261

Appendix A – Wind and wave roses

Wind and wave roses for the period between 1997 and 2003 at location 8°N, 57.5°W, located at about 150km offshore of Georgetown:

Wind:



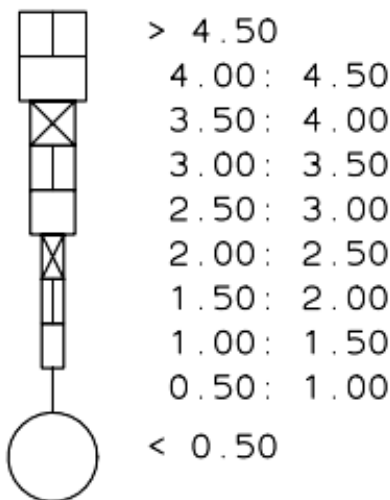
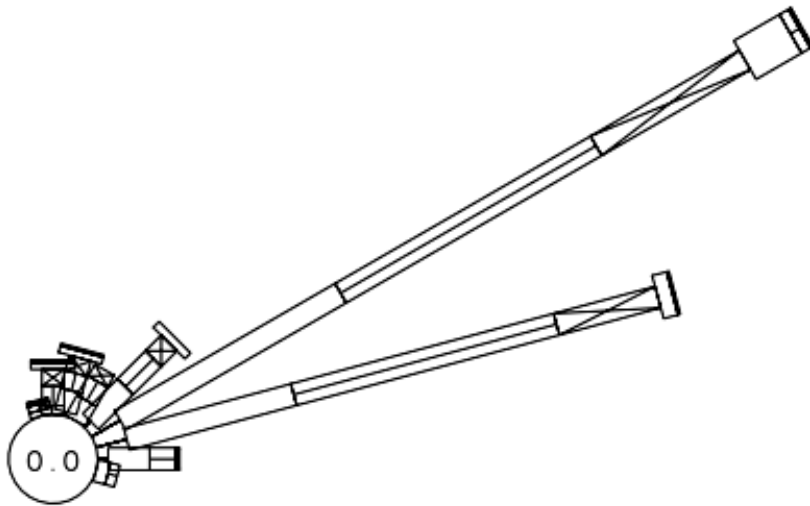
EXPLANATION

Item:	Represents:
Type of bar	Height / Speed
Direction of bar (to centre of rose)	Direction
Length of bar	Occurrence (%)
Number in centre of rose	Occurrence (%) in lowest class

20.0%

Wind speed rose at location 8N,57.5W NOAA Global Model 1997-2003	Wind	
	All Year	
DELFT HYDRAULICS	H4095	FIG.

Waves:



EXPLANATION

Item:	Represents:
Type of bar	Height / Speed
Direction of bar (to centre of rose)	Direction
Length of bar	Occurrence (%)
Number in centre of rose	Occurrence (%) in lowest class

Significant wave height (m)

20.0%

Wave height rose at 8N,57.5W NOAA Global Wave Model	Sea + Swell	
	All Year	
DELFT HYDRAULICS	H4095	FIG.

Appendix B – Mudbank migration in Guyana coast

The position and the migration plan of mudbanks along Guyana coast according to NEDECO, 1972

